Waves in Random and Complex Media
Vol. 16, No. 3, August 2006, 293–382

Taylor & Francis
Taylor & Francis

Slow light in photonic crystals

ALEX FIGOTIN* and ILYA VITEBSKIY

Department of Mathematics, University of California at Irvine, CA 92697

(Received 18 April 2005; in final form 31 May 2006)

The problem of slowing down light by orders of magnitude has been extensively discussed in the literature. Such a possibility can be useful in a variety of optical and microwave applications. Many qualitatively different approaches have been explored. Here we discuss how this goal can be achieved in linear dispersive media, such as photonic crystals. The existence of slowly propagating electromagnetic waves in photonic crystals is quite obvious and well known. The main problem, though, has been how to convert the input radiation into the slow mode without losing a significant portion of the incident light energy to absorption, reflection, etc. We show that the so-called frozen mode regime offers a unique solution to the above problem. Under the frozen mode regime, the incident light enters the photonic crystal with little reflection and, subsequently, is completely converted into the frozen mode with huge amplitude and almost zero group velocity. The linearity of the above effect allows the slowing of light regardless of its intensity. An additional advantage of photonic crystals over other methods of slowing down light is that photonic crystals can preserve both time and space coherence of the input electromagnetic wave.

1. Introduction

1.1. *What is slow light?*

It is common knowledge that, in vacuum, light propagates with constant velocity $c \approx 3 \times 10^8$ m/sec. In optically transparent nondispersive media, the speed of light propagation is different

$$v = \omega/k = c/n, \tag{1}$$

where k is the wave number, ω is the respective frequency, and n is the refractive index of the medium. At optical frequencies, the refractive index n of transparent materials usually does not exceed several units, and the speed of light propagation is of the same order of magnitude as in vacuum.

The situation can change dramatically in strongly dispersive media. Although the phase velocity of light is still determined by the same expression (1), the speed of electromagnetic pulse propagation is different from v and is determined by the group velocity [1–3]

$$u = \frac{\partial \omega}{\partial k} = c\left(n + \omega \frac{dn}{d\omega}\right)^{-1}, \tag{2}$$

*Corresponding author. E-mail: afigotin@uci.edu

Waves in Random and Complex Media
ISSN: 1745-5030 (print), 1745-5049 (online)
http://www.tandf.co.uk/journals
DOI: 10.1080/17455030600836507

which is one of the most important electromagnetic characteristics of the medium. With certain reservations, the group velocity u coincides with the electromagnetic energy velocity and is usually referred to simply as the propagation speed of light in the medium. Hereinafter, the speed of light propagation means the group velocity (2), rather then the phase velocity (1).

Strong dispersion means that the group velocity u strongly depends on the frequency and can be substantially different from c. In the slow light case, which is the subject of our interest, the electromagnetic pulse propagates through the dispersive medium at the speed $u \ll c$, regardless of the respective value of the phase velocity (1). In some cases, u can even become vanishingly small implying that the propagating electromagnetic mode at the respective frequency does not transfer energy. In another extreme case, the group velocity u can exceed c (the so-called case of superluminal pulse propagation), without contradicting the causality principle [1, 4–7]. In yet another case of a left-handed medium, the group velocity u can have the opposite sign to that of the phase velocity v [8]. But again, in this paper we will focus exclusively on the slow light and related phenomena.

Slow and ultraslow light have numerous and diverse practical applications. The related phenomena include dramatic enhancement of various light-matter interactions such as nonlinear effects (higher harmonic generation, wave mixing, etc.), magnetic Faraday rotation, as well as many other important electromagnetic properties of the optical media. Such an enhancement can facilitate design of controllable optical delay lines, phase shifters, miniature and efficient optical amplifiers and lasers, etc. In addition, ultraslow light might allow nonlinear interactions down to a single photon level, which could significantly benefit the design of ultrasensitive optical switches, quantum all-optical data storage and data processing devices. Ultraslow light can also be used in quantum communication and design of novel acousto-optical devices. This list can be continued. For more detailed information on the prospective practical applications of slow light phenomena see, for example, [9–31] and references therein.

1.2. *Temporal dispersion versus spatial dispersion*

In recent years, several different approaches have been pursued in order to slow down or even completely stop light. These approaches can be grouped into two major categories:

- those where the low group velocity results from strong temporal dispersion $dn/d\omega$ of optical media;
- those where the low speed of pulse propagation is a result of coherent interference in spatially periodic heterogeneous media, such as photonic crystals.

Let us start with a brief discussion of slow light phenomena in media with strong temporal dispersion.

1.2.1. Slow light in media with strong temporal dispersion. Assuming that the refractive index n in (2) is of the order of unity, which is usually the case at optical frequencies, one can state that a very low group velocity can only occur if n varies strongly as a function of ω

$$u \approx c\left(\omega\frac{dn}{d\omega}\right)^{-1} \ll c \qquad \text{only if } \omega\frac{dn}{d\omega} \gg 1. \tag{3}$$

Strong frequency dependence of the refractive index n can be a result of excitation of electronic or some other intrinsic resonances of the medium, which are normally accompanied by strong absorption of light. Recently, though, several techniques have been developed that allow to significantly suppress the absorption of light at the frequency where the derivative $dn/d\omega$ peaks.

One of the most successful ways to suppress light absorption is based on the effect of electromagnetically induced transparency (EIT) [35]. In such a case, the incident light interacts with atomic spin excitations forming combined excitations of photons and spins, called

dark-state polaritons. These polaritons propagate slowly through the medium in the form of a sharply compressed pulse, the energy of which is much smaller than that of the incident light pulse. Most of the incident light energy is expended to create the coherent state of the atomic spins, the rest is carried away by the control electromagnetic field. The pulse delay inside the medium is limited by the bandwidth of the transparency window, which decreases with propagation distance. At higher propagation distances the medium becomes increasingly opaque at frequencies other than the line center, further reducing the available transparency window [12, 13]. Specific physical mechanisms of such transformations are very diverse. The detailed description of EIT and related phenomena can be found in the extensive literature on the subject (see, for example, [9–14], and references therein). The techniques based on EIT have already produced some amazing results, such as reduction of the speed of pulse propagation by 7–8 orders of magnitude compared to the speed of light in vacuum, while providing a huge and controllable pulse delay.

Another method to create a transparency window in otherwise opaque substance was used in [15, 16]. This method involves the creation of a spectral hole by the periodic modulation of the ground state population at the beat frequency between the pump and the probe fields applied to the material sample. It can produce slow light in a solid-state material at room temperature. The spectral hole created by this technique can be extremely narrow (36 Hz in the experiment [15, 16]), and leads to a rapid spectral variation of refractive index. It allowed to reduce the light group velocity in a ruby crystal down to 57 m/s.

Physically, the above approaches to slowing down the light can be viewed as a reversible transformation of the input nearly monochromatic light into some kind of coherent atomic excitations (e.g., dark-state polaritons) with very low relaxation rate and low group velocity. In other words, ultraslow pulse propagating through such a medium is, in fact, an intrinsic coherent excitation triggered by the input light, rather than a light pulse per se. This process always involves some kind of a delicate resonant light-matter interaction with extremely small bandwidth. Indeed, the relation (3) yields the following limitation on the slow pulse bandwidth

$$\frac{\Delta\omega}{\omega} < \frac{u}{c}, \tag{4}$$

where the assumption is made that the refractive index n within the transparency window is of the order of unity. The condition (4) can also be viewed as a constraint on the minimal propagation speed of a light pulse with a given bandwidth $\Delta\omega$. On the positive side, the approach based on EIT or its modifications does produce an exceptionally low speed of pulse propagation, which can have some very important practical implications.

In the rest of the paper we focus exclusively on those techniques which do not involve any intrinsic resonant excitations of the medium and, therefore, do not essentially rely on strong temporal dispersion. Instead, we will focus on spatially periodic dielectric arrays, in which low group velocity results solely from spatial inhomogeneity of the optical medium.

1.2.2. Slow light in spatially periodic arrays. Well-known examples of optical periodic dielectric structures include photonic crystals [36], periodic arrays of coupled optical resonators [18–24], and line-defect waveguides [25]. Generally, a periodic heterogeneous medium can be assigned a meaningful refractive index n only if the structural period L is much smaller than the light wavelength λ

$$L \ll \lambda. \tag{5}$$

On the other hand, a significant spatial dispersion associated with heterogeneity of the medium can occur only when L and λ are comparable in value

$$L \sim \lambda. \tag{6}$$

In particular, the relation (6) defines a necessary condition under which heterogeneity of the medium can lead to low speed of electromagnetic pulse propagation. Hence, in the cases where low speed of pulse propagation is a result of strong spatial dispersion, one cannot assign a meaningful refractive index to the composite medium, and the expression (3) for the group velocity of light does not apply.

At optical frequencies, the speed of pulse propagation in periodic dielectric arrays can be reduced by two or three orders of magnitude. This is not a fundamental restriction, but rather a technological limitation related to the difficulty of building flawless periodic arrays at nanoscales. On the positive side, the dielectric components of the periodic array are not required to display strong temporal dispersion and, hence, absorption of light is not an essential and unavoidable problem in this case. In addition, the photonic crystal based approach is much more versatile in terms of the input light intensity. It allows the same photonic device to operate both at high and low intensity of the input light. By contrast, utilizing strong temporal dispersion always involves significant nonlinearity and usually is limited to a certain amplitude of the input light.

There is a natural bandwidth limitation on the slowed pulse in periodic dielectric arrays, which is similar to the case of slow light in time-dispersive media. Indeed, let $\Delta\omega$ be the frequency bandwidth of a pulse and Δk – the respective range of the Bloch wave number. The average group velocity $\langle u\rangle$ of the pulse is defined as

$$\langle u\rangle \approx \frac{\Delta\omega}{\Delta k}. \tag{7}$$

Let us make the following natural assumptions.

(i) The pulse propagating inside the periodic medium is composed of the Bloch eigenmodes belonging to the same spectral branch of the dispersion relation $\omega(k)$. This assumption implies that Δk cannot exceed the size $2\pi/L$ of the Brillouin zone

$$\Delta k < 2\pi/L, \tag{8}$$

where L is the unit cell length of the periodic array.

(ii) The refractive index of the constitutive components of the periodic array is of the order of unity and, therefore,

$$L \sim \lambda_0 = 2\pi c/\omega, \tag{9}$$

where λ_0 is the light wavelength in vacuum.

The relations (7–9) yield the following limitation on the minimal speed of pulse propagation for a pulse with a given bandwidth $\Delta\omega$

$$\langle u\rangle > \frac{L}{2\pi}\Delta\omega \sim c\frac{\Delta\omega}{\omega}. \tag{10}$$

The restriction (10) is similar to that defined by the inequality (4) and related to the case of slow light in a uniform medium with strong temporal dispersion. In either case, a higher refractive index would lower the minimal speed $\langle u\rangle$ of pulse propagation for a given pulse bandwidth $\Delta\omega$.

Any attempt to circumvent the restriction (10) would involve some kind of pulse compression techniques [17].

1.2.3. Examples of periodic arrays supporting slow light. *Coupled resonator optical waveguide.* During the last several years, a tremendous progress has been made in theory and applications of periodic arrays of coupled optical resonators. Generally, if the coupling between adjacent resonators in a periodic chain is weak, the group velocity of Bloch excitations

supported by such a periodic array is low. This is true regardless of the nature of individual resonators. The above simple idea forms the basis for one of the most popular approaches to slowing down the light. An extensive discussion on the subject and numerous examples and references can be found in [18–24, 32].

A qualitatively similar situation occurs in line-defect waveguides in a photonic crystal slab, where a periodic array of structural defects plays the role of weakly coupled optical resonators. Following [25], consider a dielectric slab with a two-dimensional periodic array of holes in it. A row of missing holes in this periodic array forms a line defect, which supports a waveguiding mode with two types of cutoff within the photonic band gap. These characteristics can be tuned by controlling the defect width. Theoretical calculations supported by interference measurements show that the single waveguiding mode of the line-defect waveguide displays extraordinarily large group dispersion. In some instances, the corresponding traveling speed is 2 orders of magnitude slower than that in air. According to [25], one of the major limiting factor here is structural imperfection of the array.

Slow light phenomena in periodic arrays of weakly coupled resonators have been the subject of a great number of recent publications, including some excellent review articles cited above. For this reason, further in this paper we will not discuss this subject any more.

Photonic crystals. Photonic crystals are spatially periodic structures composed of usually two different transparent dielectric materials [36]. Similarly to periodic arrays of coupled resonators, in photonic crystals, a low group velocity of light can result from multiple scattering of individual photons by periodic spatial inhomogeneities, rather than from temporal dispersion of the substance [22, 26–31]. The lowest group velocity achievable in photonic crystals for a given pulse bandwidth can be close to that defined by the fundamental restriction (10). For example, if we want a pulse to propagate undistorted at speed as low as $10^{-3}c$, its bandwidth $\Delta\omega$ should be less than $10^{-3}\omega$, which at optical frequencies is of the order of 10 GHz. In this respect, the situation in photonic crystals is as good as it can possibly be in any other linear passive media with limited refractive index.

Unlike the case of optical waveguides and linear arrays of coupled resonators, in photonic crystals we have bulk electromagnetic waves capable of propagating in any direction through the periodic heterogeneous structure. This results in much greater density of modes, compared to that of the above-mentioned arrays of coupled resonators. In addition, electromagnetic waves in photonic crystals can remain coherent in all three dimensions, which is also essential for a variety of practical applications.

A major problem with slow light in photonic crystals is the efficiency of conversion of the incident light into the slow mode inside the heterogeneous medium. We shall see in the next section that in most cases an incident electromagnetic wave with the frequency of one of the slow modes is simply reflected back to space, without creating the slow mode inside the photonic crystal. How to overcome this fundamental problem and, thereby, how to transform a significant fraction of the incident light energy into a slow mode with drastically enhanced amplitude, is one of the primary subjects of this paper.

The paper is organized as follows. In Section 2 we describe, in general terms, what kind of slow modes can exist in photonic crystals and under what circumstances some of these modes can be effectively excited by incident light. We show, that there is a unique situation, which we call the frozen mode regime, in which the incident light can enter the photonic crystal with little reflection and be completely converted into a slow mode with nearly zero group velocity and drastically enhanced amplitude.

Section 3 gives an overall picture of the frozen mode regime in periodic layered media, without going into the detailed analysis based on the Maxwell equations. All the statements made in this section are later proven in Sections 5 through 11.

In section 4 we define the physical conditions under which a periodic layered array can support the frozen mode regime. These conditions boil down to whether or not the electromagnetic

dispersion relation of the periodic array can develop a stationary inflection point (15). This requirement imposes quite severe restrictions on composition and geometry of the periodic layered medium. We show, in particular, that in the case of light propagating normally to the layers, the frozen mode regime can only occur if some of the layers are magnetic with significant nonreciprocal Faraday rotation. In the case of oblique light propagation, the presence of magnetic layers is not required, which makes it possible to realize the frozen mode regime at any frequency range, including optical and UV. A trade-off though is that at least some of the layers of a non-magnetic stack must display significant dielectric anisotropy with tilted orientation of the anisotropy axis.

Section 5 is devoted to electrodynamics of periodic layered media. Particular attention is given to the cases where some of the layers display dielectric and/or magnetic anisotropy, because otherwise, the electromagnetic dispersion relation $\omega(k)$ of the periodic array cannot develop a stationary inflection point (15) and, therefore, such a structure cannot support the frozen mode regime.

Sections 6 through 12 constitute the analytical basis for the entire investigation. There we present a rigorous and systematic analysis of the scattering problem for a semi-infinite periodic array of anisotropic dielectric layers. The emphasis is on the vicinity of stationary points (12) of the electromagnetic dispersion relation, where the slow electromagnetic modes can be excited. The comparative analysis of all possible stationary points shows that only a stationary inflection point (15) can provide necessary conditions for slowing down and freezing a significant fraction of incoming radiation. In all other cases, the incident wave is either reflected back to space, or gets converted into a fast propagating mode with low amplitude. The exact analytical results of these sections are supported by a number of numerical simulations.

2. Stationary points of dispersion relations and slow modes

In periodic heterogeneous media, such as photonic crystals, the velocity of light is defined as the wave group velocity

$$\vec{u} = \partial\omega/\partial\vec{k}, \tag{11}$$

where $\vec{k}$ is the Bloch wave vector and $\omega = \omega(\vec{k})$ is the respective frequency. At some frequencies, the dispersion relation $\omega(\vec{k})$ can develop stationary points

$$\partial\omega/\partial\vec{k} = 0, \tag{12}$$

where the group velocity $\vec{u}$ vanishes. Zero group velocity usually implies that the respective Bloch eigenmode does not transfer electromagnetic energy. Indeed, with certain reservations, the energy flux $\vec{S}$ of a propagating Bloch mode is

$$\vec{S} = W\vec{u}, \tag{13}$$

where W is the electromagnetic energy density associated with this mode. If W is bounded, then the group velocity $\vec{u}$ and the energy flux $\vec{S}$ vanish simultaneously at the respective stationary point (12) of the dispersion relation. Such modes are referred to as slow modes, or slow light. Some examples of stationary points (12) are shown in figure 1, where each of the frequencies ω_a, ω_b, ω_g, ω_0 is associated with a slow mode.

The electromagnetic dispersion relation of any photonic crystal displays an infinite number of stationary points like those shown in figure 1. But, a common problem with almost all of them is that the respective slow modes cannot be excited in a semi-infinite photonic crystal by

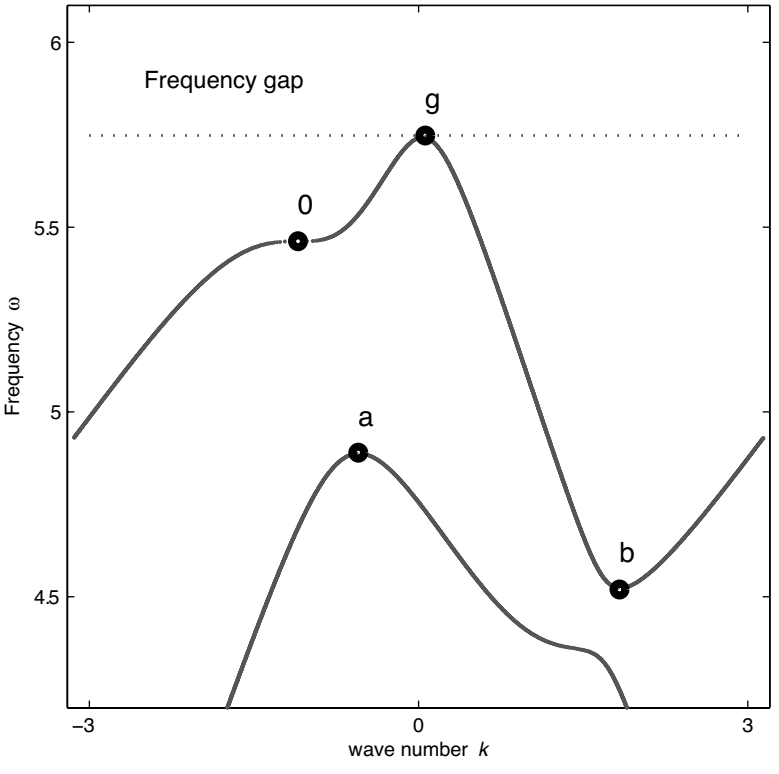

Figure 1. An example of electromagnetic dispersion relation $\omega(k)$ with various stationary points: (i) extreme points a and b of the respective spectral branches, (ii) a photonic band edge g, (iii) a stationary inflection point 0. Each stationary point is associated with slow light.

incident light. This explains why there have been only a few attempts to exploit the photonic crystals for slowing down the light. Let us take a closer look at this problem.

Consider a scattering problem of a plane monochromatic wave normally incident on a lossless semi-infinite photonic slab with the electromagnetic dispersion relation shown in figure 1. The symbol k in figure 1 denotes the normal component of the Bloch wave number $\vec{k}$ in the periodic structure, which in the case of a normal incidence is the only nonzero component of $\vec{k}$. The symbols Ψ_I, Ψ_R, and Ψ_T in figure 2 denote the incident, reflected, and transmitted waves, respectively. The transmittance τ and reflectance ρ of the semi-infinite slab are defined as

$$\tau = \frac{S_T}{S_I}, \quad \rho = -\frac{S_R}{S_I} = 1 - \tau. \tag{14}$$

where S_I, S_R and S_T are the normal energy fluxes of the respective waves.

If the frequency ω is close to the band edge frequency ω_g in figure 1, then the incident wave will be totally reflected back into space, as illustrated in figure 3. This implies that the fraction of the incident wave energy converted into the slow mode corresponding to the point g in figure 1 vanishes as $\omega \to \omega_g$.

In another case, where the incident wave frequency is close to either of the characteristic values ω_a or ω_b in figure 1, the slab transmittance remains finite, as seen in figure 3. This implies that the incident wave will be partially transmitted into the semi-infinite photonic slab. The problem, though, is that none of the transmitted light will propagate inside the slab in the

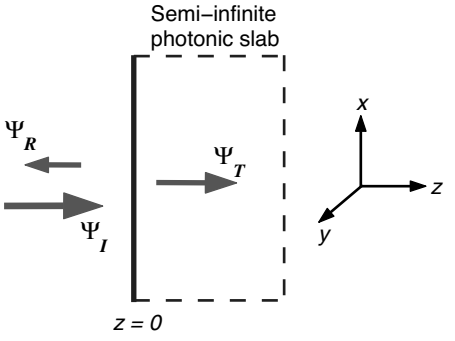

Figure 2. Plane wave normally incident on a lossless semi-infinite photonic slab. The subscripts I, R, and T refer to the incident, reflected and transmitted waves, respectively.

form of the slow mode corresponding to the respective stationary point a or b. For example, at frequency ω_a, all the transmitted light corresponds to a fast propagating mode with positive and large group velocity and the wave number different from that corresponding to the point a in figure 1. A similar situation takes place at $\omega = \omega_b$: the fraction of the transmitted light that is converted into the respective slow mode vanishes as $\omega \to \omega_b$.

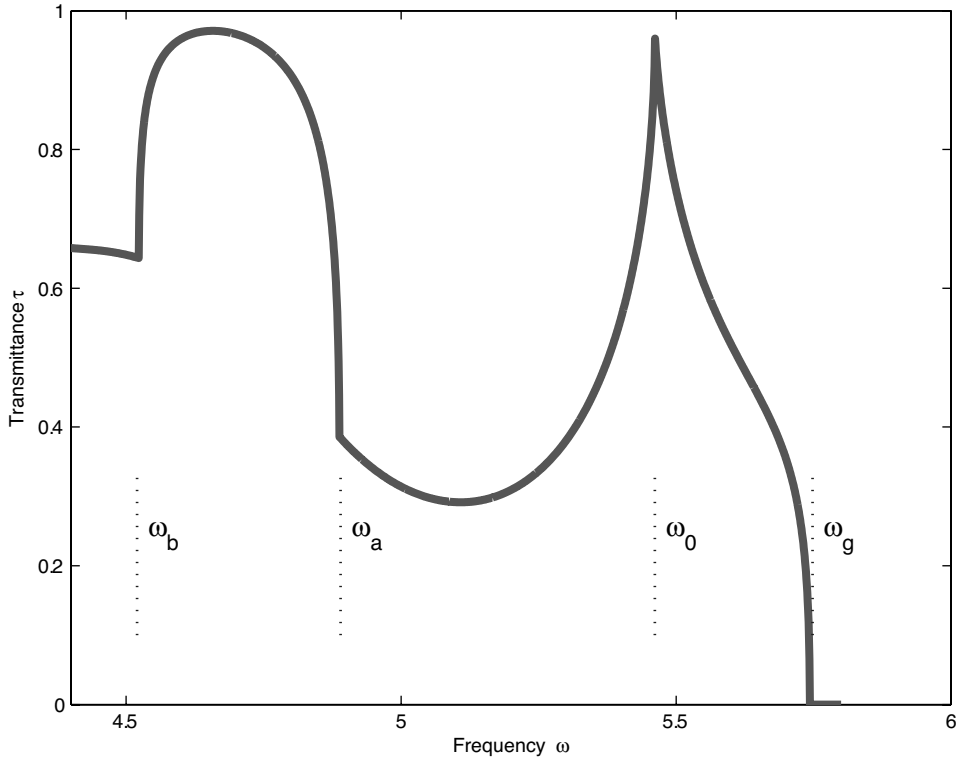

Figure 3. Transmittance τ of the semi-infinite photonic slab as a function of incident light frequency ω for the semi-infinite photonic slab with the dispersion relation presented in figure 1. The characteristic frequencies ω_a, ω_b, ω_0, and ω_g are associated with the respective stationary points in figure 1. Within the photonic band gap at $\omega \geq \omega_g$ the incident light is totally reflected by the slab.

Let us turn now to the stationary inflection point 0 in figure 1, where both the first and the second derivatives of the frequency ω with respect to k vanish, while the third derivative is finite

$$\text{at } \omega = \omega_0 \quad \text{and} \quad k = k_0: \quad \frac{\partial \omega}{\partial k} = 0; \quad \frac{\partial^2 \omega}{\partial k^2} = 0; \quad \frac{\partial^3 \omega}{\partial k^3} > 0. \tag{15}$$

In such a case, a plane wave with $\omega = \omega_0$ incident from the left can be transmitted into the semi-infinite photonic crystal with little reflection, as demonstrated in figure 3. But most remarkably, having entered the photonic slab, the light is *completely* converted into the slow mode with infinitesimal group velocity and drastically enhanced amplitude. Such a behavior is uniquely associated with stationary inflection point (15) of the dispersion relation and constitutes the *frozen mode regime* [29–31]. In the frozen mode regime, the vanishingly small group velocity u in equation (13) is offset by the diverging value of the energy density W

$$\text{as } \omega \to \omega_0: \quad u \sim |\omega - \omega_0|^{2/3} \to 0, \quad W \sim |\omega - \omega_0|^{-2/3} \to \infty, \tag{16}$$

As a result, the energy flux (13) associated with the transmitted frozen mode remains finite and comparable with that of the incident wave even at the frozen mode frequency ω_0 corresponding to the point 0 of the dispersion relation in figure 1. Such a spectacular behavior is uniquely attributed to a stationary inflection point (15) of the electromagnetic dispersion relation. Of course, in reality, the electromagnetic energy density W of the frozen mode will be limited by such factors as absorption, nonlinear effects, imperfection of the periodic dielectric array, deviation of the incident radiation from a perfect plane monochromatic wave, finiteness of the photonic slab dimensions, etc. Still, with all these limitations in place, the frozen mode regime can be very attractive for a variety of practical applications.

In the following sections we present a detailed analysis of the frozen mode regime associated with stationary inflection point (15). In the rest of this section we briefly discuss the effect of photonic crystal boundaries on slow light phenomena.

2.1. *Slow light in a finite photonic slab*

Up to this point we have considered light incident on the surface of a semi-infinite photonic crystal. Since real photonic crystals are always bounded, the question arises whether and how the photonic crystal boundaries affect the conditions of slow mode excitation and propagation.

To start with, let us recall that in an unbounded (infinite) photonic crystal, the speed of light propagation is defined as its group velocity (11), which determines the speed of pulse propagation in the medium. The spatial length l of a pulse inside the unbounded periodic medium is

$$l \sim l_0 \frac{u}{c} \tag{17}$$

where l_0 is the spatial length of the same pulse in vacuum. The quantity l_0 is directly related to the pulse bandwidth $\Delta\omega$

$$\frac{\Delta\omega}{\omega} \sim \frac{\lambda_0}{l_0} = \frac{2\pi}{\omega}\frac{c}{l_0}, \tag{18}$$

where

$$\lambda_0 = \frac{2\pi}{\omega} c$$

is the light wavelength in vacuum.

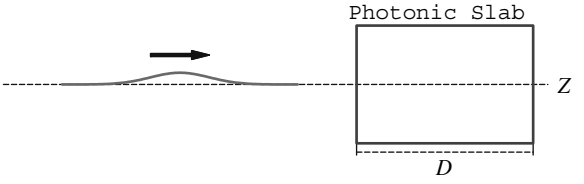

Figure 4. A pulse of length l_0 approaching a photonic slab of thickness D. The arrow shows the direction of pulse propagation. What happens after the pulse hits the slab boundary is shown in figure 5.

If instead of an infinite photonic crystal we have a bounded photonic slab of thickness D, as shown in figure 4 and 5, the simple interpretation of the group velocity u as the speed of pulse propagation can still apply, provided that the pulse length l inside the photonic slab is much smaller than the slab itself

$$l \ll D. \tag{19}$$

In other words, one can introduce the speed of pulse propagation inside the slab only if the entire pulse can fit inside the slab, as in the situation shown in figure 5. In the slow light case, the group velocity u decreases sharply, and so does the pulse length l in (17). Therefore, a slow pulse with a fixed bandwidth $\Delta\omega$ is more likely to fit inside the photonic slab than a fast pulse with the same bandwidth. The slower the pulse is, the better the condition (19) is satisfied. Taking into account the relations (17) and (18), the condition (19) can also be recast as a lower limit on the pulse bandwidth

$$\Delta\omega \gg \frac{2\pi u}{D}, \tag{20}$$

implying that in order to fit inside the slab, the pulse bandwidth should not be too narrow.

If a pulse satisfying the condition (19) or, equivalently, (20) is incident on a finite photonic slab, the slab can be treated as a semi-infinite medium until the pulse actually hits the opposite boundary of the slab. Except for the next subsection, all the results discussed in this paper relate to the case (19), where we can explicitly and literally talk about pulse propagation inside the medium and where the group velocity u in (11) does have the meaning of the speed of pulse propagation.

2.2. *Resonance effects in a finite photonic slab*

A qualitatively different picture emerges if the pulse length l defined in equation (17) is comparable in magnitude or exceeds the slab thickness D. In such a case, the slab is too thin to accommodate the entire pulse and the electromagnetic field Ψ_T inside the slab becomes a superposition of forward and backward propagating waves undergoing multiple reflections

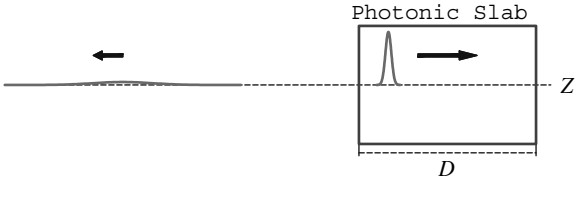

Figure 5. After hitting the slab, the pulse splits into the reflected and transmitted pulses. In a slow light situation, the transmitted pulse gets compressed in space.

from two opposite boundaries of the slab. This situation by no means can be interpreted as an individual pulse propagating through the periodic medium, because at any moment of time the electromagnetic field inside the slab cannot be viewed as a wave packet built around a single propagating mode. The term slow light does not literary apply here and, therefore, this case goes beyond the scope of this paper. Yet, it would be appropriate to discuss briefly what happens if the photonic slab becomes too thin to be treated as semi-infinite.

Assume that the photonic slab is thin enough to satisfy the inequality

$$l \gg D, \tag{21}$$

which is opposite to (19). The condition (21) establishes an upper limit on the incident pulse bandwidth

$$\Delta\omega \ll \frac{2\pi u}{D}. \tag{22}$$

Consider a plane monochromatic wave incident on a finite photonic slab in figure 6. Since a monochromatic wave packet has $l \to \infty$, the relations (21) and (22) are perfectly satisfied. If the photonic slab is lossless, its steady-state transmittance and reflectance are defined by the following expressions

$$\tau = \frac{S_P}{S_I} = \frac{S_T}{S_I}, \quad \rho = -\frac{S_R}{S_I} = 1 - \tau, \tag{23}$$

similar to those in (14) related to the semi-infinite slab. The equations (23) immediately follow from energy conservation considerations.

A typical frequency dependence of finite photonic slab transmittance (23) is shown in figures 7 *a*, *b*, and *c*. For comparison, figure 7 *d* shows the transmittance (14) of a semi-infinite photonic slab having the same periodic structure. The sharp peaks in transmittance in the vicinity of photonic band edge at larger N correspond to Fabry-Perot cavity resonances. At resonance, the electromagnetic field Ψ_T inside the slab is close to a standing wave composed of one forward and one backward propagating Bloch eigenmodes with large and nearly equal amplitudes. The slab boundaries coincide with standing wave nodes, which determines the Bloch wavenumbers of the forward and backward components

$$k_s \approx k_g \pm \frac{\pi}{D}s, \quad s = 1, 2, \ldots \tag{24}$$

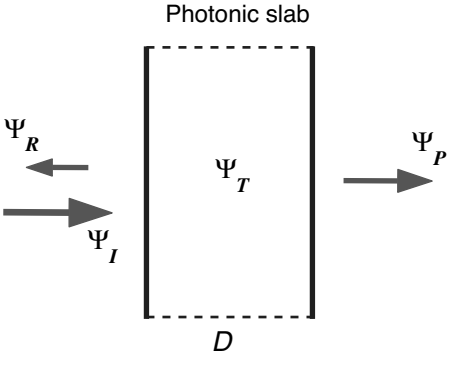

Figure 6. Light incident on a finite photonic slab of the thickness D. The subscripts I, R, and P refer to the incident, reflected, and passed waves, respectively. The transmitted wave Ψ_T inside the slab may have Bloch componets propagating in either direction.

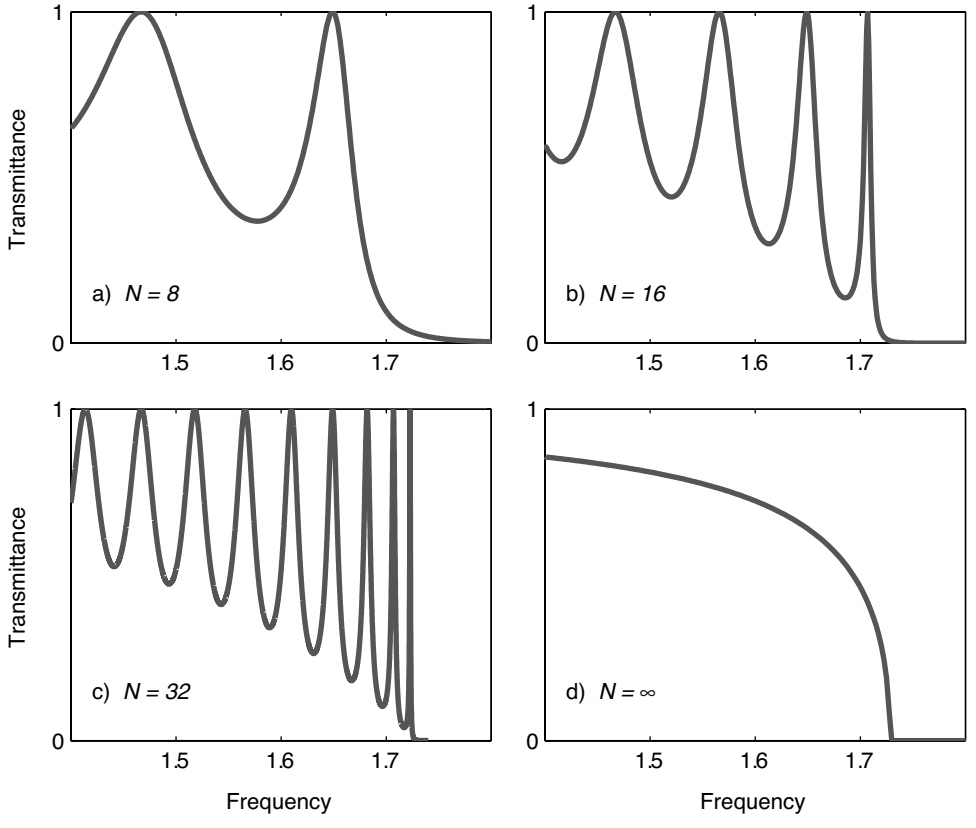

Figure 7. Typical plots of transmittance versus frequency of lossless periodic stacks composed of different number N of unit cells. The frequency range shown includes a photonic band edge. The sharp transmission peaks near the band edge frequency are associated with Fabry-Perot cavity resonance. The case $N = \infty$ corresponds to a semi-infinite photonic slab and is similar to that shown in figure 3.

where k_g corresponds to the photonic band edge. Usually, but not necessarily, k_g equals 0 or π/L. The approximation (24) is valid if $N \gg 1$ and only applies to the resonances close enough to the photonic band edge.

The dispersion function $\omega(k)$ in the vicinity of a photonic band edge can be approximated as follows

$$\omega \approx \omega_g - \frac{\omega_g''}{2}(k - k_g)^2, \quad \text{where} \tag{25}$$

where

$$\omega_g'' = \left(\frac{\partial^2 \omega}{\partial k^2}\right)_{k=k_g}.$$

The propagating mode group velocity u vanishes as $\omega \to \omega_g$

$$u = \frac{\partial \omega}{\partial k} \approx \omega_g''(k_g - k) \approx \pm\sqrt{2\omega_g''}\,(\omega_g - \omega)^{1/2}, \tag{26}$$

where $\pm$ corresponds to the forward and backward propagating waves, respectively. Inserting the resonance values (24) of the Bloch wavenumber into the dispersion relation equation (25)

yields the resonance frequencies ω_s as

$$\omega_s \approx \omega_g - \frac{\omega_g''}{2}\left(\frac{\pi}{D}s\right)^2, \quad s = 1, 2, \ldots \tag{27}$$

where $\omega_g = \omega(k_g)$ is the band edge. The dependence (27) is illustrated in figure 7*c*.

Let us focus on the Fabry-Perot cavity resonance closest to the photonic band edge. The respective frequency is

$$\omega_1 \approx \omega_g - \frac{\omega_g''}{2}\left(\frac{\pi}{D}\right)^2. \tag{28}$$

At frequency ω_1, the group velocities of the forward and backward propagating modes are

$$u_1 \approx \pm\omega_g''\frac{\pi}{D} = \pm\frac{\pi\omega_g''}{LN}, \tag{29}$$

that is inversely proportional to the number N of the unit cells L in the slab. The resonance field amplitude inside the slab is proportional to the slab thickness

$$\Psi_T(z) \approx N\Psi_0 \sin(\pi z D^{-1}) + \Psi_1, \quad 0 \le z \le D, \tag{30}$$

where Ψ_0 and Ψ_1 are periodic functions of z comparable in magnitude with the incident wave Ψ_I. So, the maximum field amplitude is reached in the middle of the slab and is proportional to the slab thickness. The bandwidth Δ_1 of the Fabry-Perot cavity resonance decreases sharply, as the number of unit cells increases

$$\Delta_1 \propto \frac{c}{LN^3} \propto \frac{\omega_1}{N^3}. \tag{31}$$

This is clearly seen in figure 7.

At this point we would like to compare the frozen mode regime introduced in the previous subsection and the Fabry-Perot cavity resonance. Both effects result from coherent interference of light and can be thought of as photons trapped inside the periodic medium. Both effects are accompanied by a huge surge in electromagnetic field amplitude inside the photonic crystal. But that is where their similarity ends. Indeed, in the case of a Fabry-Perot cavity, the entire periodic stack (photonic slab) works as a resonator in which the trapped photons are spread all over the place. For this reason, all the major characteristics of Fabry-Perot cavity resonance are essentially dependent on the slab thickness. If the slab thickness $D = NL$ is too large, then even small absorption or structural irregularity will completely smooth out the resonances. So, on the one hand, the slab should have enough layers to support distinct Fabry-Perot cavity resonances. But on the other hand, the number of layers should not be too large so that the losses and structural irregularities would not wipe out the effect. In addition, the number of layers essentially affects the resonance bandwidth. By contrast, the frozen mode regime is not a resonance in a usual sense of this word. Each trapped photon is now localized within certain small number of unit cells depending on the pulse bandwidth, while the slab size is not essential at all. Even if $N \to \infty$, it does not affect any basic characteristics of the frozen mode regime, such as the bandwidth or the frozen mode amplitude.

2.2.1. Photonic slab as a delay line. In the case (19) of a thin slab, the idea of a distinct pulse slowly propagating through the slab does not apply. On the other hand, one might be interested in the relation between the input and the output pulses, rather than in what is going on inside the photonic slab. This is the case, for example, if the photonic slab is used as a delay line. Let Ψ_I and Ψ_P be the input and output pulses, respectively, as illustrated in figure 6. The shape of the output pulse Ψ_P can be close to that of the input pulse Ψ_I regardless of whether

or not the condition (19) is met. If the shape of the pulse is indeed preserved, one can define the effective speed $\tilde{u}$ of pulse propagation through the slab as

$$\tilde{u} = \frac{D}{\tilde{t}}, \tag{32}$$

where $\tilde{t}$ is the transit time of the pulse passed through the slab. The quantity $\tilde{u}$ is referred to as the group delay. The transit time determines the pulse delay due to the presence of the slab. Of course, in the case (19) of a thick slab, the effective speed (32) coincides with the pulse group velocity u. But now we consider the opposite situation (21). It turns out that under the resonance conditions, the transit time $\tilde{t}$ of a thin photonic slab increases sharply, and the respective group delay $\tilde{u}$ can be as low as $10^{-2}c$, while the pulse passes through the slab with little reflection (see, for example, [26], and references therein). In this sense, the pulse delay can be classified as a slow light effect, although the quantity $\tilde{u}$ does not relate to the speed of any real pulse inside the photonic slab. In the rest of this section we briefly discuss this well known phenomenon.

Let us estimate the group delay associated with Fabry-Perot cavity resonance. According to equation (30), the electromagnetic energy $\mathcal{H}$ stored in the entire slab at the resonance is

$$\mathcal{H} \propto |\Psi_T|^2 D \propto |\Psi_I|^2 L N^3. \tag{33}$$

This leads to the following rough estimate for the transit time $\tilde{t}$ in (32)

$$\tilde{t}_1 \propto \frac{\mathcal{H}}{S_I} \propto c^{-1} L N^3. \tag{34}$$

The respective group delay (32) is

$$\tilde{u}_1 = \frac{D}{\tilde{t}_1} \propto \frac{c}{N^2}. \tag{35}$$

Note that if the number N is large, the value (35) of the group delay is much lower than the group velocity (29) of the propagating Bloch mode at the same frequency ω_1. The drawback, though, is that the bandwidth (31) of the Fabry-Perot cavity resonance shrinks even faster as the number N of unit cells increases. Equations (35) and (31) yield the following relation between the bandwidth Δ_1 and the group delay $\tilde{u}_1$

$$\frac{\Delta_1}{\omega_1} \propto \frac{1}{N} \frac{\tilde{u}_1}{c}. \tag{36}$$

Comparison of the slow light bandwidth (36) with its ideal value (4) shows that the Fabry-Perot cavity resonance in a finite periodic photonic slab has a fundamental bandwidth disadvantage, if used as a delay line.

Note that real optical delay lines are commonly based on periodic arrays of weakly coupled resonators, such as Fabry-Perot cavities, rather than on individual Fabry-Perot cavities (see, for example, [18–24] and references therein).

In conclusion, let us reiterate that in the cases other than (19), there is no distinct pulse propagating inside the periodic medium and, therefore, the notion of slow light does not literally apply there. Further in this paper we assume that the condition (19) is satisfied, warranting the approximation of a semi-infinite photonic crystal. This allows us to investigate the slow light phenomenon in its pure form, when it is directly related to the speed of electromagnetic pulse propagation through the medium. In this case, the frozen mode regime associated with a stationary inflection point (15) provides a unique possibility of converting a significant fraction of the incident light into a coherent mode with extremely low group velocity and drastically enhanced amplitude.

3. Slow light in periodic layered media

From now on we restrict ourselves to stratified media, which are periodic stacks of dielectric layers. Such systems are also referred to as photonic crystals with one-dimensional periodicity. A major reason for such a choice is that the electrodynamics of stratified media can be done within the framework of a rigorous analytical approach. This is particularly important since the frozen mode regime involves a unique and spectacular behavior, so it would be desirable to be sure that such a behavior is not a numerical artifact. As soon as we assume that the semi-infinite photonic slab in figure 2 is a periodic array of plane-parallel uniform layers, we can give a much more detailed and meaningful description of the frozen mode regime.

We start with some general remarks about electromagnetic eigenmodes in periodic layered media. Then we proceed to a semi-qualitative description of the situation taking place at different stationary points of the dispersion relations. A consistent and complete analysis based on the Maxwell equations will be presented in Sections 5 through 12.

3.1. *Propagating and evanescent eigenmodes in periodic stacks of anisotropic layers*

Let $\Psi_I(z)$, $\Psi_R(z)$ and $\Psi_T(z)$ denote the incident, reflected and transmitted waves, respectively, as shown in figure 2. In the frequency domain, each of these waves can be explicitly represented by a column vector

$$\Psi(z) = \begin{bmatrix} E_x(z) \\ E_y(z) \\ H_x(z) \\ H_y(z) \end{bmatrix}, \tag{37}$$

where $E_x(z)$, $E_y(z)$, $H_x(z)$, $H_y(z)$ are the transverse components of electromagnetic field. The exact definition of $\Psi(z)$ is given in (80) and (81). The incident and reflected beams are plane monochromatic waves propagating in vacuum, while the transmitted electromagnetic field $\Psi_T(z)$ inside the periodic layered medium is not a single Bloch eigenmode. At the slab boundary at $z = 0$, the three waves satisfy the standard boundary condition

$$\Psi_I(0) + \Psi_R(0) = \Psi_T(0), \tag{38}$$

implying continuity of the tangential field components (37). Note that periodic stacks capable of supporting the frozen mode regime must include anisotropic layers with misaligned and/or oblique orientation of the principal axes. As a consequence, the reflected and transmitted waves in figure 2 will have an elliptic polarization even if the incident wave is linearly polarized.

In the setting of figure 2 where the semi-infinite periodic layered array occupies the half-space $z \geq 0$, the transmitted wave $\Psi_T(z)$ is a superposition of two Bloch components (Bloch eigenmodes) with different polarizations and different values of the Bloch wave number k. There are three possibilities.

(i) Both Bloch components of the transmitted wave Ψ_T are propagating modes

$$\Psi_T(z) = \Psi_{pr1}(z) + \Psi_{pr2}(z), \quad z \geq 0, \tag{39}$$

which means that the two respective values of k are real. For example, at $\omega_b < \omega < \omega_a$ in figure 1, the transmitted wave Ψ_T is composed of two Bloch eigenmodes with two different real wave numbers k_1 and k_2 and two different group velocities $u_1 > 0$ and $u_2 > 0$. This constitutes the phenomenon of double refraction.

(ii) Both Bloch components of Ψ_T are evanescent

$$\Psi_T(z) = \Psi_{ev1}(z) + \Psi_{ev2}(z), \quad z \geq 0, \tag{40}$$

which implies that the two respective values of k are complex with $\operatorname{Im} k > 0$. For example, this is the case when the frequency ω falls into the photonic band gap at $\omega > \omega_g$ in figure 1. The fact that $\operatorname{Im} k > 0$ implies that the wave amplitude decays as the distance z from the semi-infinite slab surface increases. In the case (40), the incident wave is totally reflected back to space by the semi-infinite slab, as seen in figure 3.

(iii) Of particular interest is the case where one of the Bloch components of the transmitted wave Ψ_T is a propagating mode with $u > 0$, while the other is an evanescent mode with $\operatorname{Im} k > 0$

$$\Psi_T(z) = \Psi_{pr}(z) + \Psi_{ev}(z), \quad z \geq 0. \tag{41}$$

For example, this is the case at the frequency range

$$\omega_a < \omega < \omega_g \tag{42}$$

in figure 1. As the distance z from the slab/vacuum interface increases, the evanescent contribution Ψ_{ev} in (41) decays as $\exp(-z \operatorname{Im} k)$, and the resulting transmitted wave Ψ_T turns into a single propagating Bloch mode Ψ_{pr}.

Propagating modes with $u < 0$, as well as evanescent modes with $\operatorname{Im} k < 0$, never contribute to the transmitted wave Ψ_T inside the semi-infinite stack in figure 2. This fact is based on the following two assumptions:

- The transmitted wave Ψ_T and the reflected wave Ψ_R are originated from the plane monochromatic wave Ψ_I incident on the semi-infinite photonic slab from the left, as shown in figure 2.
- The layered array in figure 2 occupies the entire half-space and is perfectly periodic at $z > 0$.

If either of the above conditions is violated, the field Ψ_T inside the periodic stack can be a superposition of four Bloch eigenmodes with either sign of the group velocity u of propagating contributions, or either sign of $\operatorname{Im} k$ of evanescent contributions. For example, this would be the case if the periodic layered array in figure 2 had some kind of structural defects or a finite thickness like that presented in figure 6.

The propagating modes with $u > 0$ and evanescent modes with $\operatorname{Im} k > 0$ are referred to as the *forward* waves. Only forward modes contribute to the transmitted wave $\Psi_T(z)$ in the case of a periodic semi-infinite stack. The propagating modes with $u < 0$ and evanescent modes with $\operatorname{Im} k < 0$ are referred to as *backward* waves. Since the backward Bloch waves are not excited in the setting of figure 2, they play no role in further consideration.

In all three cases (39–40), the contribution of a particular Bloch eigenmode to the transmitted wave Ψ_T depends on the polarization Ψ_I of the incident wave. One can always choose the incident wave polarization so that only one Bloch component is excited. In such a case, Ψ_T is a single Bloch eigenmode.

Only propagating modes contribute to the normal component S_T of the energy flux inside a periodic semi-infinite slab. Evanescent modes do not participate in energy transfer in such a case. In the important particular case of a single propagating mode ($\Psi_T = \Psi_{pr}$), we have from (13) and (14)

$$S_T = Wu = \tau S_I, \tag{43}$$

where $W \sim |\Psi_{pr}|^2$ is the energy density associated with the transmitted propagating mode.

The assumption that the transmitted wave $\Psi_T(z)$ is a superposition of propagating and/or evanescent Bloch eigenmodes may not be valid at stationary points (12) of electromagnetic

dispersion function $\omega(k)$, because each stationary point is a degeneracy point of the frequency spectrum. For example, if the frequency ω exactly coincides with stationary inflection point defined by (15), the transmitted wave $\Psi_T(z)$ is dominated by a (non-Bloch) Floquet eigenmode linearly growing with z, which constitutes the frozen mode regime [29, 30]. At all other frequencies, the transmitted wave is a superposition of two forward Bloch modes, each of which can be either propagating or evanescent. A detailed analysis of this and related phenomena is presented further in this paper.

Knowing the eigenmode composition of the transmitted wave $\Psi_T(z)$ we can give a semi-qualitative description of what happens when the frequency ω of the incident wave approaches one of the stationary points (12) in figure 1. A complete analysis based on the Maxwell equations will be presented later in the paper.

3.2. *Photonic band edge*

We start with the simplest case of a photonic band edge. Just below the band edge frequency ω_g in figure 1, the transmitted field $\Psi_T(z)$ is a superposition (41) of one propagating and one evanescent Bloch component. Due to the boundary condition (38) at the slab/vacuum interface, the amplitude of the transmitted wave at $z = 0$ is comparable with that of the incident wave. In the case of a generic polarization of the incident light, the amplitudes of the propagating and evanescent Bloch components at $z = 0$ are also comparable to each other and to the amplitude of the incident light

$$|\Psi_{pr}(0)| \sim |\Psi_{ev}(0)| \sim |\Psi_I|, \quad \text{at } \omega \leq \omega_g. \tag{44}$$

As the distance z from the slab surface increases, the evanescent component $\Psi_{ev}(z)$ decays rapidly, while the amplitude of the propagating component remains constant. Eventually, at a certain distance from the slab surface, the transmitted wave $\Psi_T(z)$ becomes very close to its propagating Bloch component

$$\Psi_T(z) \approx \Psi_{pr}(z), \text{ at } z \gg L, \quad \omega \leq \omega_g. \tag{45}$$

The evanescent component Ψ_{ev} of the transmitted wave does not display any singularity in the vicinity of ω_g. By contrast, the propagating mode Ψ_{pr} develops a singularity as $\omega \to \omega_g - 0$, which is associated with vanishing group velocity as in (12). At $\omega > \omega_g$, the propagating mode turns into another evanescent mode in (40).

The dispersion relation in the vicinity of the band edge g in figure 1 can be approximated as

$$\omega_g - \omega \approx \frac{\omega_g''}{2}(k - k_g)^2, \quad \omega \lessapprox \omega_g.$$

This yields the following frequency dependence of the propagating mode group velocity u below the photonic band edge

$$u = \frac{\partial \omega}{\partial k} \approx \omega_g''(k_g - k) \approx \sqrt{2\omega_g''}(\omega_g - \omega)^{1/2}, \quad \omega \lessapprox \omega_g. \tag{46}$$

The energy flux (43) associated with the slow propagating mode is

$$S_T \approx \begin{cases} W\sqrt{2\omega_g''}(\omega_g - \omega)^{1/2}, & \text{at } \omega \lessapprox \omega_g \\ 0, & \text{at } \omega \geq \omega_g \end{cases}. \tag{47}$$

where

$$W \sim |\Psi_{pr}|^2 \sim |\Psi_I|^2. \tag{48}$$

The latter estimation follows from (44) and applies to the case of a generic polarization of the incident wave. The semi-infinite slab transmittance (14) in the vicinity of ω_g is

$$\tau = \frac{S_T}{S_I} \approx \begin{cases} \frac{W}{S_I}\sqrt{2\omega_g''}(\omega_g - \omega)^{1/2}, & \text{at } \omega \lessapprox \omega_g \\ 0, & \text{at } \omega \geq \omega_g \end{cases}, \tag{49}$$

where according to (48)

$$\frac{W}{S_I} \sim \frac{|\Psi_I|^2}{S_I} \sim c.$$

The relation (49) is illustrated by the numerical example in figure 3.

Equation (49) expresses the well-known fact that in the vicinity of an electromagnetic band edge, the semi-infinite photonic crystal becomes totally reflective, as illustrated in figure 3. This implies that as $\omega \to \omega_g$, only an infinitesimal fraction of the incident light energy is converted into the slow mode.

3.3. *Other extreme points of spectral branches*

For specificity, let us consider the stationary point a of the dispersion relation in figure 1, which qualitatively is not different from the point b. At frequencies right below ω_a, the transmitted wave Ψ_T is a superposition (39) of two propagating eigenmodes, one of which is the slow mode and the other is a regular forward propagating mode. The slow mode develops a singularity at $\omega = \omega_a$ similar to that of the respective slow mode in the vicinity of the band edge frequency ω_g, while the other propagating mode (the fast mode) remains regular in the vicinity of ω_a and does not produce any anomaly. The two forward modes contribute additively to the energy flux S_T, but the contribution of the fast mode remains regular in the vicinity of ω_a, while the contribution of the slow mode shows the same singular behavior as that described by equations (47) and (49). Figure 3 provides a graphic illustration of such a behavior.

The important point is that similar to the situation in the vicinity of a photonic band edge, at $\omega = \omega_a$ and $\omega = \omega_b$ the contribution of the respective slow mode to the transmitted wave Ψ_T vanishes. In other words, in terms of slow mode excitation, the stationary points a and b in figure 1 are no different from the band edge g.

3.4. *Stationary inflection point: the frozen mode regime*

A sharply different situation develops in the vicinity of a stationary inflection point (15) of the dispersion relation (point 0 in figure 1). According to (15), the dispersion relation in the vicinity of ω_0 can be approximated as follows

$$\omega - \omega_0 \approx \frac{\omega_0'''}{6}(k - k_0)^3, \tag{50}$$

where

$$\omega_0''' = \left(\frac{\partial^3 \omega}{\partial k^3}\right)_{k=k_0}.$$

The propagating mode group velocity u vanishes as ω approaches ω_0

$$u = \frac{\partial \omega}{\partial k} \approx \frac{1}{2}\omega_0'''(k - k_0)^2 \approx \frac{6^{2/3}}{2}(\omega_0''')^{1/3}(\omega - \omega_0)^{2/3}. \tag{51}$$

But remarkably, the electromagnetic energy density W associated with the transmitted frozen mode diverges as $\omega \to \omega_0$

$$W \approx \frac{2\tau S_I}{6^{2/3}}(\omega_0''')^{-1/3}(\omega - \omega_0)^{-2/3}, \tag{52}$$

where S_I is the fixed energy flux of the incident wave. The slab transmittance τ remains finite even at $\omega = \omega_0$, as illustrated in figure 3. As a result, the energy flux (43) associated with the transmitted frozen mode also remains finite and can even be close to unity in the vicinity of ω_0. The latter implies that the incident light is completely converted to the frozen mode with infinitesimal group velocity (51) and diverging energy density (52).

Let us consider the structure of the frozen mode. At $\omega \approx \omega_0$, the transmitted wave Ψ_T is a superposition (41) of one propagating and one evanescent Bloch component. In contrast to the case of a photonic band edge, in the vicinity of ω_0 both Bloch components of Ψ_T develop strong singularity. Specifically, as the frequency ω approaches ω_0, both contributions grow sharply, while remaining nearly equal and opposite in sign at the slab boundary

$$\Psi_{pr}(0) \approx -\Psi_{ev}(0) \propto |\omega - \omega_0|^{-1/3}, \quad \text{as } \omega \to \omega_0. \tag{53}$$

Due to the destructive interference (53), the resulting field

$$\Psi_T(0) = \Psi_{pr}(0) + \Psi_{ev}(0)$$

at the slab boundary is small enough to satisfy the boundary condition (38), as illustrated in figure 8. As the distance z from the slab boundary increases, the evanescent component Ψ_{ev} decays exponentially

$$\Psi_{ev}(z) \approx \Psi_{ev}(0)\exp(-z\,\mathrm{Im}\,k)$$

while the amplitude of the propagating component Ψ_{pr} remains constant and very large. As a consequence, the amplitude of the resulting transmitted wave $\Psi_T(z)$ sharply increases with the distance z from the slab boundary and, eventually, reaches its large saturation value corresponding to the propagating component Ψ_{pr}, as illustrated in figure 9.

If the frequency ω of incident light is exactly equal to the frozen mode frequency ω_0, the transmitted wave $\Psi_T(z)$ does not reduce to the sum (41) of propagating and evanescent contributions [29, 30]. Instead, it corresponds to a non-Bloch Floquet eigenmode diverging

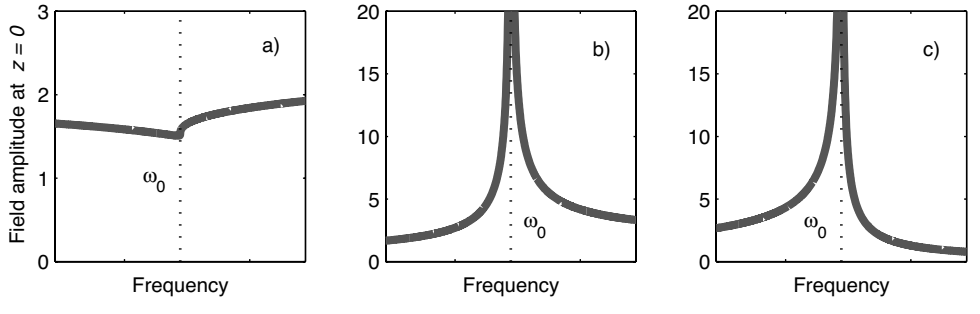

Figure 8. Destructive interference of the propagating and evanescent contributions to the resulting field Ψ_T at the slab/vacuum interface under the frozen mode regime: a) resulting field amplitude $|\Psi_T(0)|^2$, b) amplitude $|\Psi_{pr}(0)|^2$ of the propagating component, c) amplitude $|\Psi_{ev}(0)|^2$ of the evanescent component.

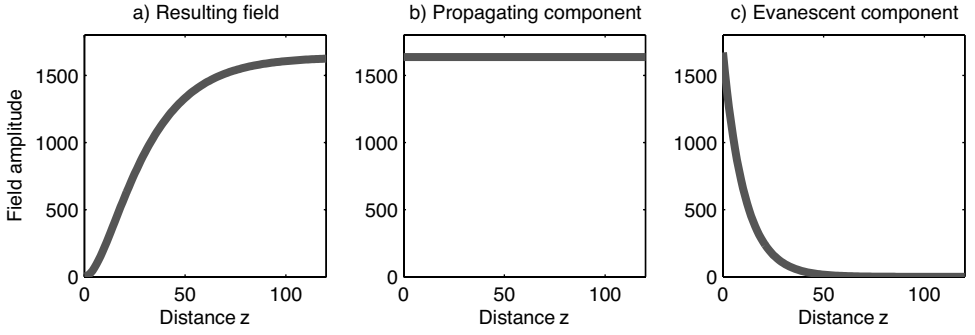

Figure 9. The transmitted electromagnetic field (41) and its propagating and evanescent components inside semi-infinite slab in close proximity of the frozen mode regime: (a) the amplitude $|\Psi_T(z)|^2$ of the resulting field, (b) the amplitude $|\Psi_{pr}(z)|^2$ of the propagating contribution, (c) the amplitude $|\Psi_{ev}(z)|^2$ of the evanescent contribution. Due to destructive interference of the propagating and evanescent components, the resulting field amplitude at $z = 0$ is small enough to satisfy the boundary conditions (38). The amplitude $|\Psi_I|^2$ of the incident wave is unity. The distance z from the slab boundary is expressed in units of L.

linearly with z

$$\Psi_T(z) - \Psi_T(0) \propto z\sqrt{\frac{\tau S_I}{\omega_0'''}}\Psi_0, \quad \text{at}\,\omega = \omega_0.$$

Evidently, the frozen mode regime associated with stationary inflection point (15) provides an ideal and unique situation in terms of slow mode excitation. Indeed, in this case virtually all the incident light energy can be converted into the slow mode with greatly enhanced amplitude.

A consistent mathematical analysis of the frozen mode regime is rather sophisticated and will take a great deal of our attention further in this paper. Specifically, the fundamental fact that at $\omega = \omega_0$, the energy flux of the frozen mode remains finite in spite of vanishing group velocity, is rigorously proven in Section 9 (see equations (421) through (449) and related explanations).

3.5. *Degenerate band edge*

While the situation with the regular band edge appears quite obvious and not particularly interesting from the perspective of slow light, the so-called degenerate band edge proves to be quite different [34]. An example of an electromagnetic dispersion relation with degenerate band edge is shown in figure 10.

In the vicinity of the degenerate band edge d, the dispersion relation can be approximated as

$$\omega_d - \omega \approx \frac{\omega_d''''}{24}(k - k_d)^4, \quad \text{where}\ \omega_d'''' = \left(\frac{\partial^4\omega}{\partial k^4}\right)_{k=k_d}. \tag{54}$$

Similarly to the regular band edge, below the degenerate band edge frequency ω_d, the transmitted field Ψ_T is a superposition (41) of one propagating and one evanescent components, while above ω_d, the transmitted wave is a combination (40) of two evanescent components. The critical difference though is that now both the Bloch components display strong singularity. Specifically, as the frequency ω approaches ω_d, both Bloch contributions grow sharply, while remaining nearly equal and opposite in sign at the slab boundary

$$\Psi_{pr}(0) \approx -\Psi_{ev}(0) \propto |\omega_d - \omega|^{-1/4}, \quad \text{as}\,\omega \to \omega_d - 0. \tag{55}$$

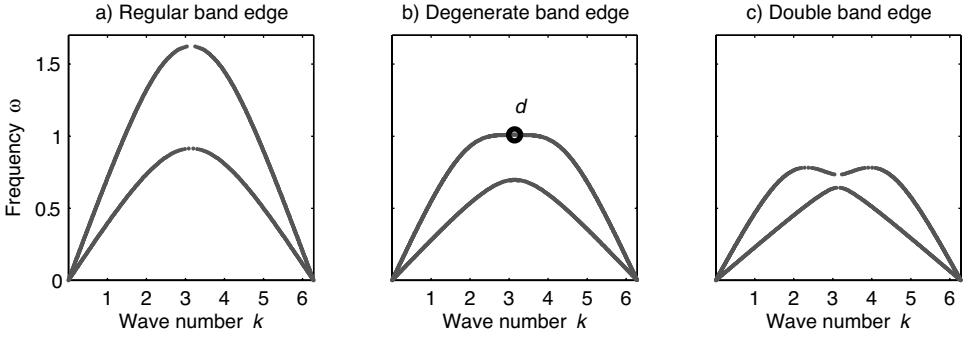

Figure 10. Dispersion relations $\omega(k)$ of three periodic stacks with slightly different layer thicknesses. The plot in the middle displays a degenerate band edge (54).

The destructive interference (55) ensures that the boundary condition (38) is satisfied, while both Bloch contributions to $\Psi_T(z)$ diverge. As the distance z from the slab boundary increases, the evanescent component $\Psi_{ev}(z)$ dies out, while the propagating component $\Psi_{pr}(z)$ remains huge. Eventually, at $z \gg L$, the resulting transmitted wave $\Psi_T(z)$ coincides with the propagating Bloch eigenmode $\Psi_{pr}(z)$. If the frequency ω of incident light is exactly equal to ω_d, the transmitted wave $\Psi_T(z)$ does not reduce to the sum (41) of propagating and evanescent contributions. Instead, it corresponds to a non-Bloch Floquet eigenmode diverging linearly with z

$$\Psi_T(z) - \Psi_T(0) \propto z\Psi_d, \quad \text{at } \omega = \omega_d.$$

The above behavior appears to be very similar to that of the frozen mode regime described in the previous subsection. In both cases, figures 8 and 9 provide a good graphical illustration of the electromagnetic field distribution inside the slab in the vicinity of the relevant stationary point. Yet, there is a crucial difference between the two cases. In spite of its huge diverging amplitude (55), the transmitted wave Ψ_T does not provide any energy flux in the immediate proximity of a degenerate band edge. Indeed, according to (55), as ω approaches ω_d, the energy density W of the transmitted wave diverges as

$$W \propto |\Psi_{pr}|^2 \propto |\omega_d - \omega|^{-1/2}, \quad \text{at } \omega \lessapprox \omega_d.$$

But, from equation (54) one can derive that the respective slow mode group velocity vanishes even faster

$$u \approx \frac{\omega_d''''}{6}(k - k_d)^3 \approx \frac{24^{3/4}}{6}(\omega_d'''')^{1/4}|\omega_d - \omega|^{3/4}, \quad \text{at } \omega \lessapprox \omega_d.$$

As the result, the energy flux of the transmitted wave vanishes, as one approaches the degenerate band edge

$$S_T = Wu \propto \begin{cases} (\omega_d - \omega)^{1/4}, & \text{at } \omega \lessapprox \omega_d \\ 0, & \text{at } \omega \geq \omega_d \end{cases},$$

and so does the slab transmittance τ

$$\tau \propto \begin{cases} (\omega_d - \omega)^{1/4}, & \text{at } \omega \lessapprox \omega_d \\ 0, & \text{at } \omega \geq \omega_d \end{cases}.$$

By contrast, in the case of the frozen mode regime the slab transmittance remains finite and a significant fraction of the incident light energy goes to the slow mode.

The situation at a degenerate band edge can be viewed as intermediate between the frozen mode regime and the vicinity of a regular band edge [34]. Indeed, on the one hand, the incident wave at $\omega = \omega_d$ is totally reflected back to space, as would be the case at a regular band edge. On the other hand, the transmitted field amplitude inside the slab becomes huge as $\omega \to \omega_d$, which is similar to what occurs in the frozen mode regime. The large amplitude of the transmitted wave at $\omega \approx \omega_d$ can be very attractive for a variety of practical applications, although such a behavior cannot be qualified as a slow light case. Detailed analysis of some peculiar electromagnetic properties associated with degenerate frequency band edge (54) can be found in [33, 34].

4. Physical conditions for the frozen mode regime in layered media

The frozen mode regime is associated with a stationary inflection point (15) of the electromagnetic dispersion relation. Leaving the proof of this statement to the following sections, here we establish the conditions under which the dispersion relation of a periodic layered array can develop the singularity (15). We will see that only special layered structures incorporating anisotropic layers can display this property. In the following sections, based on the Maxwell equations, we will show that indeed the stationary inflection point (15) is uniquely associated with the frozen mode regime.

4.1. *Axial dispersion relation: basic definitions*

We start with the generalization of the frozen mode concept to the case of oblique light incidence.

Consider a monochromatic plane wave obliquely incident on a periodic semi-infinite stack, as shown in figure 2. Let Ψ_I, Ψ_R and Ψ_T denote the incident, reflected and transmitted waves, respectively. Due to the boundary conditions (38), all three waves Ψ_I, Ψ_R and Ψ_T must be assigned the same pair of tangential components k_x, k_y of the respective wave vector [2]

$$(\vec{k}_I)_x = (\vec{k}_R)_x = (\vec{k}_T)_x, \quad (\vec{k}_I)_y = (\vec{k}_R)_y = (\vec{k}_T)_y, \tag{56}$$

while their axial (normal) components k_z can be different. Hereinafter, the normal component of the transmitted Bloch waves propagating inside the periodic layered medium will be referred to as the *wave number* and denoted by the symbol k, rather than k_z, so that inside the periodic stack (at $z > 0$)

$$\vec{k} = (k_x, k_y, k). \tag{57}$$

Unlike k_x and k_y, the z component k of the Bloch wave vector (57) is defined up to a multiple of $2\pi/L$

$$k \equiv k + 2\pi N/L, \tag{58}$$

where L is the period of the layered structure and N is an integer. For given k_x, k_y and ω, the value k is found by solving the time-harmonic Maxwell equations (79) in the periodic medium, as will be done in the following sections. The result can be represented as the *axial dispersion relation*, which gives the relation between ω and k at fixed k_x, k_y

$$\omega = \omega(k), \qquad \text{at fixed } k_x, k_y. \tag{59}$$

It can be more convenient to define the axial dispersion relation as the relation between ω and k at fixed direction $\vec{n}$ of incident light propagation

$$\omega = \omega(k), \qquad \text{at fixed}\, n_x, n_y, \tag{60}$$

where the unit vector $\vec{n}$ can be expressed in terms of the tangential components (56) of the wave vector

$$n_x = k_x c/\omega, \quad n_y = k_y c/\omega, \quad n_z = \sqrt{1 - (n_x^2 + n_y^2)}. \tag{61}$$

4.1.1. Axial stationary inflection point and the frozen mode regime. Suppose that at $\vec{k} = \vec{k}_0$ and $\omega = \omega_0 = \omega(\vec{k}_0)$, one of the axial spectral branches (59) develops a stationary inflection point for given (k_x, k_y), namely

$$\text{at}\, \omega = \omega_0 \ \text{ and } \ \vec{k} = \vec{k}_0\text{:} \ \left(\frac{\partial\omega}{\partial k}\right)_{k_x,k_y} = 0, \quad \left(\frac{\partial^2\omega}{\partial k^2}\right)_{k_x,k_y} = 0, \quad \left(\frac{\partial^3\omega}{\partial k^3}\right)_{k_x,k_y} \neq 0, \tag{62}$$

The value

$$u \equiv u_z = \left(\frac{\partial\omega}{\partial k}\right)_{k_x,k_y} \tag{63}$$

in equation (62) is the axial component of the group velocity, which vanishes at $\vec{k} = \vec{k}_0$. Observe that

$$u_x = \left(\frac{\partial\omega}{\partial k_x}\right)_{k,k_y} \ \text{ and } \ u_y = \left(\frac{\partial\omega}{\partial k_y}\right)_{k,k_x}, \tag{64}$$

representing the tangential components of the group velocity, may not be zero at $\vec{k} = \vec{k}_0$. The spectral singularity (62) is called the *axial stationary inflection point*.

One can also use another definition of axial stationary inflection point (62), which is based on the axial dispersion relation (60) rather than (59), namely

$$\text{at}\, \omega = \omega_0 \text{ and } \vec{n} = \vec{n}_0 : \left(\frac{\partial\omega}{\partial k}\right)_{n_x,n_y} = 0, \quad \left(\frac{\partial^2\omega}{\partial k^2}\right)_{n_x,\ \ n_y} = 0, \quad \left(\frac{\partial^3\omega}{\partial k^3}\right)_{n_x,n_y} \neq 0. \tag{65}$$

The partial derivatives in (65) are taken at constant (n_x, n_y), rather than at constant (k_x, k_y). Both definitions (62) and (65) are equivalent to one other. In the particular case of normal incidence in which $\vec{n} \parallel \vec{k} \parallel z$, the axial stationary inflection point (62) or, equivalently, (65) turns into a regular stationary inflection point (15).

The *axial frozen mode regime* associated with the singularity (62) is very similar to its particular case, the regular frozen mode regime, related to the regular stationary inflection point (15). Specifically, in the axial frozen mode regime, obliquely incident light can enter the semi-infinite photonic crystal with little reflection, where it is completely converted into a coherent mode with infinitesimal normal component (63) of the group velocity and drastically enhanced amplitude. The energy density of the axial frozen mode displays the same resonance-like behavior (52). The only difference between the axial and the regular frozen mode regime is that in the former case, the tangential component (64) of the group velocity remains finite at $\omega = \omega_0$. The specificity of the axial frozen mode regime as compared to the regular one is discussed in [29]. Further in this paper we will focus exclusively on the common features of these two cases. Either of them will be referred to simply as the frozen mode regime.

4.2. *Spectral asymmetry in periodic stacks*

The (axial) stationary inflection point is indeed associated with the frozen mode regime. But not every periodic layered media can display such a spectral singularity. It turns out that a necessary condition for the existence of an axial stationary inflection point and, therefore, a necessary condition for the frozen mode regime is the following property of the electromagnetic dispersion relation of the periodic stack

$$\omega(k_x, k_y, k) \neq \omega(k_x, k_y, -k) \text{ or, equivalently, } \omega(n_x, n_y, k) \neq \omega(n_x, n_y, -k). \quad (66)$$

The property (66) is referred to as *axial spectral asymmetry*. Further in this paper, we will use the simplified notation (59) for the axial dispersion relation. In this notation, the requirement (66) of axial spectral asymmetry takes the following form

$$\omega(k) \neq \omega(-k), \quad (67)$$

where k is the z component (58) of the Bloch wave vector $\vec{k}$. A robust frozen mode regime only occurs if the degree of spectral asymmetry (67) is significant. For brevity, hereinafter, the quantity k will be referred to as the Bloch wave number, although in the case of oblique propagation, k is just the normal component of the Bloch wave vector $\vec{k}$.

In the particular case of normal wave propagation, in which $\vec{n} \parallel \vec{k} \parallel z$, the requirement (66) of axial spectral asymmetry reduces to

$$\omega(\vec{k}) \neq \omega(-\vec{k}), \quad \vec{k} \parallel z. \quad (68)$$

This kind of asymmetric dispersion relation can occur only in periodic structures with some of the constitutive components being magnetic and displaying nonreciprocal Faraday rotation [40, 29]. Significant spectral asymmetry requires strong Faraday rotation. The simplest periodic array supporting the spectral asymmetry (68) is shown in figure 11.

At microwave frequencies, there exist a number of magnetic materials displaying low losses and strong Faraday rotation. But, at infrared and optical frequencies, the magnetic materials with sufficiently strong Faraday rotation are usually too lossy for our purposes. Therefore, if we are interested in optical frequencies, we have to rely on non-magnetic stacks, in which the regular spectral asymmetry (68) is impossible. By contrast, the axial spectral asymmetry

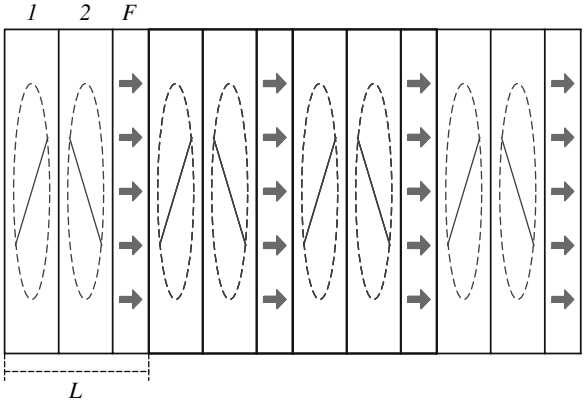

Figure 11. The simplest periodic stack supporting asymmetric dispersion relation (68). A unit cell L of this stack comprises three layers: two anisotropic layers 1 and 2 with misaligned in-plane anisotropy (the A-layers), and one magnetic layer F with magnetization shown by the arrows.

(66) or (67) does not require magnetic layers and can occur even in perfectly reciprocal non-magnetic stacks.

The physical conditions under which the electromagnetic dispersion relation of a non-magnetic layered structure can develop the (axial) spectral asymmetry (67) and, thereby, support the (axial) frozen mode regime can be grouped in two categories. The first one comprises several symmetry restrictions. The second category includes some basic qualitative recommendations which would ensure the robustness of the frozen mode regime, provided that the symmetry conditions for the regime are met. In what follows we briefly describe those conditions and then show how they apply to periodic stacks incorporating some real dielectric materials.

There are two fundamental necessary conditions for the frozen mode regime in a non-magnetic (reciprocal) periodic layered structure. The first one is that the Bloch dispersion function $\omega(\vec{k})$ in the periodic layered medium must display the axial spectral asymmetry (67). This condition is necessary for the existence of the axial stationary inflection point (62) in the electromagnetic dispersion relation of an arbitrary periodic layered medium. The second necessary condition is that for the given direction $\vec{k}$ of wave propagation, the Bloch eigenmodes $\Psi_{\vec{k}}$ with different polarizations must have the same symmetry. In the case of oblique propagation in periodic layered media, the latter condition implies that for the given $\vec{k}$, the Bloch eigenmodes are neither TE nor TM:

$$\Psi_{\vec{k}} \text{ is neither TE nor TM.} \tag{69}$$

The condition (67) imposes certain restrictions on (i) the point symmetry group G of the periodic layered array and (ii) on the direction $\vec{k}$ of the transmitted wave propagation inside the layered medium, while the condition (69) may impose an additional restriction on the direction of $\vec{k}$.

The restriction on the symmetry of the periodic stack stemming from the requirement (67) of the axial spectral asymmetry is

$$m_z \notin G \text{ and } 2_z \notin G. \tag{70}$$

where m_z is the mirror plane parallel to the layers, 2_z is the 2-fold rotation about the z axis. An immediate consequence of the criterion (70) is that at least one of the alternating layers of the periodic stack must be an anisotropic dielectric with

$$\varepsilon_{xz} \neq 0 \quad \text{and/or} \quad \varepsilon_{yz} \neq 0 \tag{71}$$

where the z direction is normal to the layers. Otherwise, the operation 2_z will be present in the symmetry group G of the periodic stack.

The simplest and the most practical example of a non-magnetic periodic stack satisfying the criterion (70) is shown in figure 12. It is made up of anisotropic A layers alternating with isotropic B layers. The respective dielectric permittivity tensors are

$$\hat{\varepsilon}_A = \begin{bmatrix} \varepsilon_{xx} & 0 & \varepsilon_{xz} \\ 0 & \varepsilon_{yy} & 0 \\ \varepsilon_{xz} & 0 & \varepsilon_{zz} \end{bmatrix}, \quad \hat{\varepsilon}_B = \begin{bmatrix} \varepsilon_B & 0 & 0 \\ 0 & \varepsilon_B & 0 \\ 0 & 0 & \varepsilon_B \end{bmatrix}. \tag{72}$$

For simplicity, we assume

$$\hat{\mu}_A = \hat{\mu}_B = \hat{I}. \tag{73}$$

The stack in figure 12 has the monoclinic symmetry

$$2_y/m_y \tag{74}$$

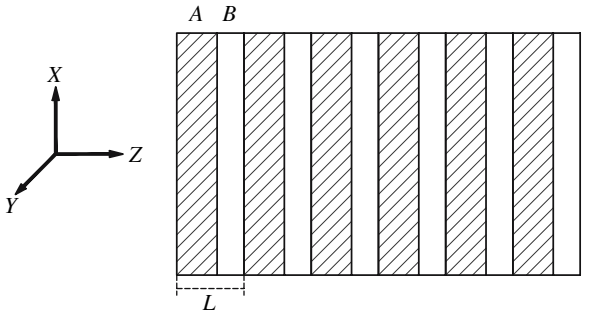

Figure 12. Periodic layered structure with two layers A and B in a unit cell L. The A layers (hatched) are anisotropic with one of the principle axes of the dielectric permittivity tensor $\hat{\varepsilon}$ making an oblique angle with the normal z to the layers ($\varepsilon_{xz} \neq 0$). The B layers can be isotropic. The $x - z$ plane coincides with the mirror plane m_y of the stack.

with the mirror plane m_y normal to the y-axis. Such a symmetry is compatible with the necessary condition (70) for the axial spectral asymmetry (67). Therefore, the periodic array in figure 12 can support the frozen mode regime, provided that incident beam lies neither in the $x - z$, nor in $y - x$ plane [29]

$$n_x \neq 0 \quad \text{and} \quad n_y \neq 0.$$

If all the above necessary conditions are met, then the (axial) frozen mode regime is, at least, not forbidden by symmetry. More details on the symmetry aspects of the frozen mode regime can be found in [30], Section II and [29], Sections I and II.

In practice, as soon as the symmetry conditions are met, one can almost certainly achieve the (axial) frozen mode regime at any desirable frequency ω within a certain frequency range. The frequency range is determined by the layer thicknesses and the dielectric materials used, while a specific value of ω within the range can be selected by the direction $\vec{n}$ of the light incidence. The problem is that unless the physical parameters of the stack layers lie within a certain range, the effects associated with the frozen mode regime can be insignificant or even practically undetectable. The basic guiding principle in choosing appropriate layer materials are discussed in Ref. [30, 31].

The biggest challenge at optical frequencies lies in the fact that most of the commercially available optical anisotropic crystals have weak anisotropy. According to [30], this would push the axial stationary inflection point (62) very close to the photonic band edge and make the photonic crystal almost 100% reflective. This indeed would be the case if we tried to realize the frozen mode regime at the lowest frequency band. But, in Ref. [31] it was shown that the above problem can be successfully solved by moving to a higher frequency band. So, a robust axially frozen mode regime with almost complete conversion of the incident light into the frozen mode can be achieved with the commercially available anisotropic dielectric materials such as $NbLiO_3$, YVO_4, etc.

5. Electrodynamics of lossless stratified media

This section starts with a description of some basic electrodynamic properties of stratified media composed of lossless anisotropic layers. Then we turn to the important particular case of unbounded periodic layered arrays (periodic stacks), where the electromagnetic eigenmodes are Bloch waves. Then we consider the problem of electromagnetic energy flux in lossless stratified media. Finally, we outline the electromagnetic scattering problem for a semi-infinite

photonic slab. The material presented in this section is sufficient for a numerical analysis of slow light phenomena in periodic layered media. This approach was used in [29–31] to analyze the frozen mode regime in magnetic and non-magnetic periodic stacks. Yet, to develop a consistent analytical picture of the frozen mode regime we shall need a more sophisticated mathematical framework based on a perturbation theory for non-diagonalizable degenerate matrices. This problem will be addressed in the following sections.

5.1. *Reduced time-harmonic Maxwell equations*

Our treatment is based on the time-harmonic Maxwell equations in heterogeneous nonconducting media

$$\nabla \times \tilde{\mathbf{E}}(\vec{r}) = i\frac{\omega}{c}\mathbf{B}(\vec{r}), \quad \nabla \times \tilde{\mathbf{H}}(\vec{r}) = -i\frac{\omega}{c}\mathbf{D}(\vec{r}). \tag{75}$$

Electric and magnetic fields and inductions in equation (75) are related through the linear constitutive equations

$$\tilde{\mathbf{D}}(\vec{r}) = \hat{\varepsilon}(\vec{r})\tilde{\mathbf{E}}(\vec{r}), \quad \tilde{\mathbf{B}}(\vec{r}) = \hat{\mu}(\vec{r})\tilde{\mathbf{H}}(\vec{r}). \tag{76}$$

All variables in equations (75) and (76) are frequency dependent. In lossless media, the material tensors $\hat{\varepsilon}(\vec{r})$ and $\hat{\mu}(\vec{r})$ are Hermitian

$$\text{In lossless media:} \quad \hat{\varepsilon}(\vec{r}) = \hat{\varepsilon}^{\dagger}(\vec{r}), \quad \hat{\mu}(\vec{r}) = \hat{\mu}^{\dagger}(\vec{r}), \tag{77}$$

where the dagger † denotes the Hermitian conjugate. In lossless non-magnetic media, both tensors $\hat{\varepsilon}$ and $\hat{\mu}$ are also real and symmetric

$$\text{In lossless non-magnetic media:} \quad \hat{\varepsilon}(\vec{r}) = \hat{\varepsilon}^{*}(\vec{r}) = \hat{\varepsilon}^{T}(\vec{r}), \quad \hat{\mu}(\vec{r}) = \hat{\mu}^{*}(\vec{r}) = \hat{\mu}^{T}(\vec{r}), \tag{78}$$

where the asterisk denotes the complex conjugate and the superscript T denotes matrix transposition. In magnetically polarized lossless media, the Hermitian material tensors (77) may have a skew-symmetric imaginary part which is responsible for the non-reciprocal effect of Faraday rotation [2].

In a stratified medium, the second rank tensors $\hat{\varepsilon}(\vec{r})$ and $\hat{\mu}(\vec{r})$ depend on a single Cartesian coordinate z, and the Maxwell equations (75) can be recast as

$$\nabla \times \tilde{\mathbf{E}}(\vec{r}) = i\frac{\omega}{c}\hat{\mu}(z)\tilde{\mathbf{H}}(\vec{r}), \quad \nabla \times \tilde{\mathbf{H}}(\vec{r}) = -i\frac{\omega}{c}\hat{\varepsilon}(z)\tilde{\mathbf{E}}(\vec{r}). \tag{79}$$

Solutions for equation (79) can be sought in the following form

$$\tilde{\mathbf{E}}(\vec{r}) = e^{i(k_x x + k_y y)}\vec{E}(z), \quad \tilde{\mathbf{H}}(\vec{r}) = e^{i(k_x x + k_y y)}\vec{H}(z), \tag{80}$$

which can be interpreted as the "tangential" Bloch representation. The substitution (80) allows separation of the tangential components of the fields into a closed system of four linear ordinary differential equations

$$\partial_z \Psi(z) = i\frac{\omega}{c}M(z)\Psi(z), \quad \Psi(z) = \begin{bmatrix} E_x(z) \\ E_y(z) \\ H_x(z) \\ H_y(z) \end{bmatrix}, \tag{81}$$

where the 4×4 matrix $M(z)$ is referred to as the (reduced) Maxwell operator. The normal field components E_z and H_z do not enter the reduced Maxwell equations (81) and can be expressed

in terms of the tangential field components from equation (81) as

$$\begin{aligned} E_z &= (-n_x H_y + n_y H_x - \varepsilon^*_{xz} E_x - \varepsilon^*_{yz} E_y)\varepsilon^{-1}_{zz}, \\ H_z &= (n_x E_y - n_y E_x - \mu^*_{xz} H_x - \mu^*_{yz} H_y)\mu^{-1}_{zz}, \end{aligned} \tag{82}$$

where $n_x = ck_x/\omega$, $n_y = ck_y/\omega$.

The explicit expression for the Maxwell operator $M(z)$ in equation (81) is

$$M(z) = \begin{bmatrix} M_{11} & M_{12} \\ M_{21} & M_{22} \end{bmatrix} \tag{83}$$

where

$$M_{11} = \begin{bmatrix} -\dfrac{\varepsilon^*_{xz}}{\varepsilon_{zz}} n_x - \dfrac{\mu_{yz}}{\mu_{zz}} n_y & \left(-\dfrac{\varepsilon^*_{yz}}{\varepsilon_{zz}} + \dfrac{\mu_{yz}}{\mu_{zz}} \right) n_x \\ -\left(\dfrac{\varepsilon^*_{xz}}{\varepsilon_{zz}} - \dfrac{\mu_{xz}}{\mu_{zz}} \right) n_y & -\dfrac{\varepsilon^*_{yz}}{\varepsilon_{zz}} n_y - \dfrac{\mu_{xz}}{\mu_{zz}} n_x \end{bmatrix},$$

$$M_{22} = \begin{bmatrix} -\dfrac{\varepsilon_{yz}}{\varepsilon_{zz}} n_y - \dfrac{\mu^*_{xz}}{\mu_{zz}} n_x & \left(\dfrac{\varepsilon_{yz}}{\varepsilon_{zz}} - \dfrac{\mu^*_{yz}}{\mu_{zz}} \right) n_x \\ \left(\dfrac{\varepsilon_{xz}}{\varepsilon_{zz}} - \dfrac{\mu^*_{xz}}{\mu_{zz}} \right) n_y & -\dfrac{\varepsilon_{xz}}{\varepsilon_{zz}} n_x - \dfrac{\mu^*_{yz}}{\mu_{zz}} n_y \end{bmatrix},$$

$$M_{12} = \begin{bmatrix} \mu^*_{xy} - \dfrac{\mu^*_{xz}\mu_{yz}}{\mu_{zz}} + \dfrac{n_x n_y}{\varepsilon_{zz}} & \mu_{yy} - \dfrac{\mu_{yz}\mu^*_{yz}}{\mu_{zz}} - \dfrac{n_x^2}{\varepsilon_{zz}} \\ -\mu_{xx} + \dfrac{\mu_{xz}\mu^*_{xz}}{\mu_{zz}} + \dfrac{n_y^2}{\varepsilon_{zz}} & -\mu_{xy} + \dfrac{\mu_{xz}\mu^*_{yz}}{\mu_{zz}} - \dfrac{n_x n_y}{\varepsilon_{zz}} \end{bmatrix},$$

$$M_{21} = \begin{bmatrix} -\varepsilon^*_{xy} + \dfrac{\varepsilon^*_{xz}\varepsilon_{yz}}{\varepsilon_{zz}} - \dfrac{n_x n_y}{\mu_{zz}} & -\varepsilon_{yy} + \dfrac{\varepsilon_{yz}\varepsilon^*_{yz}}{\varepsilon_{zz}} + \dfrac{n_x^2}{\mu_{zz}} \\ \varepsilon_{xx} - \dfrac{\varepsilon_{xz}\varepsilon^*_{xz}}{\varepsilon_{zz}} - \dfrac{n_y^2}{\mu_{zz}} & \varepsilon_{xy} - \dfrac{\varepsilon_{xz}\varepsilon^*_{yz}}{\varepsilon_{zz}} + \dfrac{n_x n_y}{\mu_{zz}} \end{bmatrix}.$$

In the important particular case of $k_x = k_y = 0$, the Maxwell operator (83) has a simpler form

$$M(z) = \begin{bmatrix} 0 & M_{12} \\ M_{21} & 0 \end{bmatrix}. \tag{84}$$

Only in this case of $\vec{k} \parallel z$, the fields $\vec{E}(z)$ and $\vec{H}(z)$ coincide with the actual electric and magnetic fields $\tilde{\mathbf{E}}(\vec{r})$ and $\tilde{\mathbf{H}}(\vec{r})$, as follows from the relation (80).

The (reduced) Maxwell operator $M(z)$ is a function of:

- the local values of material tensors $\hat{\varepsilon}(z)$ and $\hat{\mu}(z)$,
- the space coordinate z, via the material tensors $\hat{\varepsilon}(z)$ and $\hat{\mu}(z)$,
- the tangential components k_x, k_y of the wave vector,
- the frequency ω.

Different versions of the reduced Maxwell equation (81) can be found in the extensive literature on electrodynamics of stratified media (see, for example, [41] and references therein).

The 4×4 matrix $M(z)$ in equation (83) has the fundamental property of J-Hermitivity defined as

$$M^{\dagger} = JMJ, \tag{85}$$

where

$$J = J^{\dagger} = J^{-1} = \begin{bmatrix} 0 & 0 & 0 & 1 \\ 0 & 0 & -1 & 0 \\ 0 & -1 & 0 & 0 \\ 1 & 0 & 0 & 0 \end{bmatrix}. \tag{86}$$

The property (85) relates to conservation of electromagnetic energy in lossless media, it plays an important role in further consideration.

5.2. *The transfer matrix formalism*

The Cauchy problem

$$\partial_z \Psi(z) = i\frac{\omega}{c} M(z)\Psi(z), \quad \Psi(z_0) = \Psi_0 \tag{87}$$

for the reduced Maxwell equation (81) has a unique solution

$$\Psi(z) = T(z, z_0)\Psi(z_0) \tag{88}$$

where the 4×4 matrix $T(z, z_0)$ is referred to as the *transfer matrix*. From the definition (88) it follows that

$$T(z, z_0) = T(z, z')T(z', z_0), \quad T(z, z_0) = T^{-1}(z_0, z), \quad T(z, z) = I, \tag{89}$$

where I is the identity matrix. The transfer matrix $T(z, z_0)$ allows determination of the time-harmonic electromagnetic field $\Psi(z)$ at an arbitrary point z of the stratified medium once its value $\Psi(z_0)$ at any particular point z_0.

The matrix $T(z, z_0)$ itself is uniquely defined by the following Cauchy problem

$$\partial_z T(z, z_0) = i\frac{\omega}{c} M(z)T(z, z_0), \quad T(z, z) = I. \tag{90}$$

The equation (90), together with J-Hermitivity (85) of the Maxwell operator $M(z)$, implies that the transfer matrix $T(z, z_0)$ is *J-unitary*

$$T^{\dagger} = JT^{-1}J, \tag{91}$$

as shown in Ref. [30]. The J-unitarity (91) of the transfer matrix $T = T(z, z_0)$ imposes the following constraint on its set of four eigenvalues $\zeta_i,\ i = 1, 2, 3, 4$

$$\{\zeta_1^*, \zeta_2^*, \zeta_3^*, \zeta_4^*\} \equiv \left\{\zeta_1^{-1}, \zeta_2^{-1}, \zeta_3^{-1}, \zeta_4^{-1}\right\}, \tag{92}$$

which also implies that

$$|\det T| = 1. \tag{93}$$

5.2.1. The transfer matrix of a stack of uniform layers. The greatest advantage of the transfer matrix approach stems from the fact that the transfer matrix T_S of an arbitrary stack of layers is a sequential product of the transfer matrices T_m of the constituent layers

$$T_S = \prod_m T_m. \tag{94}$$

According to equation (90), if each individual layer m is homogeneous, the corresponding single-layer transfer matrices T_m can be explicitly expressed in terms of the respective Maxwell operators M_m

$$T_m = \exp\left(i\frac{\omega}{c}z_m M_m\right), \tag{95}$$

where z_m is the thickness of the m-th layer. The explicit expression for the Maxwell operator M_m of an arbitrary uniform layer of anisotropic dielectric material is given by equation (83). Thus, equation (94), together with (95) and (83), give an explicit expression for the transfer matrix T_S of an arbitrary stack of anisotropic dielectric layers. The elements of the J-unitary matrix T_S are functions of:

- the material tensors $\hat{\varepsilon}$ and $\hat{\mu}$ in each layer of the stack,
- the layer thicknesses d_m,
- the frequency ω,
- the tangential components $k_x = \frac{\omega}{c}n_x,\ k_y = \frac{\omega}{c}n_y$ of the wave vector.

In the case of $k_x = k_y = 0$, we have instead of equation (93)

$$\text{if } k_x = k_y = 0, \quad \det T_S = 1, \tag{96}$$

that can be derived directly from equations (95) and (83).

5.3. *Periodic layered arrays. Bloch eigenmodes.*

In a periodic layered medium, all material tensors are periodic functions of z

$$\hat{\varepsilon}(z) = \hat{\varepsilon}\,(z+L), \quad \hat{\mu}(z) = \hat{\mu}\,(z+L),$$

and so is the Maxwell operator $M(z)$ in equation (81),

$$M\,(z+L) = M(z), \tag{97}$$

where L is the length of a unit cell of the periodic stack. A Bloch solution $\Psi_k(z)$ of the reduced Maxwell equation (81) with the periodic operator $M(z)$ should satisfy the following relation

$$\Psi_k\,(z+L) = e^{ikL}\Psi_k(z), \tag{98}$$

where k is the normal component of the Bloch wave vector

$$k = k_z. \tag{99}$$

Unlike k_x and k_y, the z component (99) of the Bloch wave vector is defined up to a multiple of $2\pi/L$

$$k \equiv k + 2\pi N/L,$$

where N is an integer. Hereinafter, the normal component k_z of the Bloch wave vector $\vec{k}$ will be referred to simply as the *wave number* and denoted with symbol k, rather than k_z.

The definition (88) of the T-matrix together with equation (98) give

$$\Psi_k\,(z+L) = T\,(z+L, z)\Psi_k(z) = e^{ikL}\Psi_k(z). \tag{100}$$

Introducing the transfer matrix of a primitive cell

$$T_L = T\,(L, 0) \tag{101}$$

we have from equation (100)

$$T_L \Phi_k = e^{ikL} \Phi_k, \quad \text{where} \quad \Phi_k = \Psi_k(0). \tag{102}$$

Thus, the eigenvectors of the transfer matrix T_L of the unit cell are uniquely related to the eigenmodes $\Psi_k(z)$ of the reduced Maxwell equation (81) through the relations

$$\Phi_i = \Psi_i(0), \quad i = 1, 2, 3, 4. \tag{103}$$

The respective four eigenvalues

$$\zeta_i = e^{ik_i L}, \quad i = 1, 2, 3, 4 \tag{104}$$

of T_L are the roots of the characteristic equation

$$F(\zeta) = 0, \quad \text{where} \quad F(\zeta) = \det(T_L - \zeta \hat{I}). \tag{105}$$

For any given ω and (k_x, k_y), the characteristic equation (105) defines a set of four values $\{\zeta_1, \zeta_2, \zeta_3, \zeta_4\}$, or equivalently, $\{k_1, k_2, k_3, k_4\}$. Real k (or, equivalently, $|\zeta| = 1$) correspond to propagating Bloch waves (propagating modes), while complex k (or, equivalently, $|\zeta| \neq 1$) correspond to evanescent modes. Evanescent modes are relevant near photonic crystal boundaries and other structural irregularities.

The J-unitarity (91) of T_L imposes the restriction (92) on the eigenvalues (104), which can be recast as

$$\{k_1, k_2, k_3, k_4\} \equiv \{k_1^*, k_2^*, k_3^*, k_4^*\}, \tag{106}$$

for any given ω and k_x, k_y. In view of the relations (106) or (92), one can distinguish the following three different situations.

(i) All four wave numbers are real

$$k_1 \equiv k_1^*, \quad k_2 \equiv k_2^*, \quad k_3 \equiv k_3^*, \quad k_4 \equiv k_4^*. \tag{107}$$

or, equivalently,

$$|\zeta_1| = |\zeta_2| = |\zeta_3| = |\zeta_4| = 1. \tag{108}$$

The respective four Bloch eigenmodes are propagating.

(ii) Two real and to complex wave numbers

$$k_1 = k_1^*, \quad k_2 = k_2^*, \quad k_4 = k_3^*, \quad \text{where} \quad k_3 \neq k_3^*, \quad k_4 \neq k_4^*. \tag{109}$$

or, equivalently,

$$|\zeta_1| = |\zeta_2| = 1, \ \zeta_4 = 1/\zeta_3^*, \quad \text{where} \quad |\zeta_3|, \quad |\zeta_4| \neq 1. \tag{110}$$

Two of the four Bloch eigenmodes are propagating and the remaining two are evanescent with complex conjugate wave numbers.

(iii) All four wave numbers are complex

$$k_2 = k_1^*, \quad k_4 = k_3^*, \quad \text{where} \quad k_1 \neq k_1^*, \quad k_2 \neq k_2^*, \quad k_3 \neq k_3^*, \quad k_4 \neq k_4^*. \tag{111}$$

or, equivalently,

$$\zeta_2 = 1/\zeta_1^*, \quad \zeta_4 = 1/\zeta_3^*, \quad \text{where} \quad |\zeta_1|, \quad |\zeta_2|, \quad |\zeta_3|, \quad |\zeta_4| \neq 1. \tag{112}$$

This situation relates to a frequency gap, where for given ω and k_x, k_y, all four Bloch eigenmodes are evanescent.

5.4. *Symmetry of the dispersion relation*

Below we will see that the dispersion relation is symmetric under $k \to -k$ if and only if the transfer matrix T_L is similar to its inverse. Indeed, assume that

$$T_L = U^{-1} T_L^{-1} U \tag{113}$$

where U is a nonsingular 4×4 matrix. This assumption together with the property (91) of J-unitarity, imply also the similarity of T_L and $T_L^\dagger$

$$T_L = V^{-1} T_L^\dagger V, \tag{114}$$

where $V = JU$. Either of the above two relations imposes the following additional restriction on the eigenvalues (104) of T_L for given ω and k_x, k_y

$$\{\zeta_1, \zeta_2, \zeta_3, \zeta_4\} \equiv \left\{\zeta_1^{-1}, \zeta_2^{-1}, \zeta_3^{-1}, \zeta_4^{-1}\right\}, \tag{115}$$

or, equivalently,

$$\{k_1, k_2, k_3, k_4\} \equiv \{-k_1, -k_2, -k_3, -k_4\}. \tag{116}$$

The relation (116) is referred to as *axial spectral symmetry*. It applies both to propagating and evanescent solutions.

Let us consider the symmetry relation (116) in more detail. Assume that $k_1 = k_1^*$ is a real wave number corresponding to a propagating eigenmode. The relation (116) implies that for given ω and k_x, k_y, there is another real wave number $k_2 = k_2^*$ such that

$$k_2 = -k_1 \tag{117}$$

In terms of the (axial) dispersion relation $\omega(k)$, the equation (117) boils down to a simple definition of axial spectral symmetry

$$\omega(k_x, k_y, k) = \omega(k_x, k_y, -k),$$

where $k_1 = k$ and $k_2 = -k$ constitute a pair of reciprocal real wave numbers related to given ω and k_x, k_y. In the case (107) of four propagating eigenmodes, there will be an additional pair k_3 and $k_4 = -k_3$ of reciprocal wave numbers.

Now assume that while k_1 and $k_2 = -k_1$ are real, the remaining wave numbers k_3 and k_4 from the set (116) are complex, which constitutes the case (109) of two propagating and two evanescent eigenmodes. In such a case, in addition to equation (117), the relation (116) together with (106) yields

$$k_4 = -k_3 = k_3^*, \tag{118}$$

or equivalently

$$\operatorname{Re} k_4 = \operatorname{Re} k_3 = 0, \pi/L; \quad \operatorname{Im} k_4 = -\operatorname{Im} k_3. \tag{119}$$

In equation (119) we took into account that $k \equiv k + 2\pi/L$.

Consider now the case (111) of a frequency gap, where all four eigenmodes are evanescent. The relations (116) and (106) allow for two different possibilities. The first one is similar to that of equation (118)

$$\begin{aligned} k_2 &= -k_1 = k_1^*, \\ k_4 &= -k_3 = k_3^*, \end{aligned} \tag{120}$$

or, equivalently,

$$\operatorname{Re} k_2 = \operatorname{Re} k_1 = 0, \pi/L; \quad \operatorname{Im} k_2 = -\operatorname{Im} k_1,$$
$$\operatorname{Re} k_4 = \operatorname{Re} k_3 = 0, \pi/L; \quad \operatorname{Im} k_4 = -\operatorname{Im} k_3. \tag{121}$$

In the above situation, the four complex wave numbers split into two reciprocal pairs k_1, k_2 and k_3, k_4 of the conjugate values. The other possibility is

$$k_1 = -k_2^* = k_3^* = -k_4, \tag{122}$$

or, equivalently,

$$\operatorname{Re} k_1 = \operatorname{Re} k_3 = -\operatorname{Re} k_2 = -\operatorname{Re} k_4, \ \operatorname{Im} k_1 = -\operatorname{Im} k_3 = \operatorname{Im} k_2 = -\operatorname{Im} k_4. \tag{123}$$

5.4.1. Spectral asymmetry. If the sufficient condition (113) for the axial spectral symmetry is not in place, then we can have for given ω and k_x, k_y

$$\{k_1, k_2, k_3, k_4\} \neq \{-k_1, -k_2, -k_3, -k_4\}, \tag{124}$$

which implies *axial spectral asymmetry* (67). The relation (106), being a direct consequence of J-unitarity (91) of the transfer matrix T_L, remains valid.

5.5. *Electromagnetic energy flux in stratified media*

5.5.1. The J-scalar product. For future reference, consider the following scalar product involving the J -matrix (86)

$$(\Psi_1, J\Psi_2) = E_{1x}^* H_{2y} - E_{1y}^* H_{2x} + H_{1,y}^* E_{2x} - H_{1x}^* E_{2y},$$

which will be referred to as the J-scalar product. Given the importance of the above quantity, hereinafter, we will use the following special notation for it

$$[\Psi_1, \Psi_2] \equiv (\Psi_1, J\Psi_2). \tag{125}$$

The J-scalar product (125) is invariant under the following transformation involving an arbitrary J-unitary matrix T

$$[T\Psi_1, T\Psi_2] = [\Psi_1, \Psi_2] \text{ for any } \Psi_1 \text{ and } \Psi_2. \tag{126}$$

The relation (126) can also be viewed as a criterion of J-unitarity of a matrix T. This relation is similar to that involving the regular scalar product (Ψ_1, Ψ_2) and a unitary matrix U

$$(U\Psi_1, U\Psi_2) = (\Psi_1, \Psi_2) \text{ for any } \Psi_1 \text{and } \Psi_2.$$

Let $\Psi_i(z)$ and $\Psi_j(z)$ be two arbitrary solutions of the time-harmonic Maxwell equation (81). The equality (126) together with the definition (88) of the transfer matrix yields

$$[\Psi(z)_i, \Psi_j(z)] = [T(z, 0)\Psi(0)_i, T(z, 0)\Psi_j(0)] = [\Psi(0)_i, \Psi_j(0)], \tag{127}$$

which implies that the J-scalar product $[\Psi(z)_i, \Psi_j(z)]$ does not depend on the coordinate z.

Consider now the J-scalar product

$$[\Phi_i, \Phi_j] \tag{128}$$

of two eigenvectors Φ_i and Φ_j of the transfer matrix T_L

$$T_L\Phi_i = \zeta_i\Phi_i, \quad i = 1, 2, 3, 4. \tag{129}$$

The J-unitarity (126) of T_L implies that

$$[T_L\Phi_i, T_L\Phi_j] = \zeta_i^*\zeta_j[\Phi_i, \Phi_j] = [\Phi_i, \Phi_j], \tag{130}$$

which, in turn, yields the following important relation

$$[\Phi_i, \Phi_j] = 0, \text{ if } \zeta_i^*\zeta_j \neq 1, \tag{131}$$

or equivalently,

$$[\Phi_i, \Phi_j] = 0, \text{ if } k_j \neq k_i^*. \tag{132}$$

In particular

$$[\Phi_i, \Phi_i] \neq 0, \text{ only if } k_i = k_i^*, \tag{133}$$

which means that Φ_i in (133) should be a propagating Bloch mode.

5.5.2. Energy flux in stratified media. The real-valued energy flux (the Poynting vector) associated with a time-harmonic electromagnetic field is

$$\mathbf{S}(\vec{r}) = [\mathrm{Re}\,\mathbf{E}(\vec{r}) \times \mathrm{Re}\,\mathbf{H}(\vec{r})] = \frac{1}{2}\,\mathrm{Re}[\mathbf{E}^*(\vec{r}) \times \mathbf{H}(\vec{r})]. \tag{134}$$

Substitution of the "tangential" Bloch representation (80) for $\mathbf{E}(\vec{r})$ and $\mathbf{H}(\vec{r})$ in equation (134) yields

$$\mathbf{S}(\vec{r}) = \mathbf{S}(z) = \frac{1}{2}\,\mathrm{Re}[\vec{E}^*(z) \times \vec{H}(z)], \tag{135}$$

at fixed ω and k_x, k_y. equation (135) implies that in a stratified medium, at fixed ω and k_x, k_y, all three Cartesian components of the energy flux $\mathbf{S}(\vec{r})$ are independent of the tangential coordinates x and y. A simple energy conservation argument shows that the normal component S_z of the energy flux does not depend on the coordinate z either, while the tangential components S_x and S_y may depend on z. Indeed, in a lossless stratified medium we have, with consideration for equation (135)

$$\nabla \cdot \mathbf{S}(\vec{r}) = \partial_z S_z(z) = 0,$$

which yields that at fixed ω and k_x, k_y

$$S_z(\vec{r}) = S_z = \text{const}. \tag{136}$$

By contrast, the tangential components of the steady-state energy flux are dependent on the z coordinate

$$S_x(\vec{r}) = S_x(z), \quad S_y(\vec{r}) = S_y(z). \tag{137}$$

Hereinafter, the normal component of the energy flux will be referred to simply as the *energy flux*, unless otherwise specifically stated. It also will be denoted as S, rather than S_z.

The explicit expression for the normal component of the energy flux (135) can be recast as

$$S = \frac{1}{2}\,(E_x^*H_y - E_y^*H_x + E_xH_y^* - E_yH_x^*) = \frac{1}{2}[\Psi, \Psi], \tag{138}$$

where the J-scalar product $[\Psi, \Psi] \equiv (\Psi, J\Psi)$ is defined in equation (125). The fact that S in equation (138) is independent of z implies that

$$S = \frac{1}{2}\,[\Psi(z), \Psi(z)] = \frac{1}{2}\,[\Phi, \Phi], \text{ where } \Phi = \Psi(0). \tag{139}$$

Equation (139) can also be viewed as a direct consequence of J-unitarity (91) of the transfer matrix. Indeed, from the definition (88) of the transfer matrix we have

$$\Psi(z) = T(z, 0)\Psi(0) = T(z, 0)\Phi. \tag{140}$$

Substituting (140) into (138) yields

$$S = \frac{1}{2}[\Psi(z), \Psi(z)] = \frac{1}{2}[T(z, 0)\Phi, T(z, 0)\Phi].$$

Taking into account the property (126) of a J-unitary matrix, we again arrive at equation (139).

5.5.3. Energy flux in periodic stratified media. The direct relation (139) between the J-scalar product $[\Psi, \Psi]$ and the energy flux S at fixed ω and k_x, k_y allows us to make some strong statements regarding electromagnetic energy flux in periodic layered media.

Let us start with the simplest case of a single Bloch eigenmode. Equation (139) together with (133) shows that only a propagating mode can transfer electromagnetic energy

$$S_i = \frac{1}{2}[\Phi_i, \Phi_i] \neq 0 \text{ only if } k_i = k_i^*. \tag{141}$$

A single evanescent eigenmode always has zero energy flux

$$S_i = [\Phi_i, \Phi_i] = 0, \quad \text{if } k_i \neq k_i^*. \tag{142}$$

Let us turn to the case of a superposition

$$\Phi = \sum_{i=1}^{4} a_i \Phi_i.$$

of different Bloch eigenmodes with fixed ω and k_x, k_y. In such a case, the energy flux is

$$S = \frac{1}{2}[\Phi, \Phi] = \frac{1}{2}\sum_{i,j=1}^{4} a_i^* a_j [\Phi_i, \Phi_j]. \tag{143}$$

Taking into account equations (132) we can draw the following conclusions:

1) The contribution S_i of each propagating eigenmode to the total energy flux is independent of the presence or absence of other Bloch eigenmodes with the same ω and k_x, k_y

$$S = \sum_{i=1} S_i = \frac{1}{2}\sum_{i=1} |a_i|^2 [\Phi_i, \Phi_i], \tag{144}$$

where the summation runs over all propagating eigenmodes. The number of propagating modes can be 4, 2, or 0, depending on which of the cases (111), (109), or (111) we are dealing with.

2) The contribution of evanescent Bloch eigenmodes to the energy flux depends on their number.

   (a) In the case (109) of two evanescent modes Φ_3 and Φ_4 we have

$$S = \mathrm{Re}\,(a_3^* a_4 [\Phi_3, \Phi_4]), \text{ where } k_4 = k_3^*, \tag{145}$$

which implies that only a pair of evanescent modes with conjugate wave numbers can produce energy flux. The respective contribution (145) is independent of the presence of propagating modes Φ_1 and Φ_2. In accordance with equation (142), a single evanescent mode, either Φ_3 or Φ_4, does not produce energy flux on its own.

(b) In the case (111) of four evanescent modes we have

$$S = \mathrm{Re}\,(a_1^* a_2\,[\Phi_1, \Phi_2]) + \mathrm{Re}\,(a_3^* a_4\,[\Phi_3, \Phi_4]),\ \text{where } k_2 = k_1^*, k_4 = k_3^*, \quad (146)$$

which implies that either of the two pairs of evanescent modes with conjugate wave numbers contribute to the energy flux independently of each other.

5.6. *Scattering problem for a periodic semi-infinite stack*

In this final subsection we outline the standard procedure we use for solving the scattering problem of a plane monochromatic wave incident on the surface of a periodic semi-infinite stack.

In vacuum (to the left of the semi-infinite slab) the electromagnetic field $\Psi_V(z)$ is a superposition of the incident and reflected waves

$$\Psi_V(z) = \Psi_I(z) + \Psi_R(z), \quad z \le 0, \quad (147)$$

where the indices I and R relate to the incident and reflected beams, respectively. At the slab boundary we have

$$\Psi_V(0) = \Psi_I(0) + \Psi_R(0). \quad (148)$$

The transmitted wave $\Psi_T(z)$ inside the periodic semi-infinite slab is a superposition of two forward Bloch eigenmodes

$$\Psi_T(z) = \Psi_1(z) + \Psi_2(z), \quad z \ge 0. \quad (149)$$

The eigenmodes $\Psi_1(z)$ and $\Psi_2(z)$ can be both propagating (with $u > 0$), one propagating and one evanescent (with $u > 0$ and $\mathrm{Im}\,k > 0$, respectively), or both evanescent (with $\mathrm{Im}\,k > 0$), depending on which of the three cases (39), (41), or (40) we are dealing with.

Assume now that for a given frequency ω, the Bloch eigenmodes are found, which can be readily done in the case of a periodic layered array. Using the standard electromagnetic boundary conditions

$$\Psi_T(0) = \Psi_I(0) + \Psi_R(0), \quad (150)$$

one can express the reflected wave Ψ_R and the eigenmode composition of the transmitted wave Ψ_T, in terms of the amplitude and polarization of the incident wave Ψ_I. This automatically gives the electromagnetic field distribution $\Psi_T(z)$ inside the slab, as a function of the incident wave frequency, polarization, and direction of incidence.

The transmittance and reflectance coefficients of a lossless semi-infinite slab are defined by the following expressions

$$\tau = 1 - \rho = \frac{(\vec{S}_T)_z}{(\vec{S}_I)_z}, \quad \rho = -\frac{(\vec{S}_R)_z}{(\vec{S}_I)_z}, \quad (151)$$

where $(\vec{S}_I)_z$, $(\vec{S}_R)_z$ and $(\vec{S}_T)_z$ are the normal components of the energy flux of the incident, reflected, and transmitted waves, respectively. Knowing the value of the transmitted wave Ψ_T or reflected wave Ψ_R at the slab boundary, one can immediately find the respective energy flux and, thereby, the transmittance/reflectance coefficients (151).

The above-outlined standard procedure was used in all our numerical simulations. It applies both to the case of normal and oblique incidence. In the latter case, the explicit expressions

for the column vectors Ψ_I and Ψ_R in (147–150) are

$$\Psi_I = \begin{bmatrix} E_{I,x} \\ E_{I,y} \\ H_{I,x} \\ H_{I,y} \end{bmatrix}, \quad \Psi_R = \begin{bmatrix} E_{R,x} \\ E_{R,y} \\ H_{R,x} \\ H_{R,y} \end{bmatrix}, \tag{152}$$

where the complex vectors $\vec{E}_I$, $\vec{H}_I$ and $\vec{E}_R$, $\vec{H}_R$ are related to the actual electromagnetic field components $\mathbf{E}_I$, $\mathbf{H}_I$ and $\mathbf{E}_R$, $\mathbf{H}_R$ as

$$\tilde{\mathbf{E}}_I = e^{i\frac{\omega}{c}(n_x x + n_y y)}\vec{E}_I(z), \ \tilde{\mathbf{H}}_I = e^{i\frac{\omega}{c}(n_x x + n_y y)}\vec{H}_I, \tag{153}$$

$$\tilde{\mathbf{E}}_R = e^{i\frac{\omega}{c}(n_x x + n_y y)}\vec{E}_R(z), \ \tilde{\mathbf{H}}_R = e^{i\frac{\omega}{c}(n_x x + n_y y)}\vec{H}_R, \tag{154}$$

as prescribed by equation (80). Here $\vec{n}$ is the unit vector in the direction of light propagation

$$\text{for incident beam: } \vec{n} = \vec{n}_I = \left(\frac{c}{\omega}k_x, \frac{c}{\omega}k_y, \frac{c}{\omega}k_z\right), \tag{155}$$

$$\text{for reflected beam: } \vec{n} = \vec{n}_R = \left(\frac{c}{\omega}k_x, \frac{c}{\omega}k_y, -\frac{c}{\omega}k_z\right), \tag{156}$$

where

$$k_z = \frac{c}{\omega}n_z = \frac{c}{\omega}\sqrt{1 - \left(n_x^2 + n_y^2\right)}.$$

Note that the tangential components of the unit vector $\vec{n}$ of the incident wave are the same as those of the reflected wave. The electric and magnetic fields of a plane monochromatic wave in a vacuum are uniquely related to each other

$$\tilde{\mathbf{H}} = \vec{n} \times \tilde{\mathbf{E}}.$$

The same relation holds for the complex vectors $\vec{E}_I$, $\vec{H}_I$ and $\vec{E}_R$, $\vec{H}_R$ defined in (153) and (154), namely

$$\vec{H}_I = \vec{n}_I \times \vec{E}_I, \quad \vec{H}_R = \vec{n}_R \times \vec{E}_R. \tag{157}$$

6. Matrix of reflection coefficients of a semi-infinite periodic stack

This and the following sections are devoted to a rigorous mathematical analysis of the scattering problem for a plane monochromatic wave incident on a periodic semi-infinite stack. We focus on vicinities of stationary points of the electromagnetic dispersion relation and our goal is to develop an asymptotic analytical description of the frozen mode regime. Not only would that allow to rigorously prove the physical results presented earlier in this paper, it would also provide a better understanding of the very essence of the frozen mode regime. The major part of the following analysis is a perturbation theory of degenerate non-diagonalizable matrices. Specifically, we refer to the transfer matrix T_L, which develops a nontrivial Jordan block at any stationary point of the dispersion relations. The latter circumstance implies the existence of diverging non-Bloch eigenmodes, which usually do not contribute to the transmitted wave Ψ_T inside the semi-infinite photonic slab and, therefore, do not affect the scattering problem at hand. Yet, there are two important exceptions. The first one is the stationary inflection point (15), where not only the linearly diverging Floquet eigenmode dominates the transmitted wave, but it also produces a finite energy flux inside the periodic medium. Another exception is the

degenerate band edge (54), where the respective linearly divergent non-Bloch eigenmode, although dominant, does not contribute to the energy flux and, therefore, does not effectively transform the incident radiation into the slow mode.

The rest of the paper is organized as follows. In this section we re-formulate the scattering problem for a lossless periodic semi-infinite stack, introducing basic notations and definitions. In the following sections we develop a perturbation theory for degenerate non-diagonalizable 4×4 matrices and apply this theory to the transfer matrix T_L and, thereby, to the scattering problem. Special attention is given to the comparative analysis of different stationary points of the electromagnetic dispersion relation, such as a photonic band edge, a stationary inflection point, and a degenerate band edge. To simplify the rather cumbersome mathematical expressions of the following sections, we will use the following new notations for the quantities already defined earlier

$$\begin{aligned} &x_1 \to x,\ x_2 \to y, x_3 \to z, \\ &A \to \frac{\omega}{c} JM,\ T \to T_L, \\ &\mathbf{k} = (k_1, k_2, k_3) \to (ck_x, ck_y, ck_z). \end{aligned}$$

Observe that the 4×4 matrix

$$A = \frac{\omega}{c} JM \tag{158}$$

is Hermitian, while the related Maxwell operator M defined in equations (81–86) is J-Hermitian.

6.1. *Basic definitions*

A periodic semi-infinite stack is defined in terms of the related matrix function $A(x_3)$ satisfying

$$A(x_3) = \text{Const},\ -\infty < x_3 < 0;\ A(x_3 + L) = A(x_3),\ 0 < x_3 < \infty. \tag{159}$$

In vacuum, the Hermitian matrix $A(x_3)$ defined in (158) and has the form

$$A(x_3) = A^{(0)} = \begin{bmatrix} \mathbf{a}^{(0)} & \mathbf{0} \\ \mathbf{0} & \mathbf{a}^{(0)} \end{bmatrix},\ \mathbf{a}^{(0)} = \frac{1}{\omega} \begin{bmatrix} \omega^2 - k_2^2 & k_1 k_2 \\ k_1 k_2 & \omega^2 - k_1^2 \end{bmatrix}, \tag{160}$$

The above expressions immediately follow from equations (83) and (158). The tangential component $\mathbf{k}_\tau$ of the the wave vector $\mathbf{k}$ is related to its normal component k_3 by

$$k_3 = \sqrt{\omega^2 - \mathbf{k}_\tau^2} = \sqrt{\omega^2 - (k_1^2 + k_2^2)}. \tag{161}$$

Let us introduce

$$j_2 = \begin{bmatrix} 0 & -1 \\ 1 & 0 \end{bmatrix},\ J = \begin{bmatrix} 0 & -j_2 \\ j_2 & 0 \end{bmatrix} = j_2 \otimes j_2, \tag{162}$$

and notice that

$$JA^{(0)} = \begin{bmatrix} 0 & -j_2 \mathbf{a}^{(0)} \\ j_2 \mathbf{a}^{(0)} & 0 \end{bmatrix} = \begin{bmatrix} 0 & -1 \\ 1 & 0 \end{bmatrix} \otimes [j_2 \mathbf{a}^{(0)}] = j_2 \otimes [j_2 \mathbf{a}^{(0)}]. \tag{163}$$

Recall the basic properties of the tensor product operation: if A and B are square matrices and u and v are vectors of related dimensions then

$$[A \otimes B](u \otimes v) = (Au) \otimes (Bv),\ (u_1 \otimes v_1, u_2 \otimes v_2) = (u_1, u_2)(v_1, v_2). \tag{164}$$

Suppose now that we know the set of eigenvectors and eigenvalues for two square matrices A and B, namely

$$Au_j = \lambda_j u_j,\ Bv_m = \mu_m v_m. \tag{165}$$

Then (164) and (165) imply

$$[A \otimes B](u_j \otimes v_m) = \lambda_j \mu_m u_j \otimes v_m. \tag{166}$$

Using (166) and the tensor product representation (163) for $JA^{(0)}$ we can find its eigenvectors and eigenvalues as follows. First, we find that

$$j_2 u_\pm = \pm \mathrm{i} u_\pm,\ u_\pm = \frac{1}{\sqrt{2}} \begin{bmatrix} \pm \mathrm{i} \\ 1 \end{bmatrix};\quad j_2 \mathbf{a}^{(0)} v_\pm = \pm \mathrm{i} k_3 v_\pm, \tag{167}$$

$$v_\pm = v_\pm(\omega, \mathbf{k}_\tau) = \frac{1}{\gamma_{\omega,\mathbf{k}_\tau}} \begin{bmatrix} -\frac{k_3^2+k_2^2}{\pm \mathrm{i}\omega k_3 + k_1 k_2} \\ 1 \end{bmatrix},\ \gamma_{\omega,\mathbf{k}_\tau} = \sqrt{\frac{2(k_3^2+k_2^2)k_3\omega}{\omega^2 k_3^2 + k_1^2 k_2^2}}.$$

Notice also that

$$(v_+, j_2 v_-) = (v_-, j_2 v_+) = 0,\ (v_\pm, j_2 v_\pm) = \pm \mathrm{i}, \tag{168}$$

$$(v_\pm, v_\pm) = \beta_{\omega,\mathbf{k}_\tau} = \frac{\left(k_3^2+k_2^2\right)^2 + (\omega k_3)^2 + (k_1 k_2)^2}{2\left(k_3^2+k_2^2\right)k_3\omega},$$

$$(v_\mp, v_\pm) = \frac{1}{\gamma^2_{\omega,\mathbf{k}_\tau}} \left[\left(\frac{k_3^2+k_2^2}{\pm \mathrm{i}\omega k_3 + k_1 k_2} \right)^2 + 1 \right],$$

$$(u_\pm, u_\pm) = 1,\ (u_\mp, u_\pm) = 0;\ (u_\mp, j_2 u_\pm) = 0,\ (u_\pm, j_2 u_\pm) = \pm \mathrm{i}. \tag{169}$$

Using the tensor product representation (163) for $JA^{(0)}$ and (166) and (167), (168) we obtain

$$[JA^{(0)}]Z_1^\pm = \pm k_3 Z_1^\pm,\ [JA^{(0)}]Z_2^\pm = \pm k_3 Z_2^\pm,\ \ Z_j^\pm = Z_j^\pm(\omega, \mathbf{k}_\tau). \tag{170}$$

where

$$Z_1^+ = u_- \otimes v_+,\ Z_2^+ = u_+ \otimes v_-,\ Z_1^- = u_+ \otimes v_+,\ Z_2^- = u_- \otimes v_-. \tag{171}$$

The component representations for $Z_j^\pm$ are as follows

$$Z_1^+ = \frac{1}{\sqrt{2}\gamma_{\omega,\mathbf{k}_\tau}} \begin{bmatrix} \frac{\mathrm{i}\left(k_3^2+k_2^2\right)}{\mathrm{i}k_3\omega + k_1 k_2} \\ -\mathrm{i} \\ -\frac{k_3^2+k_2^2}{\mathrm{i}k_3\omega + k_1 k_2} \\ 1 \end{bmatrix},\quad Z_2^+ = \frac{1}{\sqrt{2}\gamma_{\omega,\mathbf{k}_\tau}} \begin{bmatrix} -\frac{\mathrm{i}\left(k_3^2+k_2^2\right)}{-\mathrm{i}k_3\omega + k_1 k_2} \\ \mathrm{i} \\ -\frac{k_3^2+k_2^2}{-\mathrm{i}k_3\omega + k_1 k_2} \\ 1 \end{bmatrix}, \tag{172}$$

$$Z_1^- = \frac{1}{\sqrt{2}\gamma_{\omega,\mathbf{k}_\tau}} \begin{bmatrix} -\frac{\mathrm{i}\left(k_3^2+k_2^2\right)}{\mathrm{i}k_3\omega + k_1 k_2} \\ \mathrm{i} \\ -\frac{k_3^2+k_2^2}{\mathrm{i}k_3\omega + k_1 k_2} \\ 1 \end{bmatrix},\quad Z_2^- = \frac{1}{\sqrt{2}\gamma_{\omega,\mathbf{k}_\tau}} \begin{bmatrix} \frac{\mathrm{i}\left(k_3^2+k_2^2\right)}{-\mathrm{i}k_3\omega + k_1 k_2} \\ -\mathrm{i} \\ -\frac{k_3^2+k_2^2}{-\mathrm{i}k_3\omega + k_1 k_2} \\ 1 \end{bmatrix}. \tag{173}$$

Observe that (164), (171), (169) imply

$$[Z_1^+, Z_2^+] = (Z_1^+, JZ_2^+) = (u_- \otimes v_+, [j_2 \otimes j_2]u_+ \otimes v_-) \tag{174}$$
$$= (u_- \otimes v_+, j_2u_+ \otimes j_2v_-) = \mathrm{i}(u_- \otimes v_+, u_+ \otimes j_2v_-)$$
$$= (u_-, u_+)(v_+, \mathrm{i}j_2v_-) = 0,$$
$$[Z_1^+, Z_1^+] = -\mathrm{i}(u_- \otimes v_+, u_- \otimes j_2v_+) = -\mathrm{i}(u_-, u_-)(v_+, j_2v_+) = 1, \tag{175}$$
$$[Z_1^+, Z_1^-] = -\mathrm{i}(u_- \otimes v_+, u_+ \otimes j_2v_+) = -\mathrm{i}(u_-, u_+)(v_+, j_2v_+) = 0.$$

Carrying out more evaluations similar to (174), (175) we get

$$\left[Z_j^\pm, Z_m^\mp\right] = 0,\ [Z_j^\pm, Z_m^\pm] = \pm\delta_{jm},\ \ j, m = 1, 2, \tag{176}$$

where δ_{jm} is Kronecker symbol. The relations (176) show that the system of 4 vectors $Z_j^\pm$, $j = 1, 2$ is flux-orthonormal in the sense that it is orthonormal with respect to the flux form $[\Psi_1, \Psi_2] = (\Psi_1, J\Psi_2)$.

Consider now the scalar products of 4 vectors $Z_j^\pm$, $j = 1, 2$:

$$(Z_1^+, Z_1^+) = (u_- \otimes v_+, u_- \otimes v_+) = (u_-, u_-)(v_+, v_+) = \beta_{\omega,\mathbf{k}_\tau}\beta_v, \tag{177}$$
$$(Z_1^-, Z_1^-) = (u_+ \otimes v_+, u_+ \otimes v_+) = (u_+, u_+)(v_+, v_+) = \beta_{\omega,\mathbf{k}_\tau},$$
$$(Z_1^+, Z_1^-) = (u_- \otimes v_+, u_+ \otimes v_+) = (u_-, u_+)(v_+, v_+) = 0, \tag{178}$$
$$(Z_1^+, Z_2^+) = (u_- \otimes v_+, u_+ \otimes v_-) = (u_-, u_+)(v_+, v_-) = 0.$$

Carrying out evaluations similar to (177), (178) we get the following complete set of equalities:

$$(Z_j^\pm, Z_m^\pm) = \beta_{\omega,\mathbf{k}_\tau}\delta_{jm},\ (Z_j^\pm, Z_m^\mp) = 0,\quad j, m = 1, 2. \tag{179}$$

$$\beta_{\omega,\mathbf{k}_\tau} = \frac{\left(k_3^2 + k_2^2\right)^2 + (\omega k_3)^2 + (k_1k_2)^2}{2\left(k_3^2 + k_2^2\right)k_3},$$

showing that the system $Z_j^\pm$, $j = 1, 2$ is orthogonal though, evidently, it is not orthonormal.

The set of equalities (176) and (179) show the system of vectors $Z_j^\pm$, $j = 1, 2$ has a property that both the forms, namely, the EM density form (the scalar product) and the flux form, become diagonal if it is chosen to be a basis of the space $\mathbb{C}^4$. Another advantage of choosing $Z_j^\pm$, $j = 1, 2$ to be a basis is that in this basis the flux balance equality for relevant modes takes its simplest form as in the classical scattering theory (see (214), (215), (221)). *In fact, the latter is our primary motivation.*

For the periodic semi-infinite stack with $A(x_3; \omega)$ we have the following equation defining its eigenmodes $\Psi(x_3)$ at the frequency ω

$$\partial_3\Psi(x_3) = iJA(x_3)\Psi(x_3),\ -\infty < x_3 < \infty. \tag{180}$$

The eigenmodes of the periodic semi-infinite stack are the ones corresponding to an incident wave which propagates from $-\infty$ to ∞, then it is partially reflected by the interface at $x_3 = 0$ and partially transmitted into the dielectric substance in $0 < x_3 < \infty$. We refer to such eigenmodes as relevant eigenmodes and denote the set of all relevant eigenmodes by $\mathcal{S}_\mathrm{T} = \mathcal{S}_\mathrm{T}(\omega) = \mathcal{S}_\mathrm{T}(\omega, \mathbf{k}_\tau)$.

The two extended eigenmodes $\Psi_1(x_3)$ and $\Psi_2(x_3)$ describing the standard scattering problem satisfy the following relations in the air, $x_3 < 0$,

$$\Psi_1(x_3) = e^{\mathrm{i}k_3x_3}Z_1^+ + e^{-\mathrm{i}k_3x_3}[\rho_{11}Z_1^- + \rho_{21}Z_2^-],$$
$$\Psi_2(x_3) = e^{\mathrm{i}k_3x_3}Z_2^+ + e^{-\mathrm{i}k_3x_3}[\rho_{12}Z_1^- + \rho_{22}Z_2^-], \tag{181}$$

where the matrix of reflection coefficients

$$\rho = \rho_{\omega,\mathbf{k}_\tau} = \begin{bmatrix} \rho_{11}(\omega, \mathbf{k}_\tau)\ \rho_{12}(\omega, \mathbf{k}_\tau) \\ \rho_{21}(\omega, \mathbf{k}_\tau)\ \rho_{22}(\omega, \mathbf{k}_\tau) \end{bmatrix} \tag{182}$$

carries the information about reflection properties of the slab. Its entries can be called reflection coefficients.

The set $\mathcal{S}_\mathrm{T}$ of all relevant eigenmodes $\Psi(x_3)$ happens to be a two-dimensional linear space. For every fixed real a it is uniquely determined by the two-dimensional space $\mathcal{S}_\mathrm{T}(a, \omega) = \mathcal{S}_\mathrm{T}(a; \omega, \mathbf{k}_\tau)$ of the values $\Psi(a)$ as Ψ runs over $\mathcal{S}_\mathrm{T}(\mathbf{k}_\tau)$, i.e.

$$\mathcal{S}_\mathrm{T}(a; \omega, \mathbf{k}_\tau) = \{\Psi(a) : \Psi \in \mathcal{S}_\mathrm{T}(\mathbf{k}_\tau)\}. \tag{183}$$

More precisely, all possible *relevant eigenmodes* are described by solutions to the following Cauchy problem

$$\partial_3 \Psi(x_3) = iJA(x_3)\Psi(x_3),\ \Psi(a) = \Phi \in \mathcal{S}_\mathrm{T}(a, \omega),\ -\infty < x_3 < \infty. \tag{184}$$

The two-dimensional space $\mathcal{S}_\mathrm{T}(a, \omega, \mathbf{k}_\tau)$ provides a convenient way to describe and parametrize the relevant modes. For instance, assuming that we know $\mathcal{S}_\mathrm{T}(a, \omega, \mathbf{k}_\tau)$ let us pick any $\Phi \in \mathcal{S}_\mathrm{T}(\omega, \mathbf{k}_\tau)$ and find values of the eigenmode $\Psi(x_3)$ in the air. The eigenmode $\Psi(x_3)$ can be represented as the following linear combination for $-\infty < x_3 < \infty$:

$$\begin{aligned} \Psi(x_3) &= e^{\mathrm{i}k_3 x_3}[\alpha_1^+ Z_1^+ + \alpha_2^+ Z_2^+] + e^{-\mathrm{i}k_3 x_3}[\alpha_1^- Z_1^- + \alpha_2^- Z_2^-], \\ \Psi(0) &= \alpha_1^+ Z_1^+ + \alpha_2^+ Z_2^+ + \alpha_1^- Z_1^- + \alpha_2^- Z_2^- \Phi \in \mathcal{S}_\mathrm{T}(0), \end{aligned} \tag{185}$$

where evidently the two pairs of coefficients

$$\alpha^+ = \begin{bmatrix} \alpha_1^+ \\ \alpha_2^+ \end{bmatrix} \quad \text{and } \alpha^- = \begin{bmatrix} \alpha_1^- \\ \alpha_2^- \end{bmatrix} \tag{186}$$

are respectively related to the incident and the reflected waves. As is commonly done, we choose arbitrarily the incident wave by picking the vector α^+ and then finding the the reflected wave as the vector α^- using the relations (181), (182) and (185) by the following formula

$$\alpha^- = \rho\alpha^+,\ \alpha^\pm = \begin{bmatrix} \alpha_1^\pm \\ \alpha_2^\pm \end{bmatrix},\ \rho = \begin{bmatrix} \rho_{11} & \rho_{12} \\ \rho_{21} & \rho_{22} \end{bmatrix}. \tag{187}$$

Observe then that the matrix of reflection coefficients ρ can be viewed as the following mapping relating the incident wave α^+ to the reflected wave α^-

$$\rho : \alpha^+ \to \alpha^-. \tag{188}$$

Notice also that the reflection and the transmission coefficients $r(\alpha^+)$ and $t(\alpha^+)$ corresponding to the incident wave α^+ are defined by the formulae

$$r^2(\alpha^+) = \frac{|\rho\alpha^+(\Phi)|^2}{|\alpha^+(\Phi)|^2} = \frac{|\rho\alpha^+|^2}{|\alpha^+|^2},\ t^2(\alpha^+) = 1 - r^2(\alpha^+). \tag{189}$$

It follows from (181) that the space $\mathcal{S}_\mathrm{T}(0; \omega, \mathbf{k}_\tau)$ has the following representation in terms of the vectors $Z_j^\pm$ and the reflection coefficients ρ_{jm}:

$$\mathcal{S}_\mathrm{T}(0; \omega, \mathbf{k}_\tau) = \mathrm{Span}\{(Z_1^+ + \rho_{11}Z_1^- + \rho_{21}Z_2^-), (Z_2^+ + \rho_{12}Z_1^- + \rho_{22}Z_2^-)\}. \tag{190}$$

The relation (190) shows that the space $\mathcal{S}_\mathrm{T}(0; \omega, \mathbf{k}_\tau)$ is uniquely determined by the matrix $\rho_{\omega,\mathbf{k}_\tau}$. We show in the following subsection that the matrix $\rho_{\omega,\mathbf{k}_\tau}$ is uniquely determined and can be constructed based on the space $\mathcal{S}_\mathrm{T}(0; \omega, \mathbf{k}_\tau)$.

6.2. *Basic properties of the space of relevant eigenmodes*

Let us consider now basic properties of the two-dimensional space $\mathcal{S}_{\rm T}(0;\omega)=\mathcal{S}_{\rm T}(0;\omega,\mathbf{k}_\tau)$ suppressing in the notation its dependence on $\mathbf{k}_\tau$. Notice first, that the space $\mathcal{S}_{\rm T}(0;\omega)$ has the fundamental property that it is always nonnegative with respect to flux form in the sense that

$$[\Phi,\Phi]\geq 0 \text{ for any } \Phi\in\mathcal{S}_{\rm T}(a;\omega). \tag{191}$$

The property (191) indicates that the modes related to $S_{\rm T}(a;\omega)$ must transport energy in the chosen direction.

It is a well-known result of spectral theory that no eigenmode $\Psi(x_3)$ can grow at infinity faster then polynomially. In particular, an eigenmode can not grow exponentially as $x_3\to\infty$. Since $\Psi(x_3)$ is a solution to (180) it must be a linear combination of eigenmodes of the infinite periodic stack with the relevant periodic $A(x_3;\omega)$ on the interval $0<x_3<\infty$. Consequently, such a linear combination can not include evanescent modes growing exponentially as $x_3\to\infty$. Additionally, the above-mentioned linear combination cannot include backward propagating eigenmodes (those with negative group velocity). Notice that, the related properties of $\mathcal{S}_{\rm T}(0;\omega)$ can be characterized by the spectral properties of the transfer matrix $\mathcal{T}(\omega)$. For instance, in the case when all eigenmodes are propagating and have different wave numbers as described by (108), the space $\mathcal{S}_{\rm T}(0;\omega)$ is the span of those two eigenvectors $\Phi_{\xi_1}=\Phi_{\xi_1}(\omega)$ and $\Phi_{\xi_2}=\Phi_{\xi_2}(\omega)$ that have positive fluxes, i.e.

$$\mathcal{S}_{\rm T}(0;\omega)=\text{Span}\{\Phi_{\xi_1},\Phi_{\xi_2}\},\ \text{where } [\Phi_{\xi_1},\Phi_{\xi_1}],[\Phi_{\xi_2},\Phi_{\xi_2}]>0. \tag{192}$$

Hence, there are exactly two eigenvectors having positive fluxes.

In the case (110) when there are two propagating and two evanescent modes, $\mathcal{S}_{\rm T}(0;\omega)$ is the span of the two eigenvectors $\Phi_{\xi_1}(\omega)$, having a positive flux, and $\Phi_\zeta(\omega)$ with $|\zeta|<1$, i.e.

$$\mathcal{S}_{\rm T}(0;\omega)=\text{Span}\{\Phi_{\xi_1},\Phi_\zeta\},\ \text{where } |\xi_1|=1,\ [\Phi_{\xi_1},\Phi_{\xi_1}]>0 \text{ and } |\zeta|<1. \tag{193}$$

Finally, in the case (112) when all modes are evanescent, $\mathcal{S}_{\rm T}(0;\omega)$ is the span of the two eigenvectors $\Phi_{\zeta_1}(\omega)$ and $\Phi_{\zeta_2}(\omega)$, i.e.

$$\mathcal{S}_{\rm T}(0;\omega)=\text{Span}\{\Phi_{\zeta_1},\Phi_{\zeta_2}\},\ \text{where } |\zeta_1|,|\zeta_2|<1. \tag{194}$$

If for a certain frequency ω_0 the transfer matrix $\mathcal{T}(\omega_0)$ has a non-trivial Jordan block, then the space $\mathcal{S}_{\rm T}(0;\omega_0)$ can be defined as the following limit

$$\mathcal{S}_{\rm T}(0;\omega_0)=\lim_{\omega\to\omega_0}\mathcal{S}_{\rm T}(0;\omega), \tag{195}$$

where it is assumed that for $\omega\neq\omega_0$ the matrix $\mathcal{T}(\omega)$ is diagonalizable and $\mathcal{S}_{\rm T}(0;\omega)$ is a well defined two-dimensional space. The limit (195) uses a distance d between a two subspaces S_1 and S_2 defined by the formula, [48], Section IV, §2,

$$d(S_1,S_2)=\max\{\delta(S_1,S_2),\delta(S_2,S_1)\},\ \delta(S_1,S_2)=\sup_{u\in S_1:\|u\|=1}\sup_{v\in S_2}\|u-v\|. \tag{196}$$

Hence, the limit relation in (195) is interpreted as

$$\lim_{\omega\to\omega_0}d(\mathcal{S}_{\rm T}(0;\omega),\mathcal{S}_{\rm T}(0;\omega_0))=0. \tag{197}$$

The distance $d(S_1,S_2)$ defined by (196) measures the "aperture" or "gap" between the subspaces S_1 and S_2. It has the following important property, [48], Section IV, §2, Corollary 2.6,

$$d(S_1,S_2)<1 \text{ implies } \dim S_1=\dim S_2. \tag{198}$$

The property (198) implies that if the limit (195) exists then the dimension of the space $\mathcal{S}_{\mathrm{T}}(0;\omega_0)$ must be 2 since $\dim \mathcal{S}_{\mathrm{T}}(0;\omega) = 2$ for $\omega \neq \omega_0$.

One can also verify that the limit relations (195), (197) can be conveniently recast as a limit relation between orthogonal projections onto spaces $\mathcal{S}_{\mathrm{T}}(0;\omega)$. Namely, if we introduce

$$P_{\mathcal{S}} \text{ to be the orthogonal projector on the space } \mathcal{S}, \tag{199}$$

$$\|P_{\mathcal{S}}\| = \sup_{\Phi\in\mathcal{S}} \|P_{\mathcal{S}}\Phi\|, \text{ where } \|\Phi\| \text{ is length (norm) of } \|\Phi\|. \tag{200}$$

then (195), (197) are equivalent to

$$\lim_{\omega\to\omega_0} \|P_{\mathcal{S}_{\mathrm{T}}(0;\omega)} - P_{\mathcal{S}_{\mathrm{T}}(0;\omega_0)}\| = 0. \tag{201}$$

Notice, that the relation (201) is equivalent, in turn, to the relation

$$\lim_{\omega\to\omega_0} P_{\mathcal{S}_{\mathrm{T}}(0;\omega)}\Phi = P_{\mathcal{S}_{\mathrm{T}}(0;\omega_0)}\Phi \text{ for any } \Phi \in^4, \tag{202}$$

and the relation (202) is equivalent to

$$\lim_{\omega\to\omega_0} P_{\mathcal{S}_{\mathrm{T}}(0;\omega)}\Phi = P_{\mathcal{S}_{\mathrm{T}}(0;\omega_0)}\Phi = \Phi \text{ for any } \Phi \in \mathcal{S}_{\mathrm{T}}(0;\omega_0). \tag{203}$$

Notice now that for every vector $\Phi \in \mathcal{S}_{\mathrm{T}}(0;\omega_0)$ we can define a family of vectors

$$\Phi(\omega) = P_{\mathcal{S}_{\mathrm{T}}(0;\omega)}\Phi \in \mathcal{S}_{\mathrm{T}}(0;\omega) \tag{204}$$

converging, in view of (203), as $\omega \to \omega_0$ to the vector $\Phi(\omega_0)$, i.e.

$$\lim_{\omega\to\omega_0} \Phi(\omega) = \Phi(\omega_0) = \Phi, \text{ for any } \Phi \in \mathcal{S}_{\mathrm{T}}(0;\omega_0). \tag{205}$$

6.3. *Matrix of reflection coefficients and the flux quadratic form*

In this section we look at the basic properties of the matrix of reflection coefficients $\rho = \rho_{\omega,\mathbf{k}_\tau}$ as defined in (181), (182), (187), and its relation to the flux quadratic form $[\cdot,\cdot]$, and the space $\mathcal{S}_{\mathrm{T}}(0;\omega,\mathbf{k}_\tau)$.

Observe that inserting $x_3 = 0$ into (185) yields

$$\Psi(0) = \Phi = \Phi^+ + \Phi^-, \ \Phi_\pm = \alpha_1^\pm(\Phi)Z_1^\pm + \alpha_2^\pm(\Phi)Z_2^\pm. \tag{206}$$

The equality (206) indicates that the numbers $\alpha_j^\pm(\Phi)$ are the components of the vector $\Phi \in \mathcal{S}_{\mathrm{T}}(0;\omega)$ with respect to the basis

$$\{Z_1^+, Z_2^+, Z_1^-, Z_2^-\}, \tag{207}$$

and they are determined by the following formulae. Let us introduce the two-dimensional subspaces of $\mathbb{C}^4$:

$$\mathcal{Z}^+ = \mathrm{Span}\{Z_1^+, Z_2^+\}, \ \mathcal{Z}^- = \mathrm{Span}\{Z_1^-, Z_2^-\}, \tag{208}$$

and the respectively orthogonal projections:

$$\pi^+ \text{ and } \pi^- \text{ are respectively the orthogonal projections on } \mathcal{Z}^+ \text{ and } \mathcal{Z}^-. \tag{209}$$

In view of (179) we have the following representations for $\pi_\pm$:

$$\pi^\pm\Phi = \frac{1}{\beta_{\omega,\mathbf{k}_\tau}}[(Z_1^\pm, \Phi)Z_1^\pm + (Z_2^\pm, \Phi)Z_2^\pm], \ \Phi \in \mathbb{C}^4, \tag{210}$$

and, hence,

$$\Phi = \Phi^+ + \Phi^-,\ \Phi^\pm = \pi^\pm \Phi = \alpha_1^\pm(\Phi) Z_1^\pm + \alpha_2^\pm(\Phi) Z_2^\pm, \tag{211}$$

$$\alpha^\pm(\Phi) = \frac{1}{\beta_{\omega,\mathbf{k}_\tau}} \begin{bmatrix} (Z_1^+, \Phi) \\ (Z_2^+, \Phi) \end{bmatrix}, \tag{212}$$

$$\beta_{\omega,\mathbf{k}_\tau} = \frac{\left(k_3^2 + k_2^2\right)^2 + (\omega k_3)^2 + (k_1 k_2)^2}{2\left(k_3^2 + k_2^2\right) k_3},\ k_3 = \sqrt{\omega^2 - \mathbf{k}_\tau^2}.$$

Observe, in particular, that for $\Phi \in S_{\mathrm{T}}(0; \omega, \mathbf{k}_\tau)$ the equalities (212) provide relations between the value Φ of the mode at $x_3 = 0$ and the coefficients $\alpha^\pm(\Phi)$ for the relevant incident and reflected waves.

Another simple fundamental fact is that the two-dimensional vector $\alpha^+(\Phi)$ can take any prescribed value from $\mathbb{C}^2$, i.e.:

$$\{\alpha^+(\Phi) : \Phi \in S_{\mathrm{T}}(0; \omega, \mathbf{k}_\tau)\} = \mathbb{C}^2,\ \alpha^\pm(\Phi) = \frac{1}{\beta_{\omega,\mathbf{k}_\tau}} \begin{bmatrix} (Z_1^+, \Phi) \\ (Z_2^+, \Phi) \end{bmatrix}, \tag{213}$$

The relation (213) can be considered as another fundamental property of the space $S_{\mathrm{T}}(0; \omega, \mathbf{k}_\tau)$.

Using the coefficients $\alpha^\pm(\Phi)$ and (176) we get the following representation for the flux of the mode described by Φ

$$[\Phi, \Phi] = [\Phi^+, \Phi^+] - [\Phi^-, \Phi^-] = |\alpha^+(\Phi)|^2 - |\alpha^-(\Phi)|^2, \tag{214}$$

$$\Phi = \alpha_1^+ Z_1^+ + \alpha_2^+ Z_2^+ + \alpha_1^- Z_1^- + \alpha_2^- Z_2^- \in \mathcal{S}_{\mathrm{T}}(0; \omega, \mathbf{k}_\tau).$$

The above equality reflects the fundamental energy flux balance of the classical scattering theory in its the simplest form:

$$|\alpha^+(\Phi)|^2 \text{ (Incident wave flux) } - |\alpha^-(\Phi)|^2 \text{ (Reflected wave flux)} \tag{215}$$

$$= |\alpha^+(\Phi)|^2 - |\alpha^-(\Phi)|^2 \text{ (Transmitted wave flux).}$$

The fundamental property (191) of the non-negativity of the flux on $\mathcal{S}_{\mathrm{T}}(0; \omega, \mathbf{k}_\tau)$ can be recast as

$$|\alpha^-(\Phi)|^2 = [\Phi^-, \Phi^-] \le |\alpha^+(\Phi)|^2 = [\Phi^+, \Phi^+] \text{ for any } \Phi \in S_{\mathrm{T}}(0; \omega, \mathbf{k}_\tau), \tag{216}$$

indicating the physically transparent fact that the flux of the reflected wave cannot exceed the flux of the incident wave.

Combining now the relations (187) and (216) and recalling that $\alpha^-(\Phi) = \rho\alpha^+(\Phi)$, gives

$$|\rho\alpha^+(\Phi)|^2 \le |\alpha^+(\Phi)|^2 \text{ for any } \alpha^+(\Phi) \text{ (any } \Phi \in S_{\mathrm{T}}(0; \omega, \mathbf{k}_\tau)), \tag{217}$$

which, in turn, together with (213) implies

$$\rho^\dagger \rho \le I_2. \tag{218}$$

The matrix inequality (218) signifies the fact that for any Φ, or any incident wave α^+, the reflection coefficient $r(\alpha^+)$ does not exceed 1, i.e.

$$r^2(\alpha^+) = \frac{|\alpha^-(\Phi)|^2}{|\alpha^+(\Phi)|^2} = \frac{|\rho\alpha^+(\Phi)|^2}{|\alpha^+(\Phi)|^2} = \frac{|\rho\alpha^+|^2}{|\alpha^+|^2} = \frac{(\alpha^+, [\rho^\dagger\rho]\alpha^+)}{(\alpha^+, \alpha^+)} \le 1. \tag{219}$$

As to the EM energy density using (179) we get

$$(\Phi, \Phi) = \beta_v(|\alpha^+|^2 + |\alpha^-|^2), \tag{220}$$

$$\beta_{\omega,\mathbf{k}} = \frac{\left(k_3^2 + k_2^2\right)^2 + (\omega k_3)^2 + (k_1 k_2)^2}{2\left(k_3^2 + k_2^2\right)k_3\omega},\ k_3 = \sqrt{\omega^2 - \mathbf{k}_\tau^2},$$

$$\Phi = \alpha_1^+ Z_1^+ + \alpha_2^+ Z_2^+ + \alpha_1^- Z_1^- + \alpha_2^- Z_2^- \in \mathcal{S}_{\mathrm{T}}(0; \omega, \mathbf{k}_\tau).$$

Having the energy flux balance in the form (214) was our primary motivation for choosing the vectors $Z_j^\pm$, $j = 1, 2$ as a basis in $\mathbb{C}^4$. We also want to remind the reader that the vectors $Z_j^\pm$, $j = 1, 2$ reduce both the EM energy density (the scalar product) and the flux quadratic forms to their diagonal form, as follows from the set of equalities (176) and (179).

Let us look now at the limit case $\rho^\dagger\rho = I_2$ for which, according to (214),

$$[\Phi, \Phi] = |\alpha^+(\Phi)|^2 - |\alpha^-(\Phi)|^2 = 0 \text{ for all } \alpha^+ \in \mathbb{C}^2,\ \alpha^- = \rho\alpha_+, \tag{221}$$

$$\Phi = \alpha_1^+ Z_1^+ + \alpha_2^+ Z_2^+ + \alpha_1^- Z_1^- + \alpha_2^- Z_2^- \in \mathcal{S}_{\mathrm{T}}(0; \omega, \mathbf{k}_\tau).$$

If we denote by $\mathfrak{G}_0(J)$ the set of spaces on which the flux is identically zero, then the relations (221) and (190) imply that

$$\mathcal{S}_{\mathrm{T}}(0; \omega, \mathbf{k}_\tau) = \tag{222}$$

$$= \mathrm{Span}\{(Z_1^+ + \rho_{11}Z_1^- + \rho_{21}Z_2^-), (Z_2^+ + \rho_{12}Z_1^- + \rho_{22}Z_2^-)\} \in \mathfrak{G}_0(J)$$

or, in other words, all vectors of the space $\mathcal{S}_{\mathrm{T}}(0; \omega, \mathbf{k}_\tau)$ have zero flux. On the other hand, if $\mathcal{S}_{\mathrm{T}}(0; \omega, \mathbf{k}_\tau) \in \mathfrak{G}_0(J)$ then (221) holds implying $\rho^\dagger\rho = I_2$. *Consequently, the property that the slab has complete reflection $\rho^\dagger\rho = I_2$ is equivalent to the property of having zero flux for all relevant modes*, or, symbolically,

$$\rho^\dagger\rho = I_2 \text{ is equivalent to } [\Phi, \Phi] = 0 \text{ for every } \Phi \in \mathcal{S}_{\mathrm{T}}(0; \omega, \mathbf{k}_\tau), \tag{223}$$

or, in other words,

$$\text{the reflection coefficient } r(\alpha^+) = 1 \text{ for every } \alpha^+ \in \mathbb{C}^2 \text{ is equivalent} \tag{224}$$

$$\text{to } \left[\Phi(\alpha^+), \Phi(\alpha^+)\right] = 0 \text{ for every } \alpha^+ \in \mathbb{C}^2.$$

Therefore, to establish the state of complete reflectance it is sufficient to verify that the fluxes of all relevant modes are zero.

Observe also that as a consequence of (223), (224) we have

$$\text{if there exists } \Phi \in \mathcal{S}_{\mathrm{T}}(0; \omega, \mathbf{k}_\tau) \text{ such that } [\Phi, \Phi] \neq 0, \text{ then } \rho^\dagger\rho \neq I_2, \tag{225}$$

or, in other words,

$$\text{if there exist } \Phi \in \mathcal{S}_{\mathrm{T}}(0; \omega, \mathbf{k}_\tau) \text{ such that } [\Phi, \Phi] \neq 0 \tag{226}$$

$$\text{then for almost all } \alpha^+ \in \mathbb{C}^2 :\ \text{the reflection coefficient } r(\alpha^+) < 1.$$

To establish a representation for the matrix ρ in terms of the space $\mathcal{S}_{\mathrm{T}}(0; \omega, \mathbf{k}_\tau)$ let us pick any two linearly independent vectors Φ_1 and Φ_2 in $\mathcal{S}_{\mathrm{T}}(0; \omega, \mathbf{k}_\tau)$. Then, since $\mathcal{S}_{\mathrm{T}}(0; \omega, \mathbf{k}_\tau)$ is a two-dimensional space, we have

$$\mathcal{S}_{\mathrm{T}}(0; \omega, \mathbf{k}_\tau) = \mathrm{Span}\,\{\Phi_1, \Phi_2\}\,. \tag{227}$$

Having the basis $\{\Phi_1, \Phi_2\}$ of $\mathcal{S}_{\mathrm{T}}(0; \omega, \mathbf{k}_\tau)$ we introduce the related component representation

$$\check{\Phi} = \begin{bmatrix} \varphi_1 \\ \varphi_2 \end{bmatrix},\ \Phi = \varphi_1\Phi_1 + \varphi_2\Phi_2 \in \mathcal{S}_{\mathrm{T}}(0; \omega, \mathbf{k}_\tau), \tag{228}$$

and

$$\pi^{\pm}\Phi = \alpha^{\pm}(\Phi) = Q^{\pm}\check{\Phi}, \tag{229}$$

$$Q^{\pm} = \left[Z_1^+ Z_2^+\right]^{\dagger}[\Phi_1\Phi_2] = \frac{1}{\beta_{\omega,\mathbf{k}_\tau}}\begin{bmatrix}(Z_1^{\pm},\,\Phi_1)\;(Z_1^{\pm},\,\Phi_2)\\(Z_2^{\pm},\,\Phi_1)\;(Z_2^{\pm},\,\Phi_2)\end{bmatrix}.$$

Observe now that the relation $\alpha^- = \rho\alpha^+$ together with (229) implies

$$Q^-\check{\Phi} = \rho Q^+\check{\Phi}, \tag{230}$$

where

$$\check{\Phi} = \check{\Phi}(\alpha^+) = \left[Q^+\right]^{-1}\alpha^+,\;\; \Phi(\alpha^+) = [\Phi_1\Phi_2]\,\check{\Phi}(\alpha^+) = [\Phi_1\Phi_2]\left[Q^+\right]^{-1}\alpha^+. \tag{231}$$

The relations (230) yields, in turn, the following representation for the matrix ρ

$$\rho = Q^-\left[Q^+\right]^{-1} = \begin{bmatrix}(Z_1^-,\,\Phi_1) & (Z_1^-,\,\Phi_2)\\(Z_2^-,\,\Phi_1) & (Z_2^-,\,\Phi_2)\end{bmatrix}\begin{bmatrix}(Z_1^+,\,\Phi_1) & (Z_1^+,\,\Phi_2)\\(Z_2^+,\,\Phi_1) & (Z_2^+,\,\Phi_2)\end{bmatrix}^{-1}. \tag{232}$$

Notice that the inequality (216) together with (213) implies

$$[Q^-]^{\dagger}Q^- \le [Q^+]^{\dagger}Q^+, \tag{233}$$

which is an alternative form of the inequalities (216), (218) and (219). Using (219), (229) and (232) we get the following representation for the reflection coefficient

$$r^2(\alpha^+) = \frac{(Q^-[Q^+]^{-1}\alpha^+,\,Q^-[Q^+]^{-1}\alpha^+)}{|\alpha^+|^2}, \tag{234}$$

$$r^2(\alpha^+(\Phi)) = \frac{|\alpha^-(\Phi)|^2}{|\alpha^+(\Phi)|^2} = \frac{(Q^-\check{\Phi},\,Q^-\check{\Phi})}{(Q^+\check{\Phi},\,Q^+\check{\Phi})}. \tag{235}$$

Observe also that (221) and (234) yield the following expression for the flux associated with the incident wave described by α^+

$$\begin{aligned}[\Phi(\alpha^+),\,\Phi(\alpha^+)] &= (1 - r^2(\alpha^+))|\alpha^+|^2 \\ &= \left(1 - \frac{(Q^-[Q^+]^{-1}\alpha^+,\,Q^-[Q^+]^{-1}\alpha^+)}{|\alpha^+|^2}\right)|\alpha^+|^2.\end{aligned} \tag{236}$$

The formula (236) can be recast as the following representation for the transmission coefficient $t = t(\alpha^+)$ defined by (189)

$$t^2(\alpha^+) = 1 - r^2(\alpha^+) = \frac{[\Phi(\alpha^+),\,\Phi(\alpha^+)]}{|\alpha^+|^2},\;\; \Phi(\alpha^+) = [\Phi_1\Phi_2][Q^+]^{-1}\alpha^+. \tag{237}$$

7. Transfer matrix at and near a point of degeneracy

Let us recall first the definition of degenerate points including inflection ones. A n-degenerate point k_0 of a dispersion relation $\omega(k)$ is defined as a point at which the following relations holds

$$\partial_k\omega(k_0) = \partial_k^2\omega(k_0) = \cdots = \partial_k^{n-1}\omega(k_0) = 0,\;\; \partial_k^n\omega(k_0) \neq 0. \tag{238}$$

In particular, an inflection point k_0 is a 3-fold degenerate point if

$$\omega'(k_0) = \omega''(k_0) = 0,\;\; \omega'''(k_0) \neq 0. \tag{239}$$

Hence, if k_0 is a n-degenerate point we have

$$\omega(k) = \omega(k_0) + \frac{\partial_k^n \omega(k_0)}{n!}(k - k_0)^n + O((k - k_0)^{n+1}),\ k \to k_0. \tag{240}$$

In particular, if k_0 is an inflection point then

$$\omega(k) = \omega(k_0) + \frac{\omega'''(k_0)}{6}(k - k_0)^3 + O((k - k_0)^4),\ k \to k_0. \tag{241}$$

To study the behavior of the transfer matrix T_L near ω_0 we introduce

$$\mathcal{T}(\nu) = \mathbf{T}(\omega_0 + \nu),\ \nu = \omega - \omega_0. \tag{242}$$

We assume the dependence of $\mathcal{T}(\nu)$ on ν to be analytic in some vicinity of $\nu = 0$. In our further analysis we use well known statements from the analytic perturbation theory for matrices and their spectra [48].

To find the spectrum of $\mathcal{T}(\nu)$ we consider the characteristic polynomial $\Delta_{\mathcal{T}(\nu)}(\zeta)$ and the related characteristic equation

$$\Delta_{\mathcal{T}(\nu)}(\zeta) = \det(\mathcal{T}(\nu) - \zeta I_4) = 0,\ \zeta = e^{ik}, \tag{243}$$

where I_4 is the 4×4 identity matrix, and k is the quasimomentum. Equation (243) is the dispersion relation, namely it relates to every frequency $\nu = \omega - \omega_0$ four values of ζ or, equivalently, four values of the wave number (see equation (104)).

Since $\mathcal{T}(\nu)$ is 4×4 matrix the equation (243) can be written as

$$\Delta_{\mathcal{T}(\nu)}(\zeta) = \zeta^4 + b_3(\nu)\zeta^3 + b_2(\nu)\zeta^2 + b_1(\nu)\zeta + b_0(\nu) = 0, \tag{244}$$

where the complex valued functions $b_j(\nu)$, $j = 0, 1, 2, 3$ are analytic in ν in a vicinity of $\nu = 0$.

For the frozen mode regime to occur at the frequency $\nu = 0$, i.e., $\omega = \omega_0$, the spectral decomposition of the transfer matrix $\mathcal{T}(0)$ must have a Jordan block of rank $n \geq 2$ with an algebraic eigenvalue ζ_0. In this situation the characteristic polynomial $\Delta_{\mathcal{T}(0)}(\zeta)$ takes the following special form

$$\Delta_{\mathcal{T}(0)}(\zeta) = (\zeta - \zeta_0)^n Q_n(\zeta), \tag{245}$$

where

$$Q_n(\zeta) = \zeta^{4-n} + \cdots \text{ is a polynomial of the degree } 4 - n \text{ such that } Q_n(\zeta_0) \neq 0. \tag{246}$$

It is an additional property of the transfer matrix $\mathcal{T}(\nu)$ that

$$|\zeta_0| = 1, \tag{247}$$

where the eigenvalues $\zeta_0 = e^{ik_0}$ is n-degenerate and it corresponds to a Floquet mode. Because of this degeneracy at $\nu = 0$, the perturbation theory, [48], Section II, classifies the point $\nu = 0$ as an exceptional one, and the dependence $\zeta_0(\nu)$ is described by the Puiseux series of the form

$$\zeta_0(\nu) = \zeta_0\big(1 + \alpha_1 \nu^{1/n} + \alpha_2 \nu^{2/n} + \cdots\big). \tag{248}$$

The corresponding eigenprojectors can be singular. In fact, in our case they are singular.

If the characteristic equation (243) takes the special form (245) near $\nu = 0$ then $\mathcal{T}(\nu)$ can be reduced and represented as follows

$$\mathcal{T}(\nu) = \mathcal{G}(\nu) \begin{bmatrix} T(\nu) & 0 \\ 0 & W(\nu) \end{bmatrix} \mathcal{G}^{-1}(\nu), \tag{249}$$

where $\mathcal{G}(\nu)$ is an invertible 4×4 matrix depending analytically on ν, $T(\nu)$ and $W(\nu)$ are respectively $n \times n$ and $(4-n) \times (4-n)$ matrices depending analytically on ν. Additionally

$$T(\nu) = T_0 + T_1\nu + \cdots, \tag{250}$$

where T_0 has the following Jordan form

$$T_0 = \zeta_0(I_n + D_0), \tag{251}$$

with I_n being the $n \times n$ identity matrix, and D_0 being a nilpotent matrix, [49], Section 6, such that

$$D_0^n = 0. \tag{252}$$

We would like to show $D_0 \neq 0$ and, even more, that,

$$D_0^{n-1} \neq 0. \tag{253}$$

Notice that the characteristic equation for $T(\nu)$ is

$$\det(T(\nu) - \zeta I_n) = 0, \ \zeta = e^{ik}, \tag{254}$$

which, in view of (251), takes the following form

$$\det(T(\nu) - \zeta I_3) = (\zeta - \zeta_0)^n + \sum_{s=1}^{n-1} a_{n-s}(\nu)(\zeta - \zeta_0)^{n-s} + a_0(\nu), \tag{255}$$

where the functions $a_s(\nu)$ for small ν have the following expansions $a_s(\nu) = a_s\nu + O(\nu^2)$ for some number a_s, $0 \leq s \leq n$. Hence, for small ν the characteristic equation (254) can be recast as

$$(\zeta - \zeta_0)^n + \sum_{s=1}^{n-1}[a_{n-s}\nu + O(\nu^2)](\zeta - \zeta_0)^{n-s} + a_0\nu + O(\nu^2) = 0, \tag{256}$$

where, importantly, we assume that

$$a_0 \neq 0. \tag{257}$$

It turns out, that the assumption $a_0 \neq 0$ is equivalent to the following assumption on the dispersion relation

$$\omega^{(n)}(k_0) \text{ is finite and nonzero, i.e. } 0 < |\omega^{(n)}(k_0)| < \infty, \tag{258}$$

and the following representation holds

$$a_0 = \frac{n!(\mathrm{i}\zeta_0)^n}{\omega^{(n)}(k_0)}. \tag{259}$$

To establish this representation we recall that $\zeta = e^{\mathrm{i}k}$, where k is the wave number, and notice that equation (254) or (256) relate to every $\nu = \omega - \omega_0$ certain $\zeta_j(\omega)$ and, consequently, wave vectors $k_j(\omega)$ determining dispersion relations. We can also add that the algebraic equation (256) for $\zeta = e^{\mathrm{i}k}$ is just another form of the dispersion relation (240) for $\omega(k)$. Using this observation we can derive (259) from (256) by inserting in it $\zeta = e^{\mathrm{i}k}$ and $\zeta_0 = e^{\mathrm{i}k_0}$ and, assuming $k - k_0$ to be small, we get

$$\zeta_0^n[\mathrm{i}(k - k_0)]^n + a_0\nu + O(\nu^2) + O((k - k_0)\nu) = 0, \tag{260}$$

which implies

$$a_0(\omega(k) - \omega_0) = (\mathrm{i}\zeta_0)^n(k - k_0)^n + O[(k - k_0)^{n+1}]. \tag{261}$$

Differentiating (261) with respect to k at $k = k_0$ we get

$$a_0\omega^{(n)}(k_0) = n!(\mathrm{i}\zeta_0)^n, \tag{262}$$

implying (259). Notice also that the substitution $\zeta = \zeta_0$ in (255) yields

$$\det(T(\nu) - \zeta_0 I_3) = a_0\nu + O(\nu^2). \tag{263}$$

Recall now that by the Cayley-Hamilton theorem, [49], Section 6.2, any matrix T is annulled by its characteristic polynomial, i.e. $\Delta_T(T) = 0$. Hence, (256) holds if we substitute $\zeta = T(\nu)$ treating all other complex numbers as scalar matrices, i.e.

$$(T(\nu) - \zeta_0 I_n)^n + \sum_{s=1}^{n-1}[a_{n-s}\nu + O(\nu^2)](T(\nu) - \zeta_0 I_n)^{n-s} + a_0\nu I_n + O(\nu^2) = 0. \tag{264}$$

Now substituting $T(\nu) = T_0 + T_1\nu + O(\nu^2)$ into (264) and taking in account (251) we single out the terms linear with respect to ν getting the following matrix equation

$$\zeta_0^{n-1}\sum_{s=1}^{n}\zeta_0 D_0^{n-s}T_1 D_0^{s-1} + \sum_{s=1}^{n-1}a_{n-s}\zeta_0^{n-s}D_0^{n-s} = -a_0 I_n. \tag{265}$$

Suppose now for the sake of argument that (253) does not hold, and, hence, $D_0^{n-1} = 0$. Then in the case of $n = 2$ we would have $D_0^{n-1} = D_0 = 0$ and the right-hand side of the equation (265) becomes 0 implying $a_0 = 0$ that contradicts the assumption (257). Hence, for $n = 2$, (253) holds. In the case of $n \geq 3$ the equation (265) turns into

$$\zeta_0^{n-1}\sum_{s=2}^{n-1} D_0^{n-s}T_1 D_0^{s-1} + \sum_{s=2}^{n-1}a_{n-s}\zeta_0^{n-s}D_0^{n-s} = -a_0 I_n, \tag{266}$$

so, taking the determinant of the both sides of (266) implies,

$$\det D_0\left(\zeta_0^{n-1}\sum_{s=2}^{n-1} D_0^{n-s}T_1 D_0^{s-2} + \sum_{s=2}^{n-1}a_{n-s}\zeta_0^{n-s}D_0^{n-s-1}\right) = (-a_0)^n. \tag{267}$$

But, in view of (252), evidently $\det D_0 = 0$ implying together with (267) $a_0 = 0$ that contradicts (257). Therefore, (253) is correct and the matrix $T_0 = \zeta_0(I_n + D_0)$ has nontrivial Jordan structure. In fact, in view of (252) $T_0 = \zeta_0(I_n + D_0)$ is similar to the Jordan block of rank n, i.e.

$$T_0 = \zeta_0 S_0 \begin{bmatrix} 1 & 1 & 0 & \cdots & 0 \\ 0 & \ddots & \ddots & \ddots & \vdots \\ 0 & 0 & \ddots & \ddots & 0 \\ \vdots & \ddots & \ddots & \ddots & 1 \\ 0 & \cdots & 0 & 0 & 1 \end{bmatrix} S_0^{-1} \tag{268}$$

for an invertible $n \times n$ matrix S_0. In other words, there exists a basis $f_0, f_1, \ldots, f_n$ such that

$$\zeta_0^{-1}T_0 f_0 = f_0,\ \zeta_0^{-1}T_0 f_1 = f_1 + f_0, \cdots,\ \zeta_0^{-1}T_0 f_n = f_n + f_{n-1}. \tag{269}$$

The basis $f_0, f_1, \ldots, f_n$ reducing T_0 to its canonical form is not unique. What is unique is the following set of spans

$$\mathrm{Span}\{f_0\},\ \mathrm{Span}\{f_0, f_1\},\ \mathrm{Span}\{f_0, f_1, \ldots, f_{n-1}\}. \tag{270}$$

Possible bases preserving the canonical matrix to the right of S_0 in (268) and (269) are described by the following transformations

$$S\begin{bmatrix} 1 & 1 & 0 & \cdots & 0 \\ 0 & 1 & \ddots & \ddots & \vdots \\ 0 & 0 & \ddots & \ddots & 0 \\ \vdots & \ddots & \ddots & 1 & 1 \\ 0 & \cdots & 0 & 0 & 1 \end{bmatrix} S^{-1} = \begin{bmatrix} 1 & 1 & 0 & \cdots & 0 \\ 0 & 1 & \ddots & \ddots & \vdots \\ 0 & 0 & \ddots & \ddots & 0 \\ \vdots & \ddots & \ddots & 1 & 1 \\ 0 & \cdots & 0 & 0 & 1 \end{bmatrix} \tag{271}$$

where

$$S = \begin{bmatrix} \gamma_1 & \gamma_2 & \cdots & \gamma_{n-1} & \gamma_n \\ 0 & \gamma_1 & \ddots & \ddots & \gamma_{n-1} \\ 0 & 0 & \ddots & \ddots & \vdots \\ \vdots & \ddots & \ddots & \gamma_1 & \gamma_2 \\ 0 & \cdots & 0 & 0 & \gamma_1 \end{bmatrix}, \ \gamma_j \in \mathbb{C}, \ j = 1, \cdots n. \tag{272}$$

Let us introduce now a 4×4 matrix Q reducing the matrix $\mathcal{G}^{-1}\mathcal{T}(0)\mathcal{G}(0)$ to its canonical Jordan form $Q^{-1}\mathcal{G}^{-1}\mathcal{T}(0)\mathcal{G}(0)Q$. In other words, if we denote

$$\mathcal{G}_0(\nu) = \mathcal{G}(\nu)Q \tag{273}$$

then we have

$$\mathcal{G}_0^{-1}(0)\mathcal{T}(0)\mathcal{G}_0(0) = \begin{bmatrix} T(0) & 0 \\ 0 & W(0) \end{bmatrix}, \tag{274}$$

where the both matrices $\zeta_0^{-1}T(0)$ and $W(0)$ are of the canonical Jordan form. Namely, $T(0) = T_0$ takes the following form as in (268)

$$\zeta_0^{-1}T(0) = \begin{bmatrix} 1 & 1 & 0 & \cdots & 0 \\ 0 & \ddots & \ddots & \ddots & \vdots \\ 0 & 0 & \ddots & \ddots & 0 \\ \vdots & \ddots & \ddots & \ddots & 1 \\ 0 & \cdots & 0 & 0 & 1 \end{bmatrix}, \text{ and } W(0) \text{ has canonical Jordan form.} \tag{275}$$

In the most interesting case of the inflection point for $n = 3$ the matrix $W(0)$ reduces to a scalar. In the case $n = 4$ there is no $W(0)$, and in the case $n = 2$ in a generic situation $W(0)$ will be just a diagonal matrix.

Consequently, the basis $\mathfrak{f}_j,\ j = 0, 1, 2, 3$ reducing $\mathcal{T}(0)$ to the above mentioned Jordan form (274), (275) can represented as follows

$$\mathfrak{f}_j = \mathcal{G}_0(0)\mathfrak{b}_j,\ \ j = 0, 1, 2, 3 \text{ where} \tag{276}$$

$$\mathfrak{b}_0 = \begin{bmatrix} 1 \\ 0 \\ 0 \\ 0 \end{bmatrix}, \quad \mathfrak{b}_1 = \begin{bmatrix} 0 \\ 1 \\ 0 \\ 0 \end{bmatrix}, \quad \mathfrak{b}_2 = \begin{bmatrix} 0 \\ 0 \\ 1 \\ 0 \end{bmatrix}, \quad \mathfrak{b}_3 = \begin{bmatrix} 0 \\ 0 \\ 0 \\ 1 \end{bmatrix}.$$

8. Spectral perturbation theory of the transfer matrix at a point of degeneracy

In this section we develop the spectral perturbation theory for the transfer matrix $\mathbf{T}(\omega)$ defined by (101). This problem has been considered in [30] for a stationary inflection point. For an inflection the essential part of the perturbation theory is related to perturbational spectral analysis of the Jordan block of the rank 3, i.e.

$$D_0 = D_0^{(3)} = \begin{bmatrix} 0 & 1 & 0 \\ 0 & 0 & 1 \\ 0 & 0 & 0 \end{bmatrix}. \tag{277}$$

Below we extend the spectral constructions from [30] to the case of degenerate points of the ranks 4 and 2. It turns out that as in the case of an inflection point, which is a degenerate point of the rank 3, the essential part of perturbational spectral analysis is reduced analysis of Jordan blocks of the ranks 4 and 2, i.e.

$$D_0 = D_0^{(4)} = \begin{bmatrix} 0 & 1 & 0 & 0 \\ 0 & 0 & 1 & 0 \\ 0 & 0 & 0 & 1 \\ 0 & 0 & 0 & 0 \end{bmatrix}, \quad D_0 = D_0^{(2)} = \begin{bmatrix} 0 & 1 \\ 0 & 0 \end{bmatrix}. \tag{278}$$

We use the notations

$$\mathbf{T}(\omega) = \mathbf{T}(L;\omega);\ \mathcal{T}(\nu) = \mathbf{T}(\omega_0 + \nu),\ \ \nu = \omega - \omega_0. \tag{279}$$

The transfer matrix $\mathcal{T}(\nu)$ depends analytically on ν in a vicinity of $\nu = 0$ and it can be be reduced to its canonical Jordan form (see (249)–(253), (268) and (274)–(276))

$$\mathcal{T}(\nu) = \mathcal{G}_0(\nu) \begin{bmatrix} T(\nu) & 0 \\ 0 & W(\nu) \end{bmatrix} \mathcal{G}_0^{-1}(\nu) \tag{280}$$

with help of the 4×4 invertible matrix $\mathcal{G}_0(\nu)$ depending analytically on ν in a vicinity of $\nu = 0$. The matrix $T(\nu)$ in (280) is also analytic at $\nu = 0$ and has the following representation

$$T(\nu) = T_0 + T_1\nu + \cdots,\ T_0 = \zeta_0(I_n + D_0), \tag{281}$$

where in our case $D_0 = D_0^{(n)}$ is a Jordan block (277), (278) of the order $n = 2, 3, 4$ correspondingly to the rank of the degenerate point, i.e.

$$T(0) = T_0 = \zeta_0 \quad (I_n + D_0^{(n)} \quad) = \zeta_0 \begin{bmatrix} 1 & 1 & 0 & \cdots & 0 \\ 0 & \ddots & \ddots & \ddots & \vdots \\ 0 & 0 & \ddots & \ddots & 0 \\ \vdots & \ddots & \ddots & \ddots & 1 \\ 0 & \cdots & 0 & 0 & 1 \end{bmatrix}. \tag{282}$$

It is convenient to recast (281) as

$$\begin{aligned} &T(\nu) = \zeta_0[I_n + \mathfrak{T}(\nu)],\ \mathfrak{T}(\nu) = D_0^{(n)} + \mathfrak{T}_1\nu + \mathfrak{T}_2\nu^2 + \ldots., \\ &\mathfrak{T}_s = \zeta_0^{-1}T_s,\ s = 1, 2, \ldots. \end{aligned} \tag{283}$$

Let us introduce also matrices $K_0^{(n)}$ by

$$K_0^{(2)} = \begin{bmatrix} 0 & 0 \\ 1 & 0 \end{bmatrix}, \quad K_0^{(3)} = \begin{bmatrix} 0 & 0 & 0 \\ 0 & 0 & 0 \\ 1 & 0 & 0 \end{bmatrix}, \quad K_0^{(4)} = \begin{bmatrix} 0 & 0 & 0 & 0 \\ 0 & 0 & 0 & 0 \\ 0 & 0 & 0 & 0 \\ 1 & 0 & 0 & 0 \end{bmatrix}, \tag{284}$$

and for every $n \times n$ matrix $\mathfrak{T}$ define the matrix

$$\mathfrak{T}^\natural = \mathfrak{T} - [\mathfrak{T}]_{n1}K_0^{(n)},\ \text{where } [\mathfrak{T}]_{n1} \text{ is the named entry of } \mathfrak{T}. \tag{285}$$

It turns out that the following very special case of $\mathfrak{T}(\nu)$

$$\mathfrak{T}_0(\nu) = \mathfrak{T}_0^{(n)}(\nu) = D_0^{(n)} + \nu K_0^{(n)} = \begin{bmatrix} 0 & 1 & 0 & \ldots & 0 \\ 0 & 0 & \ddots & \ddots & \vdots \\ \vdots & \ddots & \ddots & \ddots & 0 \\ 0 & \ddots & \ddots & 0 & 1 \\ \nu & 0 & \ldots & 0 & 0 \end{bmatrix} \tag{286}$$

being an exact solution to the equation

$$\mathfrak{T}_0^n(\nu) = \nu I_n \tag{287}$$

plays the key role in the spectral analysis of $\mathfrak{T}(\nu)$. For that reason we study first spectral properties of $\mathfrak{T}_0(\nu)$.

Notice that the characteristic equation $\det(\mathfrak{T}_0(\nu) - \zeta I_n) = 0$ for the eigenvalues of $\mathfrak{T}_0(\nu)$ is

$$\zeta^n - \nu = 0, \tag{288}$$

and that the matrix $\mathfrak{T}_0(\nu)$ is a companion matrix of the polynomial $\zeta^n - \nu$, [49], Sections 2.2, 2.3. Hence, if we introduce n-th roots of 1

$$\varsigma_0 = 1,\ \varsigma_1 = e^{\mathrm{i}\frac{2\pi}{n}},\ \varsigma_2 = \varsigma_1^2, \ldots, \tag{289}$$

then the n eigenvalues of $\mathfrak{T}_0(\nu)$ are

$$\nu^{\frac{1}{n}},\ \varsigma_1\nu^{\frac{1}{n}},\ \varsigma_2\nu^{\frac{1}{n}}, \ldots. \tag{290}$$

For the most interesting case of an inflection point $n = 3$ we use another natural notation for the roots

$$\varsigma_0 = 1,\ \varsigma_1 = \varsigma_+ = e^{\mathrm{i}\frac{2\pi}{3}} = -\frac{1}{2} + \frac{1}{2}\mathrm{i}\sqrt{3},\ \varsigma_2 = \varsigma_1^2 = \varsigma_- = -\frac{1}{2} - \frac{1}{2}\mathrm{i}\sqrt{3}. \tag{291}$$

The corresponding eigenvectors of the companion matrix $\mathfrak{T}_0(\nu)$ can be also found, and, if one puts them as columns in a $n \times n$ matrix $\mathfrak{S}_0(\nu)$, it takes the form, [50], section I.10–I.13, [49], section 2.11(problem 21),

$$\mathfrak{S}_0(\nu) = \begin{bmatrix} 1 & 1 & 1 & \cdots \\ \nu^{\frac{1}{n}} & \varsigma_1\nu^{\frac{1}{n}} & \varsigma_2\nu^{\frac{1}{n}} & \cdots \\ \nu^{\frac{2}{n}} & \varsigma_1^2\nu^{\frac{2}{n}} & \varsigma_2^2\nu^{\frac{2}{n}} & \cdots \\ \vdots & \vdots & \vdots & \ddots \end{bmatrix}. \tag{292}$$

Hence,

$$\mathfrak{T}_0(\nu) = \nu^{\frac{1}{n}}\mathfrak{S}_0(\nu)\Lambda_0\mathfrak{S}_0^{-1}(\nu),\ \Lambda_0 = \begin{bmatrix} 1 & 0 & 0 & \cdots \\ 0 & \varsigma_1 & 0 & \cdots \\ 0 & 0 & \varsigma_2 & \cdots \\ \vdots & \vdots & \vdots & \ddots \end{bmatrix}. \tag{293}$$

Observe that $\mathfrak{S}_0(\nu)$ is a Vandermonde matrix, [49], of order n corresponding to n numbers $1, \varsigma_1, \varsigma_2, \cdots$, and

$$\det\mathfrak{S}_0(\nu) = \det\begin{bmatrix} 1 & 1 & 1 & \cdots \\ 1 & \varsigma_1 & \varsigma_2 & \cdots \\ 1 & \varsigma_1^2 & \varsigma_2^2 & \cdots \\ \vdots & \vdots & \vdots & \ddots \end{bmatrix} = \prod_{1\le j<s\le n}(\varsigma_s - \varsigma_j) \tag{294}$$

$$= (-1)^{\frac{(n+2)(n-1)}{4}} n^{\frac{n}{2}} \nu^{\frac{n-1}{2}} = e^{-\mathrm{i}\frac{(n+2)(n-1)\pi}{4}} n^{\frac{n}{2}} \nu^{\frac{n-1}{2}}.$$

Notice also that

$$\mathfrak{S}_0^{-1}(\nu) = \frac{1}{n}\mathfrak{S}_0^{\dagger}((\bar{\nu})^{-1}) = \frac{1}{n}\begin{bmatrix} 1 & \nu^{-\frac{1}{n}} & \nu^{-\frac{2}{n}} & \cdots \\ 1 & \varsigma_1^{-1}\nu^{-\frac{1}{n}} & \varsigma_1^{-2}\nu^{-\frac{2}{n}} & \cdots \\ 1 & \varsigma_2^{-1}\nu^{-\frac{1}{n}} & \varsigma_2^{-2}\nu^{-\frac{2}{n}} & \cdots \\ \vdots & \vdots & \vdots & \ddots \end{bmatrix} \tag{295}$$

$$= \nu^{-\frac{n-1}{n}}\mathfrak{S}_0^{\flat}(\nu),\ \mathfrak{S}_0^{\flat}(\nu) = \frac{1}{n}\begin{bmatrix} \nu^{\frac{n-1}{n}} & \nu^{\frac{n-2}{n}} & \nu^{\frac{n-3}{n}} & \cdots \\ \nu^{\frac{n-1}{n}} & \varsigma_1^{-1}\nu^{\frac{n-2}{n}} & \varsigma_1^{-2}\nu^{\frac{n-3}{n}} & \cdots \\ \nu^{\frac{n-1}{n}} & \varsigma_2^{-1}\nu^{\frac{n-2}{n}} & \varsigma_2^{-2}\nu^{\frac{n-3}{n}} & \cdots \\ \vdots & \vdots & \vdots & \ddots \end{bmatrix}$$

where a $\mathfrak{S}^{\dagger}$ is conjugate transpose to a matrix $\mathfrak{S}$, and $\bar{\zeta}$ is the conjugate to a complex number ζ. Evidently the matrix $\mathfrak{S}_0^{\flat}(\nu)$ is analytic in $\nu^{1/n}$ and

$$\mathfrak{S}_0(\nu)\mathfrak{S}_0^{\flat}(\nu) = \nu^{-\frac{n-1}{n}} I_n. \tag{296}$$

Let us consider now the $[n,\,1]$ entry of the perturbed matrix $\mathfrak{T}(\nu)$ as a new variable $\tilde{\nu}$, namely

$$\tilde{\nu} = [\mathfrak{T}(\nu)]_{n1} = \sum_{s\geq 1} \mathfrak{t}_s \nu^s,\ \ \mathfrak{t}_s = [\mathfrak{T}_s]_{31},\ \ s \geq 1. \tag{297}$$

We will consider the generic case when

$$\mathfrak{t}_1 = [\mathfrak{T}_1]_{n1} \neq 0. \tag{298}$$

The above assumption (298), as we will show, is equivalent to the fundamental assumption (258) on the dispersion relation at the point k_0. Under the condition (298) the relation (297) can be inverted as

$$\nu = \sum_{s\geq 1} \mathfrak{r}_s \tilde{\nu}^s, \tag{299}$$

where the coefficients $\mathfrak{r}_s$ can be expressed recurrently in terms of $\mathfrak{t}_q,\ q \leq s$. In particular

$$\mathfrak{r}_1 = \frac{1}{\mathfrak{t}_1},\ \mathfrak{r}_2 = -\frac{\mathfrak{t}_2}{\mathfrak{t}_1^3},\ \mathfrak{r}_3 = \frac{2\mathfrak{t}_2^2 - \mathfrak{t}_1\mathfrak{t}_3}{\mathfrak{t}_1^5}. \tag{300}$$

Hence, from (299) and (300) we have

$$\nu = \frac{1}{\mathfrak{t}_1}\tilde{\nu} - \frac{\mathfrak{t}_2}{\mathfrak{t}_1^3}\tilde{\nu}^2 + \frac{2\mathfrak{t}_2^2 - \mathfrak{t}_1\mathfrak{t}_3}{\mathfrak{t}_1^5}\tilde{\nu}^3 + \cdots. \tag{301}$$

Using the new variable $\tilde{\nu}$ and (286) we recast the perturbed matrix (283) as a series in $\tilde{\nu}$:

$$\mathfrak{T}(\nu) = \mathfrak{T}_0(\tilde{\nu}) + \sum_{s\geq 1} \tilde{\nu}^s \widetilde{\mathfrak{T}}_s,\ \ [\widetilde{\mathfrak{T}}_s]_{n1} = 0,\ \ s \geq 1, \tag{302}$$

$$\mathfrak{T}_0(\nu) = \mathfrak{T}_0^{(n)}(\nu) = D_0^{(n)} + \nu K_0^{(n)} = \begin{bmatrix} 0 & 1 & 0 & \dots & 0 \\ 0 & 0 & \ddots & \ddots & \vdots \\ \vdots & \ddots & \ddots & \ddots & 0 \\ 0 & \ddots & \ddots & 0 & 1 \\ \nu & 0 & \dots & 0 & 0 \end{bmatrix},$$

where the matrix $\mathfrak{T}_0(\tilde{\nu})$ satisfies also (292), (293), and the matrices $\widetilde{\mathfrak{T}}_s$ can be expressed recurrently in terms of $\mathfrak{T}_q^\sharp,\ q \leq s$. In particular,

$$\widetilde{\mathfrak{T}}_1 = \frac{\mathfrak{T}_1^\sharp}{\mathfrak{t}_1},\ \widetilde{\mathfrak{T}}_2 = -\frac{\mathfrak{t}_2\mathfrak{T}_1^\sharp}{\mathfrak{t}_1^3} + \frac{\mathfrak{T}_2^\sharp}{\mathfrak{t}_1^2},\ \widetilde{\mathfrak{T}}_3 = \frac{\big(2\mathfrak{t}_2^2 - \mathfrak{t}_1\mathfrak{t}_3\big)\mathfrak{T}_1^\sharp}{\mathfrak{t}_1^5} - \frac{2\mathfrak{T}_2^\sharp}{\mathfrak{t}_1^4} + \frac{\mathfrak{T}_3^\sharp}{\mathfrak{t}_1^3}. \tag{303}$$

In particular, in view of (283), the equalities (303) yield

$$\widetilde{\mathfrak{T}}_1 = \frac{T_1^\sharp}{\zeta_0\mathfrak{t}_1},\ \widetilde{\mathfrak{T}}_2 = -\frac{\mathfrak{t}_2 T_1^\sharp}{\zeta_0\mathfrak{t}_1^3} + \frac{T_2^\sharp}{\zeta_0\mathfrak{t}_1^2},\ \widetilde{\mathfrak{T}}_3 = \frac{(2\mathfrak{t}_2^2 - \mathfrak{t}_1\mathfrak{t}_3)T_1^\sharp}{\zeta_0\mathfrak{t}_1^5} - \frac{2T_2^\sharp}{\zeta_0\mathfrak{t}_1^4} + \frac{T_3^\sharp}{\zeta_0\mathfrak{t}_1^3}. \tag{304}$$

Based on (292) and (295) we get the following representation for an arbitrary $n \times n$ matrix $\mathfrak{A}$

$$\nu^{\frac{n-1}{n}} \mathfrak{S}_0^{-1}(\nu)\mathfrak{A}\mathfrak{S}_0(\nu) = \sum_{q=0}^{(n-1)^2} \langle\mathfrak{A}\rangle_q \nu^{\frac{q}{n}}, \tag{305}$$

where, evidently, $\langle\mathfrak{A}\rangle_q$ are $n \times n$ matrices can be found based on the matrix $\mathfrak{A}$ from the very relation (305). In particular, one can find that

$$\langle\mathfrak{A}\rangle_0 = \frac{1}{n}\,[\mathfrak{A}]_{n1}\begin{bmatrix} 1 & 1 & \cdots & 1 \\ \varsigma_1 & \varsigma_1 & \cdots & \varsigma_1 \\ \vdots & \vdots & \ddots & \cdots \\ \varsigma_{n-1} & \varsigma_{n-1} & \cdots & \varsigma_{n-1} \end{bmatrix}, \tag{306}$$

$$\langle\mathfrak{A}\rangle_1 = \frac{1}{n}\,[\mathfrak{A}]_{n-1,1}\begin{bmatrix} 1 & 1 & \cdots & 1 \\ \varsigma_1^2 & \varsigma_1^2 & \cdots & \varsigma_1^2 \\ \vdots & \vdots & \ddots & \cdots \\ \varsigma_{n-1}^2 & \varsigma_{n-1}^2 & \cdots & \varsigma_{n-1}^2 \end{bmatrix} + \frac{1}{n}\,[\mathfrak{A}]_{n,2}\begin{bmatrix} 1 & \varsigma_1 & \cdots & \varsigma_{n-1} \\ \varsigma_1 & \varsigma_1\varsigma_1 & \cdots & \varsigma_1\varsigma_{n-1} \\ \vdots & \vdots & \ddots & \cdots \\ \varsigma_{n-1} & \varsigma_{n-1}\varsigma_1 & \cdots & \varsigma_{n-1}\varsigma_{n-1} \end{bmatrix} \tag{307}$$

showing as $\nu \to 0$ the most significant zero term in the representation (305) depends only on the entry $[\mathfrak{A}]_{n1}$ of the entire matrix $\mathfrak{A}$. This elucidates the special role played by the matrix entry $[\mathfrak{A}]_{n1}$. Then from (293), (302)–(307) we get the following important representation

$$\begin{aligned} &\mathfrak{S}_0^{-1}(\tilde{\nu})\mathfrak{T}(\nu)\mathfrak{S}_0(\tilde{\nu}) = \qquad (308)\\ &= \tilde{\nu}^{\frac{1}{n}}\Lambda_0 + \sum_{s\geq 1}\tilde{\nu}^s\mathfrak{S}_0^{-1}(\tilde{\nu})\widetilde{\mathfrak{T}}_s\mathfrak{S}_0(\tilde{\nu}) = \tilde{\nu}^{\frac{1}{n}}\Lambda_0 + \sum_{s\geq 1}\tilde{\nu}^{s-\frac{n-1}{n}}\sum_{q=0}^{(n-1)^2}\langle\widetilde{\mathfrak{T}}_s\rangle_q\tilde{\nu}^{\frac{q}{n}}\\ &= \tilde{\nu}^{\frac{1}{n}}\Lambda_0 + \sum_{s\geq 1}\tilde{\nu}^{s-\frac{n-1}{n}}\sum_{q=1}^{(n-1)^2}\langle\widetilde{\mathfrak{T}}_s\rangle_q\tilde{\nu}^{\frac{q-1}{n}}\\ &= \tilde{\nu}^{\frac{1}{n}}\big[\Lambda_0 + \tilde{\nu}^{\frac{1}{n}}\langle\widetilde{\mathfrak{T}}_1\rangle_1 + \tilde{\nu}^{\frac{2}{n}}\langle\widetilde{\mathfrak{T}}_1\rangle_2 + \tilde{\nu}^{\frac{3}{n}}\langle\widetilde{\mathfrak{T}}_1\rangle_3 + \cdots + \tilde{\nu}^{\frac{n-1}{n}}\langle\widetilde{\mathfrak{T}}_1\rangle_{n-1} + \cdots\big], \end{aligned}$$

where the matrix Λ_0 is a diagonal matrix defined by (293) and, evidently its entries $1, \varsigma_1, \ldots, \varsigma_{n-1}$ defined by (289) are all distinct. Notice that the representation (308) reduces the perturbation analysis of the initial series to the last series in (308). The perturbation theory of that series involving a diagonal matrix Λ_0 with different elements is much simpler and elementary. The relevant perturbational statements needed for the analysis are collected in the following section.

To analyze perturbations of the matrix Λ_0 we introduce first the following auxiliary variable

$$\tilde{\nu}^{\frac{1}{n}} = \mathrm{i}\acute{\nu}. \tag{309}$$

Then based on the described results and general facts on the perturbation theory for diagonal matrices [46] (the sketch of the theory is presented in the appendix 2) we get

$$\begin{aligned} &\mathfrak{T}(\nu) = \mathrm{i}\acute{\nu}\mathfrak{S}_0(\tilde{\nu})e^{-S(\mathrm{i}\acute{\nu})}(\Lambda_0 + (\mathrm{i}\acute{\nu})\Lambda_1 + (\mathrm{i}\acute{\nu})^2\Lambda_2 + \cdots)e^{S(\mathrm{i}\acute{\nu})}\mathfrak{S}_0^{-1}(\tilde{\nu}), \qquad (310)\\ &S(\mathrm{i}\acute{\nu}) = (\mathrm{i}\acute{\nu})S_1 + (\mathrm{i}\acute{\nu})^2S_2 + \cdots, \end{aligned}$$

where Λ_s, $s \geq 1$ are diagonal matrices. The above formula can be also written in the form

$$\begin{aligned} &\mathfrak{T}(\nu) = (\mathrm{i}\acute{\nu})^{-1}\mathfrak{S}_0(\tilde{\nu})e^{-S(\mathrm{i}\acute{\nu})}(\Lambda_0 + \Lambda_1(\mathrm{i}\acute{\nu}) + \Lambda_2(\mathrm{i}\acute{\nu})^2 + \cdots)e^{S(\mathrm{i}\acute{\nu})}\mathfrak{S}_0^{\flat}(\nu), \qquad (311)\\ &S(\mathrm{i}\acute{\nu}) = (\mathrm{i}\acute{\nu})S_1 + (\mathrm{i}\acute{\nu})^2S_2 + \cdots. \end{aligned}$$

We would like to point out that in the representation (310), (311) the eigenvectors collected in the Vandermonde matrix $\mathfrak{S}_0(\tilde{\nu})$ defined by (292) are invariant under any change of variables described by (271), (272). The dependence of the eigenvectors on the parameters γ_j, $j = 1, \ldots, n$ comes through terms of proper higher powers of $\acute{\nu}$.

The representation (310) and (309) imply that *the eigenvectors of the matrix $T(\nu)$ (and, hence, in view of (283), of the matrix $T(\nu)$) are the columns of the following matrix*

$$\mathfrak{S}_0(\tilde{\nu})e^{-S(\mathrm{i}\acute{\nu})} = \begin{bmatrix} 1 & 1 & 1 & \cdots \\ (\mathrm{i}\acute{\nu}) & \varsigma_1(\mathrm{i}\acute{\nu}) & \varsigma_2(\mathrm{i}\acute{\nu}) & \cdots \\ (\mathrm{i}\acute{\nu})^2 & \varsigma_1^2(\mathrm{i}\acute{\nu})^2 & \varsigma_2^2(\mathrm{i}\acute{\nu})^2 & \cdots \\ \vdots & \vdots & \vdots & \ddots \end{bmatrix} \{I_n - (\mathrm{i}\acute{\nu})S_1 + O(\acute{\nu}^2)\}. \tag{312}$$

Observe also that

$$\det \mathfrak{T}(\nu) = (\mathrm{i}\acute{\nu})^n \det \Lambda_0(1 + O(\acute{\nu})) = (\mathrm{i}\acute{\nu})^n(1 + O(\acute{\nu})) = \tilde{\nu}(1 + O(\tilde{\nu}^{1/n})). \tag{313}$$

From (283) and (313) we get

$$\det(T(\nu) - \zeta_0 I_n) = \zeta_0^n \det \mathfrak{T}(\nu) = \zeta_0^n \tilde{\nu}(1 + O(\tilde{\nu}^{1/n})). \tag{314}$$

Comparing (314) with (263) and taking into account (259) we get

$$\zeta_0^n \tilde{\nu} = a_0 \nu,\ a_0 = \frac{n!(\mathrm{i}\zeta_0)^n}{\omega^{(n)}(k_0)}. \tag{315}$$

The relation (315) combined with (301) yields the following representation for the important quantity $\mathfrak{t}_1 = [\mathfrak{T}_1]_{n1}$

$$\mathfrak{t}_1 = \frac{n!\mathrm{i}^n}{\omega^{(n)}(k_0)},\ \mathfrak{t}_1^{\frac{1}{n}} = \alpha_0 \mathrm{i},\ \alpha_0 = \left[\frac{n!}{\omega^{(n)}(k_0)}\right]^{\frac{1}{n}}. \tag{316}$$

The representation (316), in turn, implies the equivalence of the assumption (298) ($t_1 \neq 0$) to the fundamental assumption (258) on the dispersion relation at the point k_0. Combining (316) with (301) and (309) we get

$$\tilde{\nu}^{\frac{1}{n}} = \mathrm{i}\acute{\nu} = \alpha_0 \mathrm{i}\nu^{\frac{1}{n}} + O\big(\nu^{\frac{2}{n}}\big),\ \alpha_0 = \left[\frac{n!}{\omega^{(n)}(k_0)}\right]^{\frac{1}{n}}. \tag{317}$$

The diagonal matrices Λ_s, $s \geq 1$ as well the terms of the Taylor series for $S(\mathrm{i}\acute{\nu})$ can be found recursively (see the appendix 2 for the details).

Notice that the eigenvectors of the transfer matrix $\mathcal{T}(\nu)$ in view of (310) and (274)–(276) take the form

$$\mathfrak{e}_j(\nu) = \mathcal{G}_0(\nu) \begin{bmatrix} \mathfrak{S}_0(\tilde{\nu})e^{-S(\mathrm{i}\acute{\nu})} & 0 \\ 0 & I_{4-n} \end{bmatrix} \mathfrak{b}_j,\ j = 0, 1, 2, 3, \tag{318}$$

where, according to (309),

$$\mathcal{G}_0(\nu) = \mathcal{G}_0(0) + O(\nu) = \mathcal{G}_0(0) + O(\acute{\nu}^n),\ \text{where } n \text{ is the degeneracy order.} \tag{319}$$

8.1. *Spectrum of the transfer matrix at an inflection point*

In this section we derive the asymptotic formulae for the eigenvalues and eigenvectors of the transfer matrix $T(\nu)$ as $\nu = \omega - \omega_0 \to 0$ in the case when the frequency ω_0 is an inflection point, i.e. a degeneracy point of the order 3. We remind the reader that in this case according to (280), (281), (282) and (274)–(276) we have

$$\mathcal{T}(\nu) = \mathcal{G}_0(\nu) \begin{bmatrix} T(\nu) & 0 \\ 0 & W(\nu) \end{bmatrix} \mathcal{G}_0^{-1}(\nu), \tag{320}$$

where $\mathcal{G}_0(\nu)$ is a 4×4 invertible matrix $\mathcal{G}_0(\nu)$ depending analytically on ν in a vicinity of $\nu = 0$, $T(\nu)$ is a 3×3 matrix depending analytically on ν in a vicinity of $\nu = 0$, $W(\nu)$ is a complex valued function analytic in ν in a vicinity of $\nu = 0$. In addition to that, (see (425)), we have

$$T(0) = \zeta_0 \begin{bmatrix} 1 & 1 & 0 \\ 0 & 1 & 1 \\ 0 & 0 & 1 \end{bmatrix}, \quad |W(0)| = 1. \tag{321}$$

In other words, the basis $\mathfrak{f}_j$, $j = 0, 1, 2, 3$ defined by (276) reduces $\mathcal{T}(0)$ to its canonical form

$$\mathcal{T}(0) = \mathcal{G}_0(0) \begin{bmatrix} \zeta_0 & \zeta_0 & 0 & 0 \\ 0 & \zeta_0 & \zeta_0 & 0 \\ 0 & 0 & \zeta_0 & 0 \\ 0 & 0 & 0 & W(0) \end{bmatrix} \mathcal{G}_0^{-1}(0). \tag{322}$$

8.1.1. Eigenvalues of the transfer matrix. Observe that it follows from (293), (310) the eigenvalues $\eta_0(\nu)$, $\eta_+(\nu)$, $\eta_-(\nu)$ of the matrix $I_3 + \mathfrak{T}(\nu)$ from (283) are

$$\eta_0(\nu) = 1 + \tilde{\nu}^{1/3} + O(\tilde{\nu}^{2/3}), \ \eta_+(\nu) = 1 + \varsigma_+ \tilde{\nu}^{1/3} + O(\tilde{\nu}^{2/3}), \tag{323}$$
$$\eta_-(\nu) = 1 + \varsigma_- \tilde{\nu}^{1/3} + O(\tilde{\nu}^{2/3}), \ \tilde{\nu} = \mathfrak{t}_1^{1/3} \nu^{1/3} + O(\nu^{2/3}),$$

or, in view of (297),

$$\eta_0(\nu) = 1 + \mathfrak{t}_1^{1/3} \nu^{1/3} + O(\nu^{2/3}), \ \eta_+(\nu) = 1 + \mathfrak{t}_1^{1/3} \varsigma_+ \nu^{1/3} + O(\nu^{2/3}), \tag{324}$$
$$\eta_-(\nu) = 1 + \mathfrak{t}_1^{1/3} \varsigma_- \nu^{1/3} + O(\nu^{2/3}),$$

where according to (291)

$$\varsigma_0 = 1, \ \varsigma_1 = \varsigma_+ = e^{\mathrm{i}\frac{2\pi}{3}} = -\frac{1}{2} + \frac{1}{2}\mathrm{i}\sqrt{3}, \ \varsigma_2 = \varsigma_1^2 = \varsigma_- = -\frac{1}{2} - \frac{1}{2}\mathrm{i}\sqrt{3}. \tag{325}$$

Notice that we can recast (324) as

$$\eta_0(\nu) = \exp\left\{\mathfrak{t}_1^{1/3} \nu^{1/3} + O(\nu^{2/3})\right\}, \ \eta_+(\nu) = \exp\left\{\mathfrak{t}_1^{1/3} \varsigma_+ \nu^{1/3} + O(\nu^{2/3})\right\}, \tag{326}$$
$$\eta_-(\nu) = \exp\left\{\mathfrak{t}_1^{1/3} \varsigma_- \nu^{1/3} + O(\nu^{2/3})\right\}.$$

As follows from the statement (571) at least one of $\eta_j(\nu)$ must satisfy $\left|\eta_j(\nu)\right| = 1$. Without lost of generality we can choose that one to be $\eta_0(\nu)$, and, hence for sufficiently small $\delta > 0$ we have

$$\left|\eta_0(\nu)\right| = 1 \quad \text{for } |\nu| \le \delta. \tag{327}$$

The representation (324) together with (327) (see also (316) and (317)) yields

$$\mathfrak{t}_1^{1/3} = \alpha_0 \mathrm{i} \text{ with a real } \alpha_0 = \left[\frac{6}{\omega'''(k_0)}\right]^{\frac{1}{3}}, \tag{328}$$

$$\mathfrak{t}_1 = [\mathfrak{T}_1]_{31} = -\alpha_0^3 \mathrm{i} \text{ with a real } \alpha_0 = \left[\frac{6}{\omega'''(k_0)}\right]^{\frac{1}{3}}. \tag{329}$$

$$\tilde{\nu}^{1/3} = \mathrm{i}\alpha_0 \nu^{1/3} + O(\nu^{2/3}) \tag{330}$$

Hence, (326) takes the form

$$\eta_0(\nu) = \exp\left\{\mathrm{i}\alpha_0\nu^{1/3} + O(\nu^{2/3})\right\},\ \eta_+(\nu) = \exp\left\{\mathrm{i}\alpha_0\varsigma_+\nu^{1/3} + O(\nu^{2/3})\right\}, \tag{331}$$
$$\eta_-(\nu) = \exp\{\mathrm{i}\alpha_0\varsigma_-\nu^{1/3} + O(\nu^{2/3})\}.$$

Observe that (325) and (331) imply that

$$\text{if } \alpha_0\nu > 0 \text{ then } \left|\eta_0(\nu)\right| = 1,\ \left|\eta_+(\nu)\right| < 1,\ \left|\eta_-(\nu)\right| > 1, \tag{332}$$
$$\text{if } \alpha_0\nu < 0 \text{ then } \left|\eta_0(\nu)\right| = 1,\ \left|\eta_-(\nu)\right| < 1,\ \left|\eta_+(\nu)\right| > 1.$$

Now, as follows from (283), the eigenvalues $\theta_j(\nu)$ of the 3×3 transfer matrix $T(\nu)$ take the form

$$\theta_j(\nu) = \zeta_0\eta_j(\nu),\ j = 0, \pm. \tag{333}$$

If now we denote

$$\zeta_0 = e^{\mathrm{i}k_0} \text{ where } k_0 \text{ is real}, \tag{334}$$

then (331)–(334) imply

$$\theta_0(\nu) = \exp\left\{\mathrm{i}k_0 + \mathrm{i}\alpha_0\nu^{1/3} + O(\nu^{2/3})\right\} = e^{\mathrm{i}k_0+\mathrm{i}\alpha_0\nu^{1/3}}(1 + O(\nu^{2/3})), \tag{335}$$
$$\theta_+(\nu) = \exp\left\{\mathrm{i}k_0 + \mathrm{i}\alpha_0\varsigma_+\nu^{1/3} + O(\nu^{2/3})\right\} = e^{\mathrm{i}k_0+\mathrm{i}\alpha_0\varsigma_+\nu^{1/3}}(1 + O(\nu^{2/3})),$$
$$\theta_-(\nu) = \exp\left\{\mathrm{i}k_0 + \mathrm{i}\alpha_0\varsigma_-\nu^{1/3} + O(\nu^{2/3})\right\} = e^{\mathrm{i}k_0+\mathrm{i}\alpha_0\varsigma_-\nu^{1/3}}(1 + O(\nu^{2/3})).$$

Observe that

$$\text{if } \alpha_0\nu > 0 \text{ then } |\theta_0(\nu)| = 1,\ |\theta_+(\nu)| < 1,\ |\theta_-(\nu)| > 1, \tag{336}$$
$$\text{if } \alpha_0\nu < 0 \text{ then } |\theta_0(\nu)| = 1,\ |\theta_-(\nu)| < 1,\ |\theta_+(\nu)| > 1,$$

which can be recast as

$$|\theta_0(\nu)| = 1,\ \left|\theta_{\mathrm{sign}(\alpha_0\nu)}(\nu)\right| < 1,\ \left|\theta_{-\,\mathrm{sign}(\alpha_0\nu)}(\nu)\right| > 1. \tag{337}$$

Notice that if $\Delta k = k - k_0$ and $\Delta\omega = \omega - \omega_0 = \nu$ (328), (329) and (335) yield

$$\mathrm{i}\Delta k = \mathrm{t}_1^{1/3}\nu^{1/3} + O(\nu^{2/3}) \text{ or } \Delta\omega = \nu = \frac{-\mathrm{i}}{\mathrm{t}_1}\Delta k^3 + O(\Delta k^4), \tag{338}$$

implying

$$\omega'''(k_0) = \frac{6}{\mathrm{i}\mathrm{t}_1} \text{ or } \mathrm{i}\mathrm{t}_1 = \alpha_0^3 = \frac{6}{\omega'''(k_0)}. \tag{339}$$

Notice also that (259) implies

$$a_0 = -\mathrm{i}\alpha_0^3\zeta_0^3 = -\mathrm{i}\frac{6}{\omega'''(k_0)}\zeta_0^3. \tag{340}$$

It is convenient to introduce

$$\acute{\nu} = \alpha_0\nu^{1/3} \tag{341}$$

and to rewrite (335) and (337) as

$$\theta_0(\nu) = \exp\{\mathrm{i}k_0 + \mathrm{i}\acute{\nu} + O(\acute{\nu}^{2/3})\} = e^{\mathrm{i}k_0+\mathrm{i}\acute{\nu}}(1 + O(\acute{\nu}^{2/3})), \tag{342}$$
$$\theta_+(\nu) = \exp\{\mathrm{i}k_0 + \mathrm{i}\varsigma_+\acute{\nu} + O(\acute{\nu}^{2/3})\} = e^{\mathrm{i}k_0+\mathrm{i}\varsigma_+\acute{\nu}}(1 + O(\acute{\nu}^{2/3})),$$
$$\theta_-(\nu) = \exp\{\mathrm{i}k_0 + \mathrm{i}\varsigma_-\acute{\nu} + O(\acute{\nu}^{2/3})\} = e^{\mathrm{i}k_0+\mathrm{i}\varsigma_-\acute{\nu}}(1 + O(\acute{\nu}^{2/3})).$$

The relations (342), in turn, together with (326) imply

$$|\theta_0(\nu)| = 1,\ \left|\theta_{\mathrm{sign}(\acute{\nu})}(\nu)\right| < 1,\ \left|\theta_{-\,\mathrm{sign}(\acute{\nu})}(\nu)\right| > 1. \tag{343}$$

8.1.2. Eigenvectors of the transfer matrix. We recall that we work with the basis in which $T(0)$ *has its canonical Jordan form as in (281)*, namely

$$T(0) = \zeta_0 \begin{bmatrix} 1 & 1 & 0 \\ 0 & 1 & 1 \\ 0 & 0 & 1 \end{bmatrix}.$$

Recall also that the eigenvectors $e_j(\nu)$, $j = 0, 1, 2$ of the matrix $T(\nu)$ are the respective columns of the matrix $\mathfrak{S}_0(\tilde{\nu})e^{-S(\mathrm{i}\acute{\nu})}$ represented by the asymptotic equality (312). To use (312) we need to find the matrix S_1. Following the appendix 2, we first introduce a decomposition of a square matrix W into its the diagonal component $\mathrm{diag}(W)$ and the remaining part $\mathring{W} = W - \mathrm{diag}(W)$ with zero diagonal elements, i.e.

$$\begin{aligned} &W = [W_{mj}] = \mathrm{diag}(W) + \mathring{W},\ \text{where}\ \mathrm{diag}(W) = [W_{mj}\delta_{mj}] \\ &\mathring{W} = W - \mathrm{diag}(W), \end{aligned} \tag{344}$$

where δ_{mj} is the Kronecker symbol. Then we get the following expressions for the matrices Λ_1 and S_1 as follows:

$$\Lambda_1 = \mathrm{diag}(W_1),\ [S_1]_{nm} = \frac{1}{w_m - w_n}[\mathring{W}_1]_{nm},\ n \neq m;\ [S_1]_{nn} = 0, \tag{345}$$

where

$$W_1 = \langle \tilde{\mathfrak{T}}_1 \rangle_1 \text{ and } w_1 = \varsigma_0 = 1,\ w_2 = \varsigma_1 = \varsigma_+,\ w_3 = \varsigma_2 = \varsigma_-.$$

Carrying out the operations described in (345), and using (283), (285), (303), (307) we obtain

$$\begin{aligned} \langle \tilde{\mathfrak{T}}_1 \rangle_1 &= \frac{1}{3\mathfrak{t}_1} \begin{bmatrix} [\mathfrak{T}_1]_{21} + [\mathfrak{T}_1]_{32} & [\mathfrak{T}_1]_{21} + \varsigma_+[\mathfrak{T}_1]_{32} & [\mathfrak{T}_1]_{21} + \varsigma_-[\mathfrak{T}_1]_{32} \\ \varsigma_-[\mathfrak{T}_1]_{21} + \varsigma_+[\mathfrak{T}_1]_{32} & \varsigma_-([\mathfrak{T}_1]_{21} + [\mathfrak{T}_1]_{32}) & \varsigma_-[\mathfrak{T}_1]_{21} + [\mathfrak{T}_1]_{32} \\ \varsigma_+[\mathfrak{T}_1]_{21} + \varsigma_-[\mathfrak{T}_1]_{32} & \varsigma_+[\mathfrak{T}_1]_{21} + [\mathfrak{T}_1]_{32} & \varsigma_+([\mathfrak{T}_1]_{21} + [\mathfrak{T}_1]_{32}) \end{bmatrix} \\ &= \frac{1}{3\zeta_0\mathfrak{t}_1} \begin{bmatrix} [T_1]_{21} + [T_1]_{32} & [T_1]_{21} + \varsigma_+[T_1]_{32} & [T_1]_{21} + \varsigma_-[T_1]_{32} \\ \varsigma_-[T_1]_{21} + \varsigma_+[T_1]_{32} & \varsigma_-([T_1]_{21} + [\mathfrak{T}_1]_{32}) & \varsigma_-[T_1]_{21} + [T_1]_{32} \\ \varsigma_+[T_1]_{21} + \varsigma_-[T_1]_{32} & \varsigma_+[T_1]_{21} + [\mathfrak{T}_1]_{32} & \varsigma_+([T_1]_{21} + [T_1]_{32}) \end{bmatrix}, \end{aligned} \tag{346}$$

$$\Lambda_1 = \frac{[T_1]_{21} + [T_1]_{32}}{3\zeta_0\mathfrak{t}_1} \begin{bmatrix} 1 & 0 & 0 \\ 0 & \varsigma_- & 0 \\ 0 & 0 & \varsigma_+ \end{bmatrix} \tag{347}$$

$$S_1=\frac{1}{3\mathfrak{t}_1}\begin{bmatrix}0 & \dfrac{[\mathfrak{T}_1]_{21}+\varsigma_1[\mathfrak{T}_1]_{32}}{\varsigma_1-1} & \dfrac{[\mathfrak{T}_1]_{21}+\varsigma_2[\mathfrak{T}_1]_{32}}{\varsigma_2-1}\\ \dfrac{\varsigma_2[\mathfrak{T}_1]_{21}+\varsigma_1[\mathfrak{T}_1]_{32}}{1-\varsigma_1} & 0 & \dfrac{\varsigma_2[\mathfrak{T}_1]_{21}+[\mathfrak{T}_1]_{32}}{\varsigma_2-\varsigma_1}\\ \dfrac{\varsigma_1[\mathfrak{T}_1]_{21}+\varsigma_2[\mathfrak{T}_1]_{32}}{1-\varsigma_2} & \dfrac{\varsigma_1[\mathfrak{T}_1]_{21}+[\mathfrak{T}_1]_{32}}{\varsigma_1-\varsigma_2} & 0\end{bmatrix}$$

$$=\begin{bmatrix}0 & \dfrac{\tau_1+\varsigma_+\tau_2}{\varsigma_+-1} & \dfrac{\tau_1+\varsigma_-\tau_2}{\varsigma_--1}\\ \dfrac{\varsigma_-\tau_1+\varsigma_+\tau_2}{1-\varsigma_+} & 0 & \dfrac{\varsigma_-\tau_1+\tau_2}{\varsigma_--\varsigma_+}\\ \dfrac{\varsigma_+\tau_1+\varsigma_-\tau_2}{1-\varsigma_-} & \dfrac{\varsigma_+\tau_1+\tau_2}{\varsigma_+-\varsigma_-} & 0\end{bmatrix},\ \tau_1=\frac{[T_1]_{21}}{3\zeta_0\mathfrak{t}_1},\ \tau_2=\frac{[T_1]_{32}}{3\zeta_0\mathfrak{t}_1}.$$

The eigenvectors $e_0(\nu)$, $e_1(\nu)$ and $e_2(\nu)$ of the matrix $\mathfrak{T}(\nu)$ (and, hence, the matrix $T(\nu)$), corresponding respectively to the eigenvalues $\varsigma_0=1$, and $\varsigma_1=\varsigma_+=\frac{1}{2}(-1+\mathrm{i}\sqrt{3})$ and $\varsigma_2=\varsigma_-=-\frac{1}{2}(1+\mathrm{i}\sqrt{3})$ in view of (312) and (347) take the following form

$$e_0(\nu)=\begin{bmatrix}1+\mathrm{i}\tau_2\acute{\nu}+O(\acute{\nu}^2)\\ \mathrm{i}\acute{\nu}+\mathrm{i}\tau_1\acute{\nu}^2+O(\acute{\nu}^3)\\ -\acute{\nu}^2+\mathrm{i}(\tau_2-\tau_1)\acute{\nu}^3+O(\acute{\nu}^4)\end{bmatrix},\ e_1(\nu)=\begin{bmatrix}1-\frac{\mathrm{i}+\sqrt{3}}{2}\tau_2\acute{\nu}+O(\acute{\nu}^2)\\ -\frac{\mathrm{i}+\sqrt{3}}{2}\acute{\nu}-\frac{\mathrm{i}\sqrt{3}+1}{2}\tau_1\acute{\nu}^2+O(\acute{\nu}^3)\\ \frac{\mathrm{i}\sqrt{3}+1}{2}\acute{\nu}^2+\mathrm{i}(\tau_2-\tau_1)\acute{\nu}^3+O(\acute{\nu}^4)\end{bmatrix},\tag{348}$$

$$e_2(\nu)=\begin{bmatrix}1-\frac{\mathrm{i}-\sqrt{3}}{2}\tau_2\acute{\nu}+O(\acute{\nu}^2)\\ \frac{\sqrt{3}-\mathrm{i}}{2}\acute{\nu}+\frac{\mathrm{i}\sqrt{3}-1}{2}\tau_1\acute{\nu}^2+O(\acute{\nu}^3)\\ \frac{1-\mathrm{i}\sqrt{3}}{2}\acute{\nu}^2+\mathrm{i}(\tau_2-\tau_1)\acute{\nu}^3+O(\acute{\nu}^4)\end{bmatrix},\ \tau_1=\frac{[T_1]_{21}}{3\zeta_0\mathfrak{t}_1},\ \tau_2=\frac{[T_1]_{32}}{3\zeta_0\mathfrak{t}_1}.$$

The equality (348), in turn, implies

$$\frac{e_1(\nu)-e_0(\nu)}{\left(\frac{\mathrm{i}}{2}-\frac{\sqrt{3}}{6}\right)\acute{\nu}}=\begin{bmatrix}\tau_2+O(\acute{\nu})\\ 1+\frac{\sqrt{3}-\mathrm{i}}{2}\tau_1\acute{\nu}+O(\acute{\nu}^2)\\ \frac{\mathrm{i}-\sqrt{3}}{2}\acute{\nu}+O(\acute{\nu}^3)\end{bmatrix},\ \tau_1=\frac{[T_1]_{21}}{3\zeta_0\mathfrak{t}_1},\ \tau_2=\frac{[T_1]_{32}}{3\zeta_0\mathfrak{t}_1}.\tag{349}$$

Consequently

$$\lim_{\nu\to0}e_0(\nu)=\begin{bmatrix}1\\0\\0\end{bmatrix},\ \lim_{\nu\to0}\frac{e_1(\nu)-e_0(\nu)}{\left(\frac{\mathrm{i}}{2}-\frac{\sqrt{3}}{6}\right)\acute{\nu}}=\begin{bmatrix}\tau_2\\1\\0\end{bmatrix},\ \tau_2=\frac{[T_1]_{32}}{3\zeta_0\mathfrak{t}_1}.\tag{350}$$

Thus we have the following set of eigenvalues and corresponding eigenvectors

$$\theta_0(\nu)=e^{\mathrm{i}k_0+\mathrm{i}\acute{\nu}}(1+O(\acute{\nu}^2)),\ e_0(\nu)=\begin{bmatrix}1+\mathrm{i}\tau_2\acute{\nu}+O(\acute{\nu}^2)\\ \mathrm{i}\acute{\nu}+\mathrm{i}\tau_1\acute{\nu}^2+O(\acute{\nu}^3)\\ -\acute{\nu}^2+\mathrm{i}(\tau_2-\tau_1)\acute{\nu}^3+O(\acute{\nu}^4)\end{bmatrix},\tag{351}$$

$$\theta_+(\nu)=e^{\mathrm{i}k_0+\mathrm{i}\acute{\nu}\varsigma_+}(1+O(\acute{\nu}^2)),\ e_+(\nu)=\begin{bmatrix}1-\frac{\mathrm{i}+\sqrt{3}}{2}\tau_2\acute{\nu}+O(\acute{\nu}^2)\\ -\frac{\mathrm{i}+\sqrt{3}}{2}\acute{\nu}-\frac{\mathrm{i}\sqrt{3}+1}{2}\tau_1\acute{\nu}^2+O(\acute{\nu}^3)\\ \frac{\mathrm{i}\sqrt{3}+1}{2}\acute{\nu}^2+\mathrm{i}(\tau_2-\tau_1)\acute{\nu}^3+O(\acute{\nu}^4)\end{bmatrix},$$

$$\theta_-(\nu) = e^{ik_0+i\acute{\nu}\varsigma_-}(1+O(\acute{\nu}^2)),\ e_-(\nu) = \begin{bmatrix} 1-\frac{i-\sqrt{3}}{2}\tau_2\acute{\nu}+O(\acute{\nu}^2) \\ \frac{\sqrt{3}-i}{2}\acute{\nu}+\frac{i\sqrt{3}-1}{2}\tau_1\acute{\nu}^2+O(\acute{\nu}^3) \\ \frac{1-i\sqrt{3}}{2}\acute{\nu}^2+i(\tau_2-\tau_1)\acute{\nu}^3+O(\acute{\nu}^4) \end{bmatrix},$$

$$\tau_1 = \frac{[T_1]_{21}}{3\zeta_0 t_1},\ \tau_2 = \frac{[T_1]_{32}}{3\zeta_0 t_1};\ e_+(\nu) = e_1(\nu),\ e_-(\nu) = e_2(\nu).$$

Notice that in view of (343) we always have

$$|\theta_0(\nu)| = 1,\ \left|\theta_{\mathrm{sign}(\acute{\nu})}(\nu)\right| < 1, \tag{352}$$

implying that the vector $e_0(\nu)$ always corresponds to the frozen mode and the vector $e_{\mathrm{sign}(\acute{\nu})}(\nu)$ always corresponds to the evanescent mode, i.e. the one decaying exponentially away from the surface of the photonic crystal. In particular, the two-dimensional space $\mathrm{Span}\left\{e_0(\nu), e_{\mathrm{sign}(\acute{\nu})}(\nu)\right\}$ describes all possible values of the EM field of the ST (scattering theory) eigenmodes on the surface of the photonic crystal.

It readily follows from (350) that

$$\lim_{\nu\to 0}\mathrm{Span}\{e_0(\nu), e_\pm(\nu)\} = \mathrm{Span}\{f_0, f_1\},\ f_0 = \begin{bmatrix}1\\0\\0\end{bmatrix},\ f_1 = \begin{bmatrix}0\\1\\0\end{bmatrix}. \tag{353}$$

Hence, in particular, the two-dimensional space $\mathrm{Span}\{e_0(\nu), e_{\mathrm{sign}(\acute{\nu})}(\nu)\}$, which describes all possible values of the EM field of ST eigenmodes on the surface of the photonic crystal, converges as $\nu\to 0$ to the space $\mathrm{Span}\{f_0, f_1\}$, which describes the two-dimensional space of all possible values on EM field of ST eigenmodes on the surface of the photonic crystal for $\nu = 0$, i.e. at the frequency ω_0 of the frozen eigenmode.

Hence, in view of (318) and (319), we have the following representation for the eigenvectors $\mathfrak{e}_j(\nu) = \mathcal{G}_0(\nu)e_j(\nu)$, $j = 0, 1, 2, 4$ of the transfer matrix $\mathcal{T}(\nu)$

$$\mathfrak{e}_0(\nu) = \mathcal{G}_0(0)\begin{bmatrix} 1+i\tau_2\acute{\nu}+O(\acute{\nu}^2) \\ i\acute{\nu}+i\tau_1\acute{\nu}^2+O(\acute{\nu}^3) \\ -\acute{\nu}^2+O(\acute{\nu}^3) \\ O(\acute{\nu}^3)\end{bmatrix},\ \tau_1 = \frac{[T_1]_{21}}{3\zeta_0 t_1},\ \tau_2 = \frac{[T_1]_{32}}{3\zeta_0 t_1}. \tag{354}$$

$$\mathfrak{e}_1(\nu) = \mathfrak{e}_+(\nu) = \mathcal{G}_0(0)\begin{bmatrix} 1-\frac{i+\sqrt{3}}{2}\tau_2\acute{\nu}+O(\acute{\nu}^2) \\ -\frac{i+\sqrt{3}}{2}\acute{\nu}-\frac{i\sqrt{3}+1}{2}\tau_1\acute{\nu}^2+O(\acute{\nu}^3) \\ \frac{i\sqrt{3}+1}{2}\acute{\nu}^2+O(\acute{\nu}^3) \\ O(\acute{\nu}^3)\end{bmatrix},$$

$$\mathfrak{e}_2(\nu) = \mathcal{G}_0(0)\begin{bmatrix} 1-\frac{i-\sqrt{3}}{2}\tau_2\acute{\nu}+O(\acute{\nu}^2) \\ \frac{\sqrt{3}-i}{2}\acute{\nu}+\frac{i\sqrt{3}-1}{2}\tau_1\acute{\nu}^2+O(\acute{\nu}^3) \\ \frac{1-i\sqrt{3}}{2}\acute{\nu}^2+O(\acute{\nu}^3) \\ O(\acute{\nu}^3)\end{bmatrix},\ \mathfrak{e}_3(\nu) = \mathcal{G}_0(0)\begin{bmatrix}0\\0\\0\\1+O(\acute{\nu}^3)\end{bmatrix}. \tag{355}$$

Combining now (354), (355) with (319) and (276) we get the following representations for the eigenvectors $\mathfrak{e}_j(\nu)$

$$\mathfrak{e}_0(\nu) = (1 + \mathrm{i}\tau_2\acute{\nu} + O(\acute{\nu}^2))\mathfrak{f}_0 + (\mathrm{i}\acute{\nu} + \mathrm{i}\tau_1\acute{\nu}^2)\mathfrak{f}_1 - \acute{\nu}^2\mathfrak{f}_2 + O(\acute{\nu}^3), \tag{356}$$

$$\mathfrak{e}_+(\nu) = \mathfrak{e}_1(\nu) = \left(1 - \frac{\mathrm{i}+\sqrt{3}}{2}\tau_2\acute{\nu} + O(\acute{\nu}^2)\right)\mathfrak{f}_0 + \left(-\frac{\mathrm{i}+\sqrt{3}}{2}\acute{\nu} - \frac{\mathrm{i}\sqrt{3}+1}{2}\tau_1\acute{\nu}^2)\mathfrak{f}_1 + \frac{\mathrm{i}\sqrt{3}+1}{2}\acute{\nu}^2\mathfrak{f}_2 + O(\acute{\nu}^3\right),$$

$$\mathfrak{e}_-(\nu) = \mathfrak{e}_2(\nu) = \left(1 + \frac{\sqrt{3}-\mathrm{i}}{2}\tau_2\acute{\nu} + O(\acute{\nu}^2)\right)\mathfrak{f}_0 + \left(\frac{\sqrt{3}-\mathrm{i}}{2}\acute{\nu} + \frac{\mathrm{i}\sqrt{3}-1}{2}\tau_1\acute{\nu}^2)\mathfrak{f}_1 + \frac{1-\mathrm{i}\sqrt{3}}{2}\acute{\nu}^2\mathfrak{f}_2 + O(\acute{\nu}^3\right),$$

or, using the symbols $\varsigma_\pm = -\frac{1}{2} \pm \frac{\sqrt{3}\mathrm{i}}{2}$ from (291) we have

$$\mathfrak{e}_0(\nu) = \big(1 + \mathrm{i}\tau_2\acute{\nu} + O(\acute{\nu}^2)\big)\mathfrak{f}_0 + \big(\mathrm{i}\acute{\nu} + \mathrm{i}\tau_1\acute{\nu}^2\big)\mathfrak{f}_1 - \acute{\nu}^2\mathfrak{f}_2 + O(\acute{\nu}^3), \tag{357}$$

$$\mathfrak{e}_+(\nu) = \mathfrak{e}_1(\nu) = \big(1 + \mathrm{i}\varsigma_+\tau_2\acute{\nu} + O(\acute{\nu}^2)\big)\mathfrak{f}_0 + \big(\mathrm{i}\varsigma_+\acute{\nu} + \varsigma_-\tau_1\acute{\nu}^2\big)\mathfrak{f}_1 - \varsigma_-\acute{\nu}^2\mathfrak{f}_2 + O(\acute{\nu}^3),$$

$$\mathfrak{e}_-(\nu) = \mathfrak{e}_2(\nu) = \big(1 + \mathrm{i}\varsigma_-\tau_2\acute{\nu} + O(\acute{\nu}^2)\big)\mathfrak{f}_0 + \big(\mathrm{i}\varsigma_-\acute{\nu} + \varsigma_+\tau_1\acute{\nu}^2\big)\mathfrak{f}_1 - \varsigma_+\acute{\nu}^2\mathfrak{f}_2 + O(\acute{\nu}^3).$$

Notice that the equalities (357) imply

$$\lim_{\nu\to 0}\mathfrak{e}_0(\nu) = \lim_{\nu\to 0}\mathfrak{e}_\pm(\nu) = \mathfrak{f}_0, \tag{358}$$

indicating, in particular, that the three vectors $\mathfrak{e}_0(\nu)$ and $\mathfrak{e}_\pm(\nu)$ become almost parallel as $\nu \to 0$. To have a nicer way to trace the two-dimensional spaces $\mathrm{Span}\,\{\mathfrak{e}_0(\nu), \mathfrak{e}_\pm(\nu)\}$ we introduce the following two vectors

$$\mathfrak{h}_+(\nu) = \tfrac{\mathfrak{e}_+(\nu)-\mathfrak{e}_0(\nu)}{\mathrm{i}\acute{\nu}(\varsigma_+-1)} = [\tau_2 + O(\acute{\nu})]\,\mathfrak{f}_0 + \left[1 + \tfrac{\varsigma_- -\mathrm{i}}{\mathrm{i}(\varsigma_+-1)}\acute{\nu}\right]\mathfrak{f}_1 + \tfrac{1-\varsigma_-}{\mathrm{i}(\varsigma_+-1)}\acute{\nu}\mathfrak{f}_2 + O(\acute{\nu}^2); \tag{359}$$

$$\mathfrak{h}_-(\nu) = \tfrac{\mathfrak{e}_-(\nu)-\mathfrak{e}_0(\nu)}{\mathrm{i}\acute{\nu}(\varsigma_--1)} = [\tau_2 + O(\acute{\nu})]\,\mathfrak{f}_0 + \left[1 + \tfrac{\varsigma_+ -\mathrm{i}}{\mathrm{i}(\varsigma_--1)}\acute{\nu}\right]\mathfrak{f}_1 + \tfrac{1-\varsigma_+}{\mathrm{i}(\varsigma_--1)}\acute{\nu}\mathfrak{f}_2 + O(\acute{\nu}^2).$$

Notice that the equalities (354), (359) imply

$$\lim_{\nu\to 0}\mathfrak{h}_\pm(\nu) = \tau_2\mathfrak{f}_0 + \mathfrak{f}_1,\ \ \tau_2 = \frac{[T_1]_{32}}{3\zeta_0\mathfrak{t}_1}. \tag{360}$$

Then the relations (358), (359) and (360) yield

$$\mathrm{Span}\,\{\mathfrak{e}_0(\nu), \mathfrak{e}_\pm(\nu)\} = \mathrm{Span}\,\{\mathfrak{e}_0(\nu), \mathfrak{h}_\pm(\nu)\}, \tag{361}$$

$$\lim_{\nu\to 0}\mathrm{Span}\,\{\mathfrak{e}_0(\nu), \mathfrak{e}_\pm(\nu)\} = \mathrm{Span}\,\{\mathfrak{f}_0, \mathfrak{f}_1\}.$$

8.2. *Spectrum of the transfer matrix at a degeneracy point of the order 4*

In this section we derive the asymptotic formulae for the eigenvalues and eigenvectors of the transfer matrix $T(\nu)$ as $\nu = \omega - \omega_0 \to 0$ in the case when the frequency ω_0 is a degenerate point of order 4. In this case since $n = 4$ the transfer matrix $\mathcal{T}(\nu)$ defined by (242) is such that $\mathcal{T}(0)$ is a Jordan block of order 4, as it follows from the analysis carried out in the previous section. The mentioned analysis implies also that the matrix $T(\nu)$ defined by (249) is a 4×4 matrix and that $\mathcal{T}(\nu) = T(\nu)$.

Without loss of generality we assume that $\omega_0 = \omega(k_0)$ is a point of local minimum of the dispersion relation $\omega(k)$ in a vicinity of k_0. In the later case for $\nu = \omega - \omega_0 > 0$ and ν small there must be two propagating Bloch modes and two evanescent modes. Consequently, there will be two eigenvalues of the matrix $T(\nu)$ with absolute value 1, one eigenvalue with absolute values lesser than 1 and one eigenvalue with absolute value larger than 1.

8.2.1. Eigenvalues of the transfer matrix. Observe that it follows from (293), (310) that the eigenvalues $\eta_j(\nu)$, $j = 0, 1, 2, 3$ of the matrix $I_4 + \mathfrak{T}(\nu)$ from (283) are

$$\eta_j(\nu) = 1 + \varsigma_j \tilde{\nu}^{1/4} + O(\tilde{\nu}^{1/2}), \quad j = 0, 1, 2, 3, \tag{362}$$

or, in view of (297),

$$\eta_j(\nu) = 1 + \mathfrak{t}_1^{1/4} \varsigma_j \nu^{1/4} + O(\tilde{\nu}^{1/2}), \quad j = 0, 1, 2, 3, \tag{363}$$

where

$$\varsigma_j = e^{\mathrm{i}\frac{\pi}{2} j}, \quad j = 0, 1, 2, 3. \tag{364}$$

Notice, we can recast (363) as

$$\eta_j(\nu) = \exp\left\{\mathfrak{t}_1^{1/4} \varsigma_j \nu^{1/4} + O(\tilde{\nu}^{1/2})\right\}, \quad j = 0, 1, 2, 3. \tag{365}$$

As we have found at the beginning of the section, $\left|\eta_j(\nu)\right| = 1$ for exactly two values of $j = 0, 1, 2, 3$. Using (316) and (317) we get

$$\mathfrak{t}_1^{1/4} = \alpha_0 \mathrm{i} \text{ with a real } \alpha_0 = \left[\frac{24}{\omega^{(4)}(k_0)}\right]^{\frac{1}{4}} > 0, \tag{366}$$

and

$$\mathfrak{t}_1 = [\mathfrak{T}_1]_{41} = \alpha_0^4 \text{ with a real } \alpha_0 = \left[\frac{24}{\omega^{(4)}(k_0)}\right]^{\frac{1}{4}} > 0. \tag{367}$$

$$\tilde{\nu}^{1/4} = \mathrm{i}\alpha_0 \nu^{1/4} + O(\nu^{1/2}). \tag{368}$$

Hence, (365) takes the form

$$\eta_j(\nu) = \exp\left\{\mathrm{i}\alpha_0 \varsigma_j \nu^{1/4} + O(\tilde{\nu}^{1/2})\right\}, \quad j = 0, 1, 2, 3. \tag{369}$$

Observe that for $\alpha_0 > 0$, (369) implies that

$$\left|\eta_0(\nu)\right| = \left|\eta_2(\nu)\right| = 1, \quad \left|\eta_1(\nu)\right| < 1, \quad \left|\eta_3(\nu)\right| > 1. \tag{370}$$

Now as it follows from (283) the eigenvalues $\theta_j(\nu)$ of the 4×4 transfer matrix $T(\nu)$ take the form

$$\theta_j(\nu) = \zeta_0 \eta_j(\nu), \quad j = 0, 1, 2, 3. \tag{371}$$

If now we denote

$$\zeta_0 = e^{\mathrm{i}k_0} \text{ where } k_0 \text{ is real}, \tag{372}$$

then (369)–(372) imply

$$\begin{aligned} \theta_j(\nu) &= \exp\left\{\mathrm{i}k_0 + \mathrm{i}\alpha_0 \varsigma_j \nu^{1/4} + O(\nu^{1/2})\right\} \\ &= e^{\mathrm{i}k_0 + \mathrm{i}\alpha_0 \nu^{1/4}}(1 + O(\nu^{1/2})), \quad j = 0, 1, 2, 3. \end{aligned} \tag{373}$$

Observe that

$$|\theta_0(\nu)| = |\theta_2(\nu)| = 1, \quad |\theta_1(\nu)| < 1, \quad |\theta_3(\nu)| > 1. \tag{374}$$

Notice also that (259) implies

$$a_0 = \alpha_0^4 \zeta_0^4 = \frac{24}{\omega^{(4)}(k_0)} \zeta_0^4. \tag{375}$$

It is convenient to introduce

$$\acute{\nu} = \alpha_0 \nu^{1/4}, \tag{376}$$

and to rewrite (373) as

$$\theta_j(\nu) = \exp\{\mathrm{i}k_0 + \mathrm{i}\varsigma_j \acute{\nu} + O(\acute{\nu}^2)\} = e^{\mathrm{i}k_0 + \mathrm{i}\varsigma_j \acute{\nu}}(1 + O(\acute{\nu}^2)), \quad j = 0, 1, 2, 3. \tag{377}$$

8.2.2. Eigenvectors of the transfer matrix. We begin this section with the reminder that we work with the basis in which $T(0)$ *has its canonical Jordan form as in (281)*, namely

$$T(0) = \zeta_0 \begin{bmatrix} 1 & 1 & 0 & 0 \\ 0 & 1 & 1 & 0 \\ 0 & 0 & 1 & 1 \\ 0 & 0 & 0 & 1 \end{bmatrix}.$$

Based on (283), (310), (311), (317) and (318) we can find the eigenvectors $e_j(\nu)$ of $T(\nu)$ corresponding to its eigenvalues $\theta_j(\nu)$.

Recall also that the eigenvectors $e_j(\nu)$, $j = 0, 1, 2, 4$ of the matrix $T(\nu)$ are the respective columns of the matrix $\mathfrak{S}_0(\tilde{\nu})e^{-S(\mathrm{i}\acute{\nu})}$ represented by the asymptotic equality (312). To use (312) we need to find the matrix S_1. Following the appendix 2, first we introduce a decomposition of a square matrix W into its diagonal part $\mathrm{diag}(W)$ and the remaining part $\mathring{W} = W - \mathrm{diag}(W)$ with zero diagonal elements (as in (344))

$$W = [W_{mj}] = \mathrm{diag}(W) + \mathring{W}, \text{ where } \mathrm{diag}(W) = [W_{mj}\delta_{mj}], \ \mathring{W} = W - \mathrm{diag}(W),$$

where δ_{mj} is the Kronecker symbol. Then we get the following expressions for the matrices Λ_1 and S_1

$$\Lambda_1 = \mathrm{diag}(W_1), \quad [S_1]_{nm} = \frac{1}{\varsigma_{m-1} - \varsigma_{n-1}} \left[\mathring{W}_1\right]_{nm}, \quad n \neq m; \ [S_1]_{nn} = 0, \tag{378}$$

where

$$W_1 = \left\langle \widetilde{\mathfrak{T}}_1 \right\rangle_1, \varsigma_0 = 1, \quad \varsigma_1 = \mathrm{i}, \quad \varsigma_2 = -1, \ \varsigma_3 = -\mathrm{i}.$$

Carrying out the operations described in (378), and using (283), (285), (303), (307) we obtain

$$\langle \widetilde{\mathfrak{T}}_1 \rangle_1 = \begin{bmatrix} \tau_1 + \tau_2 & \tau_1 + \tau_2\varsigma_1 & \tau_1 + \tau_2\varsigma_2 & \tau_1 + \tau_2\varsigma_3 \\ \varsigma_1(\tau_1\varsigma_1 + \tau_2) & \varsigma_1^2(\tau_1 + \tau_2) & \varsigma_1(\tau_1\varsigma_1 + \tau_2\varsigma_2) & \varsigma_1(\tau_1\varsigma_1 + \tau_2\varsigma_3) \\ \varsigma_2(\tau_1\varsigma_2 + \tau_2) & \varsigma_2(\tau_1\varsigma_2 + \tau_2\varsigma_1) & \varsigma_2^2(\tau_1 + \tau_2) & \varsigma_2(\tau_1\varsigma_2 + \tau_2\varsigma_3) \\ \varsigma_3(\tau_1\varsigma_3 + \tau_2) & \varsigma_3(\tau_1\varsigma_3 + \tau_2\varsigma_1) & \varsigma_3(\tau_1\varsigma_3 + \tau_2\varsigma_2) & \varsigma_3^2(\tau_1 + \tau_2) \end{bmatrix}, \tag{379}$$

$$\tau_1 = \frac{[T_1]_{31}}{4\zeta_0 \mathfrak{t}_1}, \quad \tau_2 = \frac{[T_1]_{42}}{4\zeta_0 \mathfrak{t}_1},$$

$$S_1 = \begin{bmatrix} 0 & \frac{\tau_1 + \tau_2\varsigma_1}{\varsigma_1 - 1} & \frac{\tau_1 + \tau_2\varsigma_2}{\varsigma_2 - 1} & \frac{\tau_1 + \tau_2\varsigma_3}{\varsigma_3 - 1} \\ \frac{\varsigma_1(\tau_1\varsigma_1 + \tau_2)}{1 - \varsigma_1} & 0 & \frac{\varsigma_1(\tau_1\varsigma_1 + \tau_2\varsigma_2)}{\varsigma_2 - \varsigma_1} & \frac{\varsigma_1(\tau_1\varsigma_1 + \tau_2\varsigma_3)}{\varsigma_3 - 1} \\ \frac{\varsigma_2(\tau_1\varsigma_2 + \tau_2)}{1 - \varsigma_2} & \frac{\varsigma_2(\tau_1\varsigma_2 + \tau_2\varsigma_1)}{\varsigma_1 - \varsigma_2} & 0 & \frac{\varsigma_2(\tau_1\varsigma_2 + \tau_2\varsigma_3)}{\varsigma_3 - 1} \\ \frac{\varsigma_3(\tau_1\varsigma_3 + \tau_2)}{1 - \varsigma_3} & \frac{\varsigma_3(\tau_1\varsigma_3 + \tau_2\varsigma_1)}{\varsigma_1 - \varsigma_3} & \frac{\varsigma_3(\tau_1\varsigma_3 + \tau_2\varsigma_2)}{\varsigma_2 - \varsigma_3} & 0 \end{bmatrix}. \tag{380}$$

The eigenvectors $e_j(\nu)$, $j = 0, 1, 2, 3$ of the matrix $\mathfrak{T}(\nu)$ (and, hence, the matrix $T(\nu)$), corresponding to respectively the eigenvalues $\varsigma_j = \exp(\frac{2\pi \mathrm{i} j}{4})$, $j = 0, 1, 2, 3$ in view of (312) and (347) take the following form

$$e_0(\nu) = \begin{bmatrix} 1 + \mathrm{i}(\tau_1 + 3\tau_2)\acute{\nu} + O(\acute{\nu}^2) \\ \mathrm{i}\acute{\nu} + (\tau_1 - \tau_2)\acute{\nu}^2 + O(\acute{\nu}^3) \\ -\acute{\nu}^2 + \mathrm{i}(3\tau_1 + \tau_2)\acute{\nu}^3 + O(\acute{\nu}^4) \\ -\mathrm{i}\acute{\nu}^3 + 3(\tau_1 - \tau_2)\acute{\nu}^4 + O(\acute{\nu}^5) \end{bmatrix}, \quad e_1(\nu) = \begin{bmatrix} 1 - (\tau_1 + 3\tau_2)\acute{\nu} + O(\acute{\nu}^2) \\ -\acute{\nu} + (\tau_2 - \tau_1)\acute{\nu}^2 + O(\acute{\nu}^3) \\ \acute{\nu}^2 + (3\tau_1 + \tau_2)\acute{\nu}^3 + O(\acute{\nu}^4) \\ -\acute{\nu}^3 + 3(\tau_1 - \tau_2)\acute{\nu}^4 + O(\acute{\nu}^5) \end{bmatrix}, \tag{381}$$

$$e_2(\nu) = \begin{bmatrix} 1 - \mathrm{i}(\tau_1 + 3\tau_2)\acute{\nu} + O(\acute{\nu}^2) \\ -\mathrm{i}\acute{\nu} + (\tau_1 - \tau_2)\acute{\nu}^2 + O(\acute{\nu}^3) \\ -\acute{\nu}^2 - \mathrm{i}(3\tau_1 + \tau_2)\acute{\nu}^3 + O(\acute{\nu}^4) \\ \mathrm{i}\acute{\nu}^3 + 3(\tau_1 - \tau_2)\acute{\nu}^4 + O(\acute{\nu}^5) \end{bmatrix}, \quad e_3(\nu) = \begin{bmatrix} 1 + (\tau_1 + 3\tau_2)\acute{\nu} + O(\acute{\nu}^2) \\ \acute{\nu} + (\tau_2 - \tau_1)\acute{\nu}^2 + O(\acute{\nu}^3) \\ \acute{\nu}^2 - (3\tau_1 + \tau_2)\acute{\nu}^3 + O(\acute{\nu}^4) \\ \acute{\nu}^3 + 3(\tau_1 - \tau_2)\acute{\nu}^4 + O(\acute{\nu}^5) \end{bmatrix},$$

$$\tau_1 = \frac{[T_1]_{31}}{8\zeta_0 \mathfrak{t}_1}, \quad \tau_2 = \frac{[T_1]_{42}}{8\zeta_0 \mathfrak{t}_1}.$$

The equality (381), in turn, implies

$$\frac{e_0(\nu) - e_1(\nu)}{(1 + \mathrm{i})\acute{\nu}} = \begin{bmatrix} \tau_1 + 3\tau_2 + O(\acute{\nu}) \\ 1 + (1 - \mathrm{i})(\tau_1 - \tau_2)\acute{\nu} + O(\acute{\nu}^2) \\ (\mathrm{i} - 1)\acute{\nu} + (3\tau_1 + \tau_2)\acute{\nu}^2 + O(\acute{\nu}^3) \\ -\mathrm{i}\acute{\nu}^2 + O(\acute{\nu}^3) \end{bmatrix}. \tag{382}$$

Consequently,

$$\lim_{\nu \to 0} e_0(\nu) = \begin{bmatrix} 1 \\ 0 \\ 0 \\ 0 \end{bmatrix}, \quad \lim_{\nu \to 0} \frac{e_j(\nu) - e_0(\nu)}{\mathrm{i}(\varsigma_j - 1)\acute{\nu}} = \begin{bmatrix} \tau_1 + 3\tau_2 \\ 1 \\ 0 \\ 0 \end{bmatrix}, \quad j = 1, 2, 3, \tag{383}$$

$$\tau_1 = \frac{[T_1]_{31}}{8\zeta_0 \mathfrak{t}_1}, \quad \tau_2 = \frac{[T_1]_{42}}{8\zeta_0 \mathfrak{t}_1}.$$

In view of the above and (377), we have the following complete set of eigenvalues and corresponding eigenvectors of $T(\nu)$

$$\theta_0(\nu) = e^{ik_0 + i\acute{\nu}}(1 + O(\acute{\nu}^2)), \quad e_0(\nu) = \begin{bmatrix} 1 + i(\tau_1 + 3\tau_2)\acute{\nu} + O(\acute{\nu}^2) \\ i\acute{\nu} + (\tau_1 - \tau_2)\acute{\nu}^2 + O(\acute{\nu}^3) \\ -\acute{\nu}^2 + i(3\tau_1 + \tau_2)\acute{\nu}^3 + O(\acute{\nu}^4) \\ -i\acute{\nu}^3 + 3(\tau_1 - \tau_2)\acute{\nu}^4 + O(\acute{\nu}^5) \end{bmatrix}, \tag{384}$$

$$\theta_1(\nu) = e^{ik_0 + i\acute{\nu}\varsigma_1}(1 + O(\acute{\nu}^2)), \quad e_1(\nu) = \begin{bmatrix} 1 - (\tau_1 + 3\tau_2)\acute{\nu} + O(\acute{\nu}^2) \\ -\acute{\nu} + (\tau_2 - \tau_1)\acute{\nu}^2 + O(\acute{\nu}^3) \\ \acute{\nu}^2 + (3\tau_1 + \tau_2)\acute{\nu}^3 + O(\acute{\nu}^4) \\ -\acute{\nu}^3 + 3(\tau_1 - \tau_2)\acute{\nu}^4 + O(\acute{\nu}^5) \end{bmatrix},$$

$$\theta_2(\nu) = e^{ik_0 + i\acute{\nu}\varsigma_2}(1 + O(\acute{\nu}^2)), \quad e_2(\nu) = \begin{bmatrix} 1 - i(\tau_1 + 3\tau_2)\acute{\nu} + O(\acute{\nu}^2) \\ -i\acute{\nu} + (\tau_1 - \tau_2)\acute{\nu}^2 + O(\acute{\nu}^3) \\ -\acute{\nu}^2 - i(3\tau_1 + \tau_2)\acute{\nu}^3 + O(\acute{\nu}^4) \\ i\acute{\nu}^3 + 3(\tau_1 - \tau_2)\acute{\nu}^4 + O(\acute{\nu}^5) \end{bmatrix},$$

$$\theta_3(\nu) = e^{ik_0 + i\acute{\nu}\varsigma_2}(1 + O(\acute{\nu}^2)), \quad e_3(\nu) = \begin{bmatrix} 1 + (\tau_1 + 3\tau_2)\acute{\nu} + O(\acute{\nu}^2) \\ \acute{\nu} + (\tau_2 - \tau_1)\acute{\nu}^2 + O(\acute{\nu}^3) \\ \acute{\nu}^2 - (3\tau_1 + \tau_2)\acute{\nu}^3 + O(\acute{\nu}^4) \\ \acute{\nu}^3 + 3(\tau_1 - \tau_2)\acute{\nu}^4 + O(\acute{\nu}^5) \end{bmatrix},$$

$$\tau_1 = \frac{[T_1]_{31}}{8\zeta_0 \mathfrak{t}_1}, \quad \tau_2 = \frac{[T_1]_{42}}{8\zeta_0 \mathfrak{t}_1}.$$

Notice that in view of (374) we always have

$$|\theta_0(\nu)| = 1, \ |\theta_1(\nu)| < 1, \tag{385}$$

implying that the vector $e_0(\nu)$ always corresponds to the frozen mode and the vector $e_1(\nu)$ always corresponds to the evanescent mode, i.e. the one decaying exponentially away from the surface of the photonic crystal.

Hence, in view of (318) and (319), we have the following representation for the eigenvectors $\mathfrak{e}_j(\nu) = \mathcal{G}_0(\nu)e_j(\nu)$, $j = 0, 1, 2, 4$ of the transfer matrix $\mathcal{T}(\nu)$

$$\mathfrak{e}_0(\nu) = \mathcal{G}_0(0) \begin{bmatrix} 1 + i(\tau_1 + 3\tau_2)\acute{\nu} + O(\acute{\nu}^2) \\ i\acute{\nu} + (\tau_1 - \tau_2)\acute{\nu}^2 + O(\acute{\nu}^3) \\ -\acute{\nu}^2 + i(3\tau_1 + \tau_2)\acute{\nu}^3 + O(\acute{\nu}^4) \\ -i\acute{\nu}^3 + O(\acute{\nu}^4) \end{bmatrix}, \tag{386}$$

$$\mathfrak{e}_1(\nu) = \mathcal{G}_0(0) \begin{bmatrix} 1 - (\tau_1 + 3\tau_2)\acute{\nu} + O(\acute{\nu}^2) \\ -\acute{\nu} + (\tau_2 - \tau_1)\acute{\nu}^2 + O(\acute{\nu}^3) \\ \acute{\nu}^2 + (3\tau_1 + \tau_2)\acute{\nu}^3 + O(\acute{\nu}^4) \\ -\acute{\nu}^3 + O(\acute{\nu}^4) \end{bmatrix},$$

$$\mathfrak{e}_2(\nu) = \mathcal{G}_0(0)\begin{bmatrix} 1 - \mathrm{i}(\tau_1 + 3\tau_2)\acute{\nu} + O(\acute{\nu}^2) \\ -\mathrm{i}\acute{\nu} + (\tau_1 - \tau_2)\acute{\nu}^2 + O(\acute{\nu}^3) \\ -\acute{\nu}^2 - \mathrm{i}(3\tau_1 + \tau_2)\acute{\nu}^3 + O(\acute{\nu}^4) \\ \mathrm{i}\acute{\nu}^3 + O(\acute{\nu}^4) \end{bmatrix}, \tag{387}$$

$$\mathfrak{e}_3(\nu) = \mathcal{G}_0(0)\begin{bmatrix} 1 + (\tau_1 + 3\tau_2)\acute{\nu} + O(\acute{\nu}^2) \\ \acute{\nu} + (\tau_2 - \tau_1)\acute{\nu}^2 + O(\acute{\nu}^3) \\ \acute{\nu}^2 - (3\tau_1 + \tau_2)\acute{\nu}^3 + O(\acute{\nu}^4) \\ \acute{\nu}^3 + O(\acute{\nu}^4) \end{bmatrix}.$$

Combining now (386), (387) with (319) and (276) we get the following representations for the eigenvectors $\mathfrak{e}_j(\nu)$

$$\begin{aligned} \mathfrak{e}_0(\nu) &= [1 + \mathrm{i}(\tau_1 + 3\tau_2)\acute{\nu} + O(\acute{\nu}^2)]\mathfrak{f}_0 + [\mathrm{i}\acute{\nu} + (\tau_1 - \tau_2)\acute{\nu}^2 + O(\acute{\nu}^3)]\mathfrak{f}_1 \\ &\quad + [-\acute{\nu}^2 + \mathrm{i}(3\tau_1 + \tau_2)\acute{\nu}^3]\mathfrak{f}_2 - \mathrm{i}\acute{\nu}^3\mathfrak{f}_3 + O(\acute{\nu}^4), \\ \mathfrak{e}_1(\nu) &= [1 - (\tau_1 + 3\tau_2)\acute{\nu} + O(\acute{\nu}^2)]\mathfrak{f}_0 + [-\acute{\nu} + (\tau_2 - \tau_1)\acute{\nu}^2 + O(\acute{\nu}^3)]\mathfrak{f}_1 \\ &\quad + [\acute{\nu}^2 + (3\tau_1 + \tau_2)\acute{\nu}^3]\mathfrak{f}_2 - \acute{\nu}^3\mathfrak{f}_3 + O(\acute{\nu}^4), \\ \mathfrak{e}_2(\nu) &= [1 - \mathrm{i}(\tau_1 + 3\tau_2)\acute{\nu} + O(\acute{\nu}^2)]\mathfrak{f}_0 + [-\mathrm{i}\acute{\nu} + (\tau_1 - \tau_2)\acute{\nu}^2 + O(\acute{\nu}^3)]\mathfrak{f}_1 \\ &\quad + [-\acute{\nu}^2 - \mathrm{i}(3\tau_1 + \tau_2)\acute{\nu}^3]\mathfrak{f}_2 + \mathrm{i}\acute{\nu}^3\mathfrak{f}_3 + O(\acute{\nu}^4), \\ \mathfrak{e}_3(\nu) &= [1 + (\tau_1 + 3\tau_2)\acute{\nu} + O(\acute{\nu}^2)]\mathfrak{f}_0 + [\acute{\nu} + (\tau_2 - \tau_1)\acute{\nu}^2 + O(\acute{\nu}^3)]\mathfrak{f}_1 \\ &\quad + [\acute{\nu}^2 - (3\tau_1 + \tau_2)\acute{\nu}^3]\mathfrak{f}_2 + \acute{\nu}^3\mathfrak{f}_3 + O(\acute{\nu}^4). \end{aligned} \tag{388}$$

It readily follows from (384) and (388) that

$$\lim_{\nu\to 0} e_j(\nu) = \begin{bmatrix} 1 \\ 0 \\ 0 \\ 0 \end{bmatrix}, \quad j = 0, 1, 2, 3, \tag{389}$$

$$\lim_{\nu\to 0} \frac{e_j(\nu) - e_0(\nu)}{\mathrm{i}\acute{\nu}(\varsigma_j - 1)} = \begin{bmatrix} \tau_1 + 3\tau_2 \\ 1 \\ 0 \\ 0 \end{bmatrix}, \quad j = 1, 2, 3.$$

$$\lim_{\nu\to 0} \mathfrak{e}_j(\nu) = \mathfrak{f}_0, \quad j = 0, 1, 2, 3, \tag{390}$$

$$\lim_{\nu\to 0} \frac{\mathfrak{e}_j(\nu) - \mathfrak{e}_0(\nu)}{\mathrm{i}\acute{\nu}(\varsigma_j - 1)} = (\tau_1 + 3\tau_2)\mathfrak{f}_0 + \mathfrak{f}_1, \quad j = 1, 2, 3,$$

indicating, in particular, that all four vectors $\mathfrak{e}_j(\nu)$, $j = 0, 1, 2, 3$ become almost parallel as $\nu \to 0$. To have a nicer way to trace the two-dimensional spaces $\mathrm{Span}\{\mathfrak{e}_0(\nu), \mathfrak{e}_1(\nu)\}$ we introduce the following vector

$$\mathfrak{h}_1(\nu) = \frac{\mathfrak{e}_1(\nu) - \mathfrak{e}_0(\nu)}{\mathrm{i}\acute{\nu}(\varsigma_1 - 1)} = \frac{\mathfrak{e}_1(\nu) - \mathfrak{e}_0(\nu)}{\mathrm{i}\acute{\nu}(\mathrm{i} - 1)} = \frac{\mathfrak{e}_0(\nu) - \mathfrak{e}_1(\nu)}{\acute{\nu}(\mathrm{i} + 1)} = (\tau_1 + 3\tau_2)\mathfrak{f}_0 + \mathfrak{f}_1 + O(\acute{\nu}). \tag{391}$$

Notice that the equalities (390) imply

$$\lim_{\nu\to 0} \mathfrak{h}_1(\nu) = (\tau_1 + 3\tau_2)\mathfrak{f}_0 + \mathfrak{f}_1. \tag{392}$$

Then the relations (390)–(392) yield

$$\mathrm{Span}\{\mathfrak{e}_0(\nu), \mathfrak{e}_1(\nu)\} = \mathrm{Span}\{\mathfrak{e}_0(\nu), \mathfrak{h}_1(\nu)\}, \tag{393}$$

$$\lim_{\nu\to 0} \mathrm{Span}\,\{\mathfrak{e}_0(\nu), \mathfrak{e}_1(\nu)\} = \lim_{\nu\to 0} \mathrm{Span}\{\mathfrak{e}_0(\nu), \mathfrak{h}_1(\nu)\} = \mathrm{Span}\{\mathfrak{f}_0, \mathfrak{f}_1\}.$$

8.3. *Spectrum of the transfer matrix at a degenerate point of order 2*

In this section we derive the asymptotic formulae for the eigenvalues and eigenvectors of the transfer matrix $T(\nu)$ as $\nu = \omega - \omega_0 \to 0$ in the case when the frequency ω_0 is a degenerate point of order 2. In this case since $n = 2$ the transfer matrix $\mathcal{T}(\nu)$ defined by (242) is such that $\mathcal{T}(0)$ is a Jordan block of 2, that follows from the analysis carried out in the previous Section.

Without loss of generality we assume that $\omega_0 = \omega(k_0)$ is a point, say, of local minimum of the dispersion relation $\omega(k)$ in a vicinity of k_0. In the later case for $\nu = \omega - \omega_0 > 0$ and ν small there must be two propagating Bloch modes associated with the chosen branch $\omega(k)$ and two modes which either both are propagating or both are evanescent modes.

8.3.1. Eigenvalues of the transfer matrix. Observe that it follows from (293), (310) the eigenvalues $\eta_0(\nu)$, $\eta_1(\nu)$ of the matrix $I_2 + \mathfrak{T}(\nu)$ from (283) are

$$\eta_0(\nu) = 1 + \sqrt{\tilde{\nu}} + O(\tilde{\nu}), \quad \eta_1(\nu) = 1 - \sqrt{\tilde{\nu}} + O(\tilde{\nu}), \tag{394}$$

or, in view of (297),

$$\eta_0(\nu) = 1 + \sqrt{\mathfrak{t}_1}\sqrt{\nu} + O(\nu), \quad \eta_1(\nu) = 1 - \sqrt{\mathfrak{t}_1}\sqrt{\nu} + O(\nu), \tag{395}$$

where, we recall, according to (291)

$$\varsigma_0 = 1, \quad \varsigma_1 = -1. \tag{396}$$

Notice, that we can recast (395) as

$$\eta_0(\nu) = \exp\{\sqrt{\mathfrak{t}_1}\sqrt{\nu} + O(\nu)\}, \quad \eta_1(\nu) = \exp\{-\sqrt{\mathfrak{t}_1}\sqrt{\nu} + O(\nu)\}. \tag{397}$$

Since we have two propagating modes for sufficiently small positive ν there exists a sufficiently small $\delta > 0$ such that

$$|\eta_0(\nu)| = \eta_1(\nu) = 1 \quad \text{for} \quad |\nu| \le \delta. \tag{398}$$

Using (316) and (317) we get

$$\sqrt{\mathfrak{t}_1} = \alpha_0\,\mathrm{i} \text{ with a real } \alpha_0 = \sqrt{\frac{2}{\omega''(k_0)}} > 0, \tag{399}$$

$$\mathfrak{t}_1 = [\mathfrak{T}_1]_{31} = -\alpha_0^2 \text{ with a real } \alpha_0 = \sqrt{\frac{2}{\omega''(k_0)}} > 0, \tag{400}$$

$$\sqrt{\tilde{\nu}} = \mathrm{i}\alpha_0\sqrt{\nu} + O(\nu). \tag{401}$$

Hence, (397) takes the form

$$\eta_0(\nu) = \exp\{\mathrm{i}\alpha_0\sqrt{\nu} + O(\nu)\}, \quad \eta_1(\nu) = \exp\{-\mathrm{i}\alpha_0\sqrt{\nu} + O(\nu)\}. \tag{402}$$

Now as follows from (283), the eigenvalues $\theta_j(\nu)$ of the 2×2 transfer matrix $T(\nu)$ take the form

$$\theta_j(\nu) = \zeta_0 \eta_j(\nu), \quad j = 0, 1. \tag{403}$$

Recalling that

$$\zeta_0 = e^{\mathrm{i}k_0}, \tag{404}$$

where k_0 is real, we get from (402)–(404)

$$\theta_0(\nu) = \exp\{\mathrm{i}k_0 + \mathrm{i}\alpha_0\sqrt{\nu} + O(\nu)\} = e^{\mathrm{i}k_0 + \mathrm{i}\alpha_0\sqrt{\nu}}(1 + O(\nu)), \tag{405}$$
$$\theta_1(\nu) = \exp\{\mathrm{i}k_0 - \mathrm{i}\alpha_0\sqrt{\nu} + O(\nu)\} = e^{\mathrm{i}k_0 - \mathrm{i}\alpha_0\sqrt{\nu}}(1 + O(\nu)).$$

Notice also that (259) implies

$$a_0 = -\alpha_0^2\zeta_0^2 = \frac{2}{\omega''(k_0)}\zeta_0^2. \tag{406}$$

It is convenient to introduce

$$\acute{\nu} = \alpha_0\sqrt{\nu}, \tag{407}$$

and to rewrite (335) and (337) as

$$\theta_0(\nu) = \exp\{\mathrm{i}k_0 + \mathrm{i}\acute{\nu} + O(\acute{\nu}^2)\} = e^{\mathrm{i}k_0 + \mathrm{i}\acute{\nu}}(1 + O(\acute{\nu}^2)), \tag{408}$$
$$\theta_1(\nu) = \exp\{\mathrm{i}k_0 - \mathrm{i}\acute{\nu} + O(\acute{\nu}^2)\} = e^{\mathrm{i}k_0 - \mathrm{i}\acute{\nu}}(1 + O(\acute{\nu}^2)).$$

8.3.2. Eigenvectors of the transfer matrix. We recall that we work with the basis in which $T(0)$ *has its canonical Jordan form as in (281)*, namely

$$T(0) = \zeta_0 \begin{bmatrix} 1 & 1 \\ 0 & 1 \end{bmatrix}.$$

Based on (283), (310), (311), (317) and (318) we can find the eigenvectors $e_j(\nu)$ of $T(\nu)$ corresponding to its eigenvalues $\theta_j(\nu)$.

Recall also that the eigenvectors $e_j(\nu)$, $j = 0, 1$ of the matrix $T(\nu)$ are the respective columns of the matrix $\mathfrak{S}_0(\tilde{\nu})e^{-S(\mathrm{i}\acute{\nu})}$ represented by the asymptotic equality (312). To use (312) we need to find the matrix S_1 following the section "Perturbation theory for diagonal matrix" in the appendix. Namely, first we introduce a decomposition of a square matrix W into its the diagonal component $\mathrm{diag}(W)$ and the remaining part $\mathring{W} = W - \mathrm{diag}(W)$ with zero diagonal elements, i.e.

$$\Lambda_1 = \mathrm{diag}(W_1), \ [S_1]_{nm} = \frac{1}{\varsigma_{m-1} - \varsigma_{n-1}}[\mathring{W}_1]_{nm}, \ n \neq m; \ [S_1]_{nn} = 0, \tag{409}$$

where

$$W_1 = \langle\widetilde{\mathfrak{T}}_1\rangle_1, \ \varsigma_0 = 1, \ \varsigma_1 = -1,$$

Carrying out the operations described in (409), and using (283), (285), (303), (307) we obtain

$$\langle\widetilde{\mathfrak{T}}_1\rangle_1 = \frac{[T_1]_{22}}{2\zeta_0\mathfrak{t}_1}\begin{bmatrix} 1 & -1 \\ -1 & 1 \end{bmatrix}, \quad S_1 = \frac{[T_1]_{22}}{4\zeta_0\mathfrak{t}_1}\begin{bmatrix} 0 & 1 \\ -1 & 0 \end{bmatrix}. \tag{410}$$

The first two eigenvectors $e_0(\nu)$ and $e_1(\nu)$ of the matrix $\mathfrak{T}(\nu)$ (and, hence, the matrix $T(\nu)$), corresponding to eigenvalues $\varsigma_0 = 1$ and $\varsigma_1 = \mathrm{i}$ in view of (312) and (347) take the following

form

$$e_0(\nu)=\begin{bmatrix}1+\mathrm{i}\tau\acute{\nu}+O(\acute{\nu}^2)\\ \mathrm{i}\acute{\nu}+\mathrm{i}\tau\acute{\nu}^2+O(\acute{\nu}^3)\end{bmatrix},\quad e_1(\nu)=\begin{bmatrix}1-\mathrm{i}\tau\acute{\nu}+O(\acute{\nu}^2)\\ -\mathrm{i}\acute{\nu}+\mathrm{i}\tau\acute{\nu}^2+O(\acute{\nu}^3)\end{bmatrix},\qquad(411)$$

$$\tau=\frac{[T_1]_{22}}{4\zeta_0\mathfrak{t}_1}.$$

Thus using (411) and (405) we get the following complete set of the eigenvalues and corresponding eigenvectors of $T(\nu)$

$$\theta_0(\nu)=e^{\mathrm{i}k_0+\mathrm{i}\acute{\nu}}(1+O(\acute{\nu}^2)),\ e_0(\nu)=\begin{bmatrix}1+\mathrm{i}\tau\acute{\nu}+O(\acute{\nu}^2)\\ \mathrm{i}\acute{\nu}+\mathrm{i}\tau\acute{\nu}^2+O(\acute{\nu}^3)\end{bmatrix},\qquad(412)$$

$$\theta_1(\nu)=e^{\mathrm{i}k_0-\mathrm{i}\acute{\nu}}(1+O(\acute{\nu}^2)),\ e_1(\nu)=\begin{bmatrix}1-\mathrm{i}\tau\acute{\nu}+O(\acute{\nu}^2)\\ -\mathrm{i}\acute{\nu}+\mathrm{i}\tau\acute{\nu}^2+O(\acute{\nu}^3)\end{bmatrix}.$$

Hence, in view of (318) and (319), we have the following representation for the eigenvectors $\mathfrak{e}_j(\nu)=\mathcal{G}_0(\nu)e_j(\nu)$, $j=0,1,2,3$ of the transfer matrix $\mathcal{T}(\nu)$

$$\mathfrak{e}_0(\nu)=\mathcal{G}_0(0)\begin{bmatrix}1+\mathrm{i}\tau\acute{\nu}+O(\acute{\nu}^2)\\ \mathrm{i}\acute{\nu}+O(\acute{\nu}^2)\\ O(\acute{\nu}^2)\\ O(\acute{\nu}^2)\end{bmatrix},\quad \mathfrak{e}_1(\nu)=\mathcal{G}_0(0)\begin{bmatrix}1-\mathrm{i}\tau\acute{\nu}+O(\acute{\nu}^2)\\ -\mathrm{i}\acute{\nu}+O(\acute{\nu}^2)\\ O(\acute{\nu}^2)\\ O(\acute{\nu}^2)\end{bmatrix},\qquad(413)$$

$$\mathfrak{e}_2(\nu)=\mathcal{G}_0(0)\begin{bmatrix}O(\acute{\nu}^2)\\ O(\acute{\nu}^2)\\ 1+O(\acute{\nu}^2)\\ O(\acute{\nu}^2)\end{bmatrix},\quad \mathfrak{e}_3(\nu)=\mathcal{G}_0(0)\begin{bmatrix}O(\acute{\nu}^2)\\ O(\acute{\nu}^2)\\ O(\acute{\nu}^2)\\ 1+O(\acute{\nu}^2)\end{bmatrix}.\qquad(414)$$

Combining now (413) with (319) and (276) we get the following representations for the eigenvectors $\mathfrak{e}_j(\nu)$

$$\mathfrak{e}_0(\nu)=[1+\mathrm{i}\tau\acute{\nu}]\mathfrak{f}_0+\mathrm{i}\acute{\nu}\mathfrak{f}_1+O(\acute{\nu}^2),\quad \mathfrak{e}_1(\nu)=[1-\mathrm{i}\tau\acute{\nu}]\mathfrak{f}_0-\mathrm{i}\acute{\nu}\mathfrak{f}_1+O(\acute{\nu}^2),\qquad(415)$$

$$\mathfrak{e}_2(\nu)=\mathfrak{f}_2+O(\acute{\nu}^2),\quad \mathfrak{e}_3(\nu)=\mathfrak{f}_3+O(\acute{\nu}^2).$$

It readily follows from (413) and (415) that,

$$\lim_{\nu\to0}e_j(\nu)=\begin{bmatrix}1\\0\end{bmatrix},\quad j=0,1;\ \lim_{\nu\to0}\frac{e_1(\nu)-e_0(\nu)}{-2\mathrm{i}\acute{\nu}}=\begin{bmatrix}\tau\\1\end{bmatrix},\quad \tau=\frac{[T_1]_{22}}{4\zeta_0\mathfrak{t}_1}.\qquad(416)$$

$$\lim_{\nu\to0}\mathfrak{e}_j(\nu)=\mathfrak{f}_0,\quad j=0,1;\lim_{\nu\to0}\frac{\mathfrak{e}_1(\nu)-\mathfrak{e}_0(\nu)}{-2\mathrm{i}\acute{\nu}}=\tau\mathfrak{f}_0+\mathfrak{f}_1,\quad \tau=\frac{[T_1]_{22}}{4\zeta_0\mathfrak{t}_1}.\qquad(417)$$

indicating, in particular, that the two vectors $\mathfrak{e}_0(\nu)$ and $\mathfrak{e}_1(\nu)$ become almost parallel as $\nu\to0$. To have a nicer way to trace the two-dimensional spaces $\mathrm{Span}\{\mathfrak{e}_0(\nu),\mathfrak{e}_1(\nu)\}$ we introduce the following vector

$$\mathfrak{h}_1(\nu)=\frac{\mathfrak{e}_1(\nu)-\mathfrak{e}_0(\nu)}{-2\mathrm{i}\acute{\nu}}.\qquad(418)$$

Notice that the equalities (417) and (418) imply

$$\lim_{\nu\to0}\mathfrak{h}_1(\nu)=\tau\mathfrak{f}_0+\mathfrak{f}_1,\quad \tau=\frac{[T_1]_{22}}{4\zeta_0\mathfrak{t}_1}.\qquad(419)$$

Then the relations (418)–(419) yield

$$\begin{aligned} \operatorname{Span}\{\mathfrak{e}_0(\nu), \mathfrak{e}_1(\nu)\} &= \operatorname{Span}\{\mathfrak{e}_0(\nu), \mathfrak{h}_1(\nu)\}, \\ \lim_{\nu\to 0} \operatorname{Span}\{\mathfrak{e}_0(\nu), \mathfrak{e}_1(\nu)\} &= \lim_{\nu\to 0} \operatorname{Span}\{\mathfrak{e}_0(\nu), \mathfrak{h}_1(\nu)\} = \operatorname{Span}\{\mathfrak{f}_0, \mathfrak{f}_1\}. \end{aligned} \tag{420}$$

9. Transfer matrix and the flux

9.1. *Transfer matrix and the flux for an inflection point*

The case of an inflection point is the case with degeneracy index $n = 3$. In this case according to (249), the matrix $T(\nu)$ is a 3×3 matrix and $W(\nu)$ is a 1×1 matrix, i.e. just a complex number $W(\nu)$. Let the matrix $T(\nu)$ be defined by (249). Consider first the matrix at the frequency of the frozen mode ω_0, i.e. for $\nu = 0$:

$$T(0) = T_0 = \zeta_0(I_3 + D_0), \quad |\zeta_0| = 1, \quad D_0^3 = 0 \quad \text{and } D_0^2 \neq 0. \tag{421}$$

Then there exists a canonical basis f_0, f_1, f_2 related to the matrix D such that

$$D_0^3 f_2 = 0, \quad f_0 = D_0^2 f_2, \quad f_1 = D_0 f_2. \tag{422}$$

In fact, the basis f_0, f_1, f_2 is not unique and is defined up to some transformations. The equalities (421) and (422) imply the following representation for T_0

$$\zeta_0^{-1} T_0 f_0 = f_0, \quad \zeta_0^{-1} T_0 f_1 = f_1 + f_0, \quad \zeta_0^{-1} T_0 f_2 = f_2 + f_1. \tag{423}$$

or, in the basis f_0, f_1, f_2 we have

$$T_0 = \zeta_0 \begin{bmatrix} 1 & 1 & 0 \\ 0 & 1 & 1 \\ 0 & 0 & 1 \end{bmatrix}, \quad \det T_0 = \zeta_0^3. \tag{424}$$

In addition to that, (249) and (424) imply $\det \mathcal{T}(\nu) = \det T(0) W(0) = \zeta_0^3 W(0) = 1$, and, since $|\zeta_0| = 1$ we get

$$W(0) = \zeta_0^{-3}, \quad |W(0)| = 1. \tag{425}$$

We reiterate that our fundamental assumption is that ζ_0 is triply degenerate and $W(0)$ is an eigenvalue of $\mathcal{T}(0)$ that differs from ζ_0, i.e.

$$W(0) \neq \zeta_0. \tag{426}$$

Observe now that since according to (425) $|W(0)| = 1$ then $\overline{W(0)} = [W(0)]^{-1}$ and, hence, the relation (426) can be rewritten as

$$\zeta_0 \overline{W(0)} \neq 1. \tag{427}$$

Recalling again the relation (249) between the 3×3 matrix $T(0)$ and the original 4×4 matrix $\mathcal{T}(0)$ we introduce a basis $\mathfrak{f}_0$, $\mathfrak{f}_1$, $\mathfrak{f}_2$, $\mathfrak{f}_3$ in the four-dimensional space such that

$$f_j = P_3 \mathcal{S}^{-1}(0) \mathfrak{f}_j, \quad j = 0, 1, 2, \quad \text{where } P_3 \begin{bmatrix} X_1 \\ X_2 \\ X_3 \\ X_4 \end{bmatrix} = \begin{bmatrix} X_1 \\ X_2 \\ X_3 \end{bmatrix}. \tag{428}$$

and the fourth vector $\mathfrak{f}_3$ is the eigenvector $\mathcal{T}(0)$ related to the eigenvalue $W(0)$. Evidently the vectors $\mathfrak{f}_0$, $\mathfrak{f}_1$, $\mathfrak{f}_2$ are 4-dimensional representation of respective vectors f_0, f_1, f_2. Based on the above and the relations (423) we get

$$\mathcal{T}_0\mathfrak{f}_0 = \zeta_0\mathfrak{f}_0, \quad \mathcal{T}_0\mathfrak{f}_1 = \zeta_0\mathfrak{f}_1 + \zeta_0\mathfrak{f}_0, \quad \mathcal{T}_0\mathfrak{f}_2 = \zeta_0\mathfrak{f}_2 + \zeta_0\mathfrak{f}_1, \tag{429}$$

$$\mathcal{T}_0\mathfrak{f}_3 = W(0)\mathfrak{f}_3. \tag{430}$$

In particular, the matrix $\mathcal{T}_0$ has just two genuine eigenvectors $\mathfrak{f}_0$ and $\mathfrak{f}_3$ with corresponding distinct eigenvalues ζ_0 and $W(0)$. The vectors $\mathfrak{f}_0$ and $\mathfrak{f}_3$ correspond respectively to the frozen mode and the only propagating mode at the origin. The vectors $\mathfrak{f}_1$ and $\mathfrak{f}_2$ correspond respectively to linearly and quadratically growing Floquet modes at the origin.

Recall now that $\mathcal{T}_0$ is a J-unitary matrix, i.e.

$$\mathcal{T}_0^\dagger J\mathcal{T}_0 = J, \quad [\mathcal{T}_0\Phi_1, \mathcal{T}_0\Phi_2] = [\Phi_1, \Phi_2] \quad \text{for any } \Phi_1, \Phi_2. \tag{431}$$

Using (429) and (431) we obtain the following identities

$$[\mathfrak{f}_0, \mathfrak{f}_1] = [\mathcal{T}_0\mathfrak{f}_0, \mathcal{T}_0\mathfrak{f}_1] = [\mathfrak{f}_0, \mathfrak{f}_1 + \mathfrak{f}_0] = [\mathfrak{f}_0, \mathfrak{f}_1] + [\mathfrak{f}_0, \mathfrak{f}_0], \tag{432}$$

$$[\mathfrak{f}_0, \mathfrak{f}_2] = [\mathcal{T}_0\mathfrak{f}_0, \mathcal{T}_0\mathfrak{f}_2] = [\mathfrak{f}_0, \mathfrak{f}_2 + \mathfrak{f}_1] = [\mathfrak{f}_0, \mathfrak{f}_2] + [\mathfrak{f}_0, \mathfrak{f}_1], \tag{433}$$

readily implying that

$$[\mathfrak{f}_0, \mathfrak{f}_0] = 0, \quad [\mathfrak{f}_0, \mathfrak{f}_1] = 0. \tag{434}$$

Then using (429), (431) again we get

$$[\mathfrak{f}_1, \mathfrak{f}_2] = [\mathcal{T}_0\mathfrak{f}_1, \mathcal{T}_0\mathfrak{f}_2] = [\mathfrak{f}_1 + \mathfrak{f}_0, \mathfrak{f}_2 + \mathfrak{f}_1] = [\mathfrak{f}_1, \mathfrak{f}_2] + [\mathfrak{f}_0, \mathfrak{f}_2] + [\mathfrak{f}_1, \mathfrak{f}_1] + [\mathfrak{f}_0, \mathfrak{f}_1]. \tag{435}$$

The equalities (434) together with (435) yield

$$[\mathfrak{f}_0, \mathfrak{f}_2] + [\mathfrak{f}_1, \mathfrak{f}_1] = 0. \tag{436}$$

and, since $[\mathfrak{f}_1, \mathfrak{f}_1]$ is a real number, we consequently have

$$[\mathfrak{f}_0, \mathfrak{f}_2] = [\mathfrak{f}_2, \mathfrak{f}_0] = -[\mathfrak{f}_1, \mathfrak{f}_1], \quad \mathrm{Im}\{[\mathfrak{f}_0, \mathfrak{f}_2]\} = 0. \tag{437}$$

We also have the relation

$$[\mathfrak{f}_1, \mathfrak{f}_1] = [\mathcal{T}_0\mathfrak{f}_1, \mathcal{T}_0\mathfrak{f}_1] = [\mathfrak{f}_1 + \mathfrak{f}_0, \mathfrak{f}_1 + \mathfrak{f}_0] = [\mathfrak{f}_1, \mathfrak{f}_1] + [\mathfrak{f}_0, \mathfrak{f}_1] + [\mathfrak{f}_1, \mathfrak{f}_0] + [\mathfrak{f}_0, \mathfrak{f}_0], \tag{438}$$

but, in view of (434), it is already satisfied and does not produce a new relation. The remaining relation is

$$[\mathfrak{f}_2, \mathfrak{f}_2] = [\mathcal{T}_0\mathfrak{f}_2, \mathcal{T}_0\mathfrak{f}_2] = [\mathfrak{f}_2 + \mathfrak{f}_1, \mathfrak{f}_2 + \mathfrak{f}_1] = [\mathfrak{f}_2, \mathfrak{f}_2] + [\mathfrak{f}_1, \mathfrak{f}_2] + [\mathfrak{f}_2, \mathfrak{f}_1] + [\mathfrak{f}_1, \mathfrak{f}_1], \tag{439}$$

yielding

$$[\mathfrak{f}_1, \mathfrak{f}_2] + [\mathfrak{f}_2, \mathfrak{f}_1] + [\mathfrak{f}_1, \mathfrak{f}_1] = 0. \tag{440}$$

Notice that for a natural number $m \geq 2$ we have

$$\begin{bmatrix} 1 & 1 & 0 \\ 0 & 1 & 1 \\ 0 & 0 & 1 \end{bmatrix}^m = \begin{bmatrix} 1 & m & \dfrac{(m-1)m}{2} \\ 0 & 1 & m \\ 0 & 0 & 1 \end{bmatrix}. \tag{441}$$

This identity together (429) and (431) imply

$$\left[\zeta_0^{-1}\mathcal{T}_0\right]^m \mathfrak{f}_0 = \mathfrak{f}_0, \quad \mathcal{T}_0^m \mathfrak{f}_1 = \mathfrak{f}_1 + m\mathfrak{f}_0, \tag{442}$$

$$\left[\zeta_0^{-1}\mathcal{T}_0\right]^m \mathfrak{f}_2 = \mathfrak{f}_2 + m\mathfrak{f}_1 + \frac{(m-1)m}{2}\mathfrak{f}_0,$$

$$\left(\left[\zeta_0^{-1}\mathcal{T}_0\right]^m\right)^\dagger J\left[\zeta_0^{-1}\mathcal{T}_0\right]^m = J. \tag{443}$$

Notice that the vectors $\mathcal{T}_0^m\mathfrak{f}_1$ and $\mathcal{T}_0^m\mathfrak{f}_2$ representing the EM field at points mL grow respectively linearly and quadratically as $m \to \infty$.

Using (442) and (443) we obtain

$$[\mathfrak{f}_2, \mathfrak{f}_2] = \left[\mathfrak{f}_2 + m\mathfrak{f}_1 + \frac{(m-1)m}{2}\mathfrak{f}_0, \mathfrak{f}_2 + m\mathfrak{f}_1 + \frac{(m-1)m}{2}\mathfrak{f}_0\right] = [\mathfrak{f}_2, \mathfrak{f}_2] + m^2[\mathfrak{f}_1, \mathfrak{f}_1]$$

$$+ m[\mathfrak{f}_1, \mathfrak{f}_2] + m[\mathfrak{f}_2, \mathfrak{f}_1] + \frac{(m-1)m}{2}([\mathfrak{f}_0, \mathfrak{f}_2] + [\mathfrak{f}_2, \mathfrak{f}_0]), \tag{444}$$

implying

$$m[\mathfrak{f}_1, \mathfrak{f}_1] + [\mathfrak{f}_1, \mathfrak{f}_2] + [\mathfrak{f}_2, \mathfrak{f}_1] + \frac{(m-1)}{2}([\mathfrak{f}_0, \mathfrak{f}_2] + [\mathfrak{f}_2, \mathfrak{f}_0]) = 0. \tag{445}$$

Combining (445) with (437) we get

$$[\mathfrak{f}_1, \mathfrak{f}_1] + [\mathfrak{f}_1, \mathfrak{f}_2] + [\mathfrak{f}_2, \mathfrak{f}_1] = 0. \tag{446}$$

which is identical to (440). Consider now

$$[\mathfrak{f}_2, \mathfrak{f}_1] = \left[\mathfrak{f}_2 + m\mathfrak{f}_1 + \frac{(m-1)m}{2}\mathfrak{f}_0, \mathfrak{f}_1 + m\mathfrak{f}_0\right] = [\mathfrak{f}_2, \mathfrak{f}_1] + m[\mathfrak{f}_1, \mathfrak{f}_1] + m[\mathfrak{f}_2, \mathfrak{f}_0], \tag{447}$$

implying

$$[\mathfrak{f}_1, \mathfrak{f}_1] + [\mathfrak{f}_2, \mathfrak{f}_0] = 0, \tag{448}$$

which is equivalent to (436). So, consideration of powers $\mathcal{T}_0^m$ of the transfer matrix have not produced new identities. Observe now that (427), (430) and (131) imply

$$[\mathfrak{f}_0, \mathfrak{f}_3] = 0. \tag{449}$$

Collecting (434), (436), (440) and (449) we get the following system

$$[\mathfrak{f}_0, \mathfrak{f}_0] = 0, \tag{450}$$

$$[\mathfrak{f}_0, \mathfrak{f}_1] = 0, \tag{451}$$

$$[\mathfrak{f}_0, \mathfrak{f}_2] + [\mathfrak{f}_1, \mathfrak{f}_1] = 0, \tag{452}$$

$$[\mathfrak{f}_1, \mathfrak{f}_2] + [\mathfrak{f}_2, \mathfrak{f}_1] + [\mathfrak{f}_1, \mathfrak{f}_1] = 0, \tag{453}$$

$$[\mathfrak{f}_0, \mathfrak{f}_3] = 0. \tag{454}$$

Notice that since J is Hermitian (452) implies

$$\mathrm{Im}\{[\mathfrak{f}_0, \mathfrak{f}_2]\} = \mathrm{Im}\{[\mathfrak{f}_1, \mathfrak{f}_1]\} = 0, \quad [\mathfrak{f}_0, \mathfrak{f}_2] = \mathrm{Re}\{[\mathfrak{f}_0, \mathfrak{f}_2]\}. \tag{455}$$

In addition to that, (452) and (453) yield

$$[\mathfrak{f}_0, \mathfrak{f}_2] = \mathrm{Re}\{[\mathfrak{f}_0, \mathfrak{f}_2]\} = -[\mathfrak{f}_1, \mathfrak{f}_1], \tag{456}$$

$$2\,\mathrm{Re}\{[\mathfrak{f}_1, \mathfrak{f}_2]\} = -[\mathfrak{f}_1, \mathfrak{f}_1]. \tag{457}$$

Let us show now that

$$[\mathfrak{f}_1, \mathfrak{f}_1] \neq 0. \tag{458}$$

Indeed, assume for the sake of the argument that $[\mathfrak{f}_1, \mathfrak{f}_1] = 0$. Then, in view of (450)–(452) and (454) we have

$$[\mathfrak{f}_0, \mathfrak{f}_j] = 0, \quad j = 0, 1, 2, 3, \tag{459}$$

or, in other words,

$$(J\mathfrak{f}_0, \mathfrak{f}_j), \quad j = 0, 1, 2, 3. \tag{460}$$

Since $\mathfrak{f}_0, \mathfrak{f}_1, \mathfrak{f}_2, \mathfrak{f}_3$ is a basis in the 4-dimensional space the relations (460) imply that $J\mathfrak{f}_0 = 0$, and, consequently, that $\mathfrak{f}_0 = 0$ since evidently J is an invertible matrix. $\mathfrak{f}_0 = 0$ is impossible, and we must conclude that the relation (458) holds.

Since $[\mathfrak{f}_1, \mathfrak{f}_1]$ *is the flux corresponding to the Floquet mode described by* f_1 *the relation (458) signifies a fundamental fact that the Floquet mode described by* f_1 *has nonzero flux.*

Observe that (456), (457) and (458) imply

$$2\,\mathrm{Re}\{[\mathfrak{f}_1, \mathfrak{f}_2]\} = \mathrm{Re}\{[\mathfrak{f}_0, \mathfrak{f}_2]\} = -[\mathfrak{f}_1, \mathfrak{f}_1] \neq 0. \tag{461}$$

Notice also that in view of (450), (451) we have

$$[\alpha f_0 + \beta f_1, \alpha f_0 + \beta f_1] = |\beta|^2 [f_1, f_1], \tag{462}$$

$$[f_2 + \alpha f_0 + \beta f_1, f_2 + \alpha f_0 + \beta f_1] = [f_2, f_2] - 2\,\mathrm{Re}\{\alpha\}[f_1, f_1] + 2\,\mathrm{Re}\{\beta[f_2, f_1]\} + |\beta|^2 [f_1, f_1], \tag{463}$$

and, hence, we have:

$$\text{as } u \text{ runs over } \mathrm{Span}\,(f_0, f_1) \frac{[u,u]}{[f_1, f_1]}\text{, then runs over } [0, +\infty), \tag{464}$$

$$\text{as } u \text{ runs over } \mathrm{Span}\,(f_0, f_1, f_2) \frac{[u,u]}{[f_1, f_1]}\text{, then runs over } (-\infty, +\infty). \tag{465}$$

The relation (465) follows from (463) if we set $\beta = 0$ and let α run over all real values $(-\infty, +\infty)$. In other words, for all vectors u from the $\mathrm{Span}(f_0, f_1)$ the corresponding fluxes have the same sign, whereas in the case of $\mathrm{Span}(f_0, f_1, f_2)$ the flux can be any real number.

9.2. *Transfer matrix and the fluxes for a degenerate point of order 4*

In the case of a degenerate point of order 4 the transfer matrix becomes a Jordan block of rank 4 and according to (269) there exists a basis $\mathfrak{f}_j$, $j = 0, 1, 2, 3$ in $\mathbb{C}^4$ for which we have

$$\mathcal{T}_0\mathfrak{f}_0 = \zeta_0\mathfrak{f}_0, \ \mathcal{T}_0\mathfrak{f}_1 = \zeta_0\mathfrak{f}_1 + \zeta_0\mathfrak{f}_0, \ \mathcal{T}_0\mathfrak{f}_2 = \zeta_0\mathfrak{f}_2 + \zeta_0\mathfrak{f}_1, \tag{466}$$

$$\mathcal{T}_0\mathfrak{f}_3 = \zeta_0\mathfrak{f}_3 + \zeta_0\mathfrak{f}_2. \tag{467}$$

Notice that the three equations (466) are exactly the same as the three equations (429) for the inflection point. Hence, the identities (450)–(453) in this case are

$$[\mathfrak{f}_0, \mathfrak{f}_0] = 0, \tag{468}$$

$$[\mathfrak{f}_0, \mathfrak{f}_1] = 0, \tag{469}$$

$$[\mathfrak{f}_0, \mathfrak{f}_2] + [\mathfrak{f}_1, \mathfrak{f}_1] = 0, \tag{470}$$

$$[\mathfrak{f}_1, \mathfrak{f}_2] + [\mathfrak{f}_2, \mathfrak{f}_1] + [\mathfrak{f}_1, \mathfrak{f}_1] = 0. \tag{471}$$

Using now (431), (466) and (467) we obtain

$$[\mathfrak{f}_0, \mathfrak{f}_3] = [\mathcal{T}_0\mathfrak{f}_0, \mathcal{T}_0\mathfrak{f}_3] = [\mathfrak{f}_0, \mathfrak{f}_3 + \mathfrak{f}_2], \tag{472}$$

implying

$$[\mathfrak{f}_0, \mathfrak{f}_2] = 0, \tag{473}$$

which together with (470) and (471) yields

$$[\mathfrak{f}_1, \mathfrak{f}_1] = 0, \quad [\mathfrak{f}_1, \mathfrak{f}_2] + [\mathfrak{f}_2, \mathfrak{f}_1] = 0. \tag{474}$$

Observe an important difference of the case of a degenerate band edge compared to the case of an inflection point. Namely, as follows from (474) in the case of a degenerate point of order 4 we have $[\mathfrak{f}_1, \mathfrak{f}_1] = 0$ where in the case of an inflection point, according to (458), $[\mathfrak{f}_1, \mathfrak{f}_1] \neq 0$.

Using again (431) together with (466), (467) and (473) we get

$$[\mathfrak{f}_1, \mathfrak{f}_3] = [\mathcal{T}_0\mathfrak{f}_1, \mathcal{T}_0\mathfrak{f}_3] = [\mathfrak{f}_1 + \mathfrak{f}_0, \mathfrak{f}_3 + \mathfrak{f}_2] = [\mathfrak{f}_1, \mathfrak{f}_3] + [\mathfrak{f}_0, \mathfrak{f}_3] + [\mathfrak{f}_1, \mathfrak{f}_2] + [\mathfrak{f}_0, \mathfrak{f}_2], \tag{475}$$

readily implying

$$[\mathfrak{f}_0, \mathfrak{f}_3] + [\mathfrak{f}_1, \mathfrak{f}_2] = 0. \tag{476}$$

Summarizing (468)–(471), (473), (474), (476)

$$[\mathfrak{f}_0, \mathfrak{f}_0] = 0, \ [\mathfrak{f}_0, \mathfrak{f}_1] = 0, \quad [\mathfrak{f}_1, \mathfrak{f}_1] = 0, \quad [\mathfrak{f}_0, \mathfrak{f}_2] = 0, \tag{477}$$

and

$$[\mathfrak{f}_1, \mathfrak{f}_2] + [\mathfrak{f}_2, \mathfrak{f}_1] = 0, \quad [\mathfrak{f}_0, \mathfrak{f}_3] + [\mathfrak{f}_1, \mathfrak{f}_2] = 0. \tag{478}$$

Notice that the first identity in (478) implies that $[\mathfrak{f}_1, \mathfrak{f}_2]$ is pure imaginary, i.e.

$$\mathrm{Re}\{[\mathfrak{f}_1, \mathfrak{f}_2]\} = 0, \quad [\mathfrak{f}_1, \mathfrak{f}_2] = \mathrm{i}\,\mathrm{Im}[\mathfrak{f}_1, \mathfrak{f}_2]. \tag{479}$$

In particular, the first three identities in (477) imply that

$$\text{for any } \mathfrak{f} \in \mathrm{Span}\{\mathfrak{f}_0, \mathfrak{f}_1\} : [\mathfrak{f}, \mathfrak{f}] = 0. \tag{480}$$

As we have already pointed out this behavior of fluxes reflected by (480) is very different from the case of an inflection point for which always $[\mathfrak{f}_1, \mathfrak{f}_1] \neq 0$.

9.3. *Transfer matrix and the fluxes for a degenerate point of order 2*

In the case of a degenerate point of order 2 the transfer matrix has a Jordan block of rank 2 and according to (269) there exists a basis $\mathfrak{f}_j$, $j = 0, 1, 2, 3$ in $\mathbb{C}^4$ for which we have

$$\mathcal{T}_0\mathfrak{f}_0 = \zeta_0\mathfrak{f}_0, \quad \mathcal{T}_0\mathfrak{f}_1 = \zeta_0\mathfrak{f}_1 + \zeta_0\mathfrak{f}_0, \quad |\zeta_0| = 1, \tag{481}$$

$$\mathcal{T}_0\mathfrak{f}_2 = \zeta\mathfrak{f}_2, \quad \zeta \neq \zeta_0, \tag{482}$$

where $|\zeta| = 1$ or $|\zeta| \neq 1$. There are some additional relations not given here. Notice that for (481) the relation (432) applies yielding

$$[\mathfrak{f}_0, \mathfrak{f}_0] = 0. \tag{483}$$

Observe that since $\zeta \neq \zeta_0$, in both cases we have $|\zeta| = 1$ or $|\zeta| \neq 1$, in view of (131) and (133), then

$$[\mathfrak{f}_0, \mathfrak{f}_2] = 0. \tag{484}$$

Notice that $\zeta \neq \zeta_0$ implies $\overline{\zeta_0}\zeta \neq 1$. Using (431) together with (481) and (482) we obtain

$$[\mathfrak{f}_1, \mathfrak{f}_2] = [\mathcal{T}_0\mathfrak{f}_1, \mathcal{T}_0\mathfrak{f}_2] = \overline{\zeta_0}\zeta[\mathfrak{f}_1 + \mathfrak{f}_0, \mathfrak{f}_2] = \overline{\zeta_0}\zeta[\mathfrak{f}_1, \mathfrak{f}_2], \tag{485}$$

implying, in view of $\overline{\zeta_0}\zeta \neq 1$,

$$[\mathfrak{f}_1, \mathfrak{f}_2] = 0. \tag{486}$$

Notice that (438) applied in this case yielding

$$[\mathfrak{f}_0, \mathfrak{f}_1] + [\mathfrak{f}_1, \mathfrak{f}_0] = 0. \tag{487}$$

Evidently,

$$\mathrm{Re}[\mathfrak{f}_0, \mathfrak{f}_1] = 0, \quad [\mathfrak{f}_0, \mathfrak{f}_1] = \mathrm{i}\,\mathrm{Im}[\mathfrak{f}_0, \mathfrak{f}_1]. \tag{488}$$

10. Perturbation theory for the matrix of reflection coefficients

In Section 6 we have introduce and studied the matrix ρ of reflection coefficients and its relation to the space $S_{\mathrm{T}}(0; \omega, \mathbf{k}_\tau)$. In this section we study the behavior of the matrix ρ at frequencies ω close to the frequency of a degenerate point ω_0, i.e. as $\nu = \omega - \omega_0 \to 0$. To do that we first describe the space $S_{\mathrm{T}}(0; \omega, \mathbf{k}_\tau)$ by the formula (227) where the vectors Φ_1 and Φ_2 depend on the frequency ν. As we know by now that this dependence has the form (see (309) and the section on the perturbation theory, and also (317))

$$\Phi_j(\nu) = \Phi_{j0} + \Phi_{j0}\acute{\nu} + +O(\acute{\nu}^2), \quad j = 1, 2, \tag{489}$$

$$\acute{\nu} = -\mathrm{i}\tilde{\nu}^{\frac{1}{n}} = \alpha_0\nu^{\frac{1}{n}} + O\big(\nu^{\frac{2}{n}}\big), \quad \alpha_0 = \left[\frac{n!}{\omega^{(n)}(k_0)}\right]^{\frac{1}{n}},$$

where $n = 2, 3, 4$ is the degeneracy index. To get an expansion for $\rho(\nu)$ we use the relations (228)-(235). First we need obtain an expansion for the matrices $Q^{\pm}(\nu)$

$$Q^{\pm}(\nu) = Q_0^{\pm} + Q_1^{\pm}\acute{\nu} + O(\acute{\nu}^2), \quad \text{where } Q_0^{\pm} = Q^{\pm}(0), \tag{490}$$

based on (229) and (232). Notice that according to (229) we have

$$Q_0^{\pm} = Q^{\pm}(0) = [Z_1^+ Z_2^+]^{\dagger}[\Phi_1(0)\Phi_2(0)] = \frac{1}{\beta_{\omega,\mathbf{k}_\tau}}\begin{bmatrix}(Z_1^{\pm}, \Phi_1(0)) & (Z_1^{\pm}, \Phi_2(0))\\ (Z_2^{\pm}, \Phi_1(0)) & (Z_2^{\pm}, \Phi_2(0))\end{bmatrix}. \tag{491}$$

We assume that the vectors $\Phi_1(\nu)$ and $\Phi_2(\nu)$ are chosen so that for $\nu = 0$ they are linearly independent, i.e.

$$\{\Phi_1(0), \Phi_2(0)\} = \{\Phi_{10}, \Phi_{20}\} \text{ are linearly independent.} \tag{492}$$

The fulfillment of the condition (492) allows the limit space $\mathrm{Span}\{\Phi_1(\nu), \Phi_2(\nu)\}$ as $\nu \to 0$ to be described as the two-dimensional space $\mathrm{Span}\{\Phi_1(0), \Phi_2(0)\}$. It is also necessary for the invertibility of the matrix $Q^{\pm}(0)$ defined by (491), i.e. for

$$\det Q^{\pm}(0) \neq 0. \tag{493}$$

In fact, we should always have

$$\det Q^{\pm}(\nu) \neq 0 \quad \text{for any } \nu, \tag{494}$$

for any semi-infinite slab problem.

Based on the above, we get the following asymptotic expansions for $[Q^+(\nu)]^{-1}$ and $\rho(\nu)$

$$\begin{aligned}
[Q^+(\nu)]^{-1} &= [Q_0^+]^{-1} - Q_0^+ Q_1^+ [Q_0^+]^{-1} \acute{\nu} + O(\acute{\nu}^2),\\
\rho(\nu) &= Q^-(\nu)[Q^+(\nu)]^{-1} = \{Q_0^- + Q_1^- \acute{\nu} + O(\acute{\nu}^2)\}\{Q_0^+ + Q_1^+ \acute{\nu} + O(\acute{\nu}^2)\}^{-1}\\
&= \{Q_0^- + Q_1^- \acute{\nu} + O(\acute{\nu}^2)\}\{[Q_0^+]^{-1} - Q_0^+ Q_1^+ [Q_0^+]^{-1} \acute{\nu} + O(\acute{\nu}^2)\}\\
&= Q_0^- [Q_0^+]^{-1} - [Q_0^-]^{-1}\{Q_0^- Q_1^- - Q_0^+ Q_1^+\}[Q_0^+]^{-1} \acute{\nu} + O(\acute{\nu}^2), \qquad (495)
\end{aligned}$$

or

$$\begin{aligned}
&\rho(\nu) = \rho_0 + \rho_1 \acute{\nu} + O(\acute{\nu}^2), \quad \text{where}\\
&\rho_0 = Q_0^- [Q_0^+]^{-1},\ \rho_1 = [Q_0^-]^{-1}\{Q_0^- Q_1^- - Q_0^+ Q_1^+\}[Q_0^+]^{-1}. \qquad (496)
\end{aligned}$$

The relation (496) readily implies

$$\rho^\dagger(\nu)\rho(\nu) = \rho_0^\dagger \rho_0 + \rho_0^\dagger \rho_1 \acute{\nu} + \rho_1^\dagger \rho_0 \overline{\acute{\nu}} + O(\acute{\nu}^2) \qquad (497)$$

$$\begin{aligned}
r^2(\alpha^+;\nu) &= \frac{|\rho_0\alpha^+|^2}{|\alpha^+|^2} + \frac{2\,\mathrm{Re}\{(\rho_1\alpha^+, \rho_0\alpha^+)\}}{|\alpha^+|^2}\acute{\nu} + O(\acute{\nu}^2)\\
&= r^2(\alpha^+;0) + \frac{2\,\mathrm{Re}\{(\rho_1\alpha^+, \rho_0\alpha^+)\}}{|\alpha^+|^2}\acute{\nu} + O(\acute{\nu}^2) \qquad (498)
\end{aligned}$$

The relation (498) together with (236) yield the following expression for the flux associated with incident wave described by α^+

$$\begin{aligned}
[\Phi(\alpha^+;\nu), \Phi(\alpha^+;\nu)] &= (1 - r^2(\alpha^+;\nu))|\alpha^+|^2\\
&= \left(1 - \frac{|\rho_0\alpha^+|^2}{|\alpha^+|^2} - \frac{2\,\mathrm{Re}\{(\rho_1\alpha^+, \rho_0\alpha^+)\}}{|\alpha^+|^2}\acute{\nu} + O(\acute{\nu}^2)\right). \qquad (499)
\end{aligned}$$

11. Relevant modes near a degenerate point

In this section we describe in detail the properties of the space of relevant modes $\mathcal{S}_{\mathrm{T}}(0;\omega) = \mathcal{S}_{\mathrm{T}}(0;\omega,\mathbf{k}_\tau)$ (suppressing in the notation its dependence on $\mathbf{k}_\tau$) in a vicinity of a degenerate point for all the three cases, namely, an inflection point, $n = 3$, and band edges of orders $n = 2, 4$.

The general framework determining the basic properties of the space $\mathcal{S}_{\mathrm{T}}(0;\omega)$ has been considered in the subsections "Basic properties of the space of relevant eigenmodes" and "Matrix of reflection coefficients and the flux quadratic form". At this point having investigated the spectral properties of the transfer matrix $\mathcal{T}(\nu)$, $\nu = \omega - \omega_0$ at a degenerate point ω_0 and as $\nu \to 0$ (see Section "Spectral perturbation theory of the transfer matrix a point of degeneracy"), we can provide more details of the properties of $\mathcal{S}_{\mathrm{T}}(0;\omega)$ including the asymptotic behavior of the flux and the reflection coefficients of the relevant eigenmodes for a semi-infinite slab as $\nu \to 0$.

11.1. *Relevant modes near an inflection point*

In this section we study the basic properties of the relevant eigenmodes and, in particular, the space $\mathcal{S}_{\mathrm{T}}(0;\omega)$ as functions of the frequency ω in a vicinity of an inflection point ω_0, i.e. for $\omega = \omega_0 + \nu$ when ν is small.

Using the equalities (357) and (450)–(454) we get the following asymptotic formulae as $\nu \to 0$ for the fluxes

$$[\mathfrak{e}_0(\nu), \mathfrak{e}_0(\nu)] = \acute{\nu}^2[\mathfrak{f}_1, \mathfrak{f}_1] - 2\acute{\nu}^2 \operatorname{Re}[\mathfrak{f}_0, \mathfrak{f}_2] + O(\acute{\nu}^3) = \\ = 3\acute{\nu}^2[\mathfrak{f}_1, \mathfrak{f}_1] + O(\acute{\nu}^3) = 3\alpha_0^2\nu^{2/3}[\mathfrak{f}_1, \mathfrak{f}_1] + O(\nu). \tag{500}$$

where, in view of (339)–(341),

$$\acute{\nu} = \alpha_0\nu^{1/3}, \quad \mathrm{i}\,\mathfrak{t}_1 = \alpha_0^3 = \frac{6}{\omega'''(k_0)}. \tag{501}$$

Notice now that the relations (131–133), together with (357) and (426) yield the following formulae for the fluxes

$$[\mathfrak{e}_1(\nu), \mathfrak{e}_1(\nu)] = [\mathfrak{e}_2(\nu), \mathfrak{e}_2(\nu)] = 0, [\mathfrak{e}_3(\nu), \mathfrak{e}_3(\nu)] = [\mathfrak{f}_3, \mathfrak{f}_3] + O(\nu) \\ [\mathfrak{e}_0(\nu), \mathfrak{e}_1(\nu)] = [\mathfrak{e}_0(\nu), \mathfrak{e}_2(\nu)] = [\mathfrak{e}_0(\nu), \mathfrak{e}_3(\nu)] = 0, \\ [\mathfrak{e}_3(\nu), \mathfrak{e}_0(\nu)] = [\mathfrak{e}_3(\nu), \mathfrak{e}_1(\nu)] = [\mathfrak{e}_3(\nu), \mathfrak{e}_2(\nu)] = 0. \tag{502}$$

To handle in a uniform fashion both positive and negative ν we introduce

$$\mathfrak{e}_1^\sharp(\nu) = \mathfrak{e}_{\operatorname{sign}\nu}(\nu) = \begin{cases} \mathfrak{e}_+(\nu) & \text{if } \nu \geq 0 \\ \mathfrak{e}_-(\nu) & \text{if } \nu < 0 \end{cases}, \quad \theta_1^\sharp(\nu) = \begin{cases} \theta_1(\nu) \text{ if } \nu \geq 0 \\ \theta_2(\nu) \text{ if } \nu < 0 \end{cases}. \tag{503}$$

$$\mathfrak{e}_+(\nu) = \mathfrak{e}_1(\nu), \ \mathfrak{e}_-(\nu) = \mathfrak{e}_2(\nu).$$

Then it follows from (342), (351) that

$$|\theta_1^\sharp(\nu)| = e^{-\frac{\sqrt{3}}{2}|\acute{\nu}|}(1 + O(\acute{\nu}^{2/3})). \tag{504}$$

Notice that, as follows from (500), the vector $\mathfrak{e}_0(\nu)$ has a positive flux and, hence, corresponds to a propagating mode. As to $\mathfrak{e}_1^\sharp(\nu)$, in view of (504), it corresponds to an evanescent mode decaying as $x_3 \to \infty$. So, based on (193), we obtain

$$\mathcal{S}_{\mathrm{T}}(0; \omega_0 + \nu) = \operatorname{Span}\{\mathfrak{e}_0(\nu), \mathfrak{e}_1^\sharp(\nu)\}. \tag{505}$$

Then using (361) one verifies that the following limit exists

$$\mathcal{S}_{\mathrm{T}}(0; \omega_0) = \lim_{\nu \to 0} \mathcal{S}_{\mathrm{T}}(0; \omega_0 + \nu) = \operatorname{Span}\{\mathfrak{f}_0, \mathfrak{f}_1\}. \tag{506}$$

Observe that the representation (506) for the space $\mathcal{S}_{\mathrm{T}}(0; \omega_0)$ together with (458) and (462) yield

$$[\beta_0\mathfrak{f}_0 + \beta_1\mathfrak{f}_1, \beta_0\mathfrak{f}_0 + \beta_1\mathfrak{f}_1] = |\beta_1|^2[\mathfrak{f}_1, \mathfrak{f}_1] \neq 0 \quad \text{if } \beta_1 \neq 0. \tag{507}$$

The relation (507) combined with (226) imply the following very important property of the reflection coefficient $r(\alpha^+; 0)$ at the inflection point ω_0, i.e. $\nu = 0$,

$$\text{for almost all } \alpha^+ \in \mathbb{C}^2 : \text{ the reflection coefficient } r(\alpha^+; 0) < 1. \tag{508}$$

The relation (508) clearly indicates that the reflection coefficients $r(\alpha^+; 0)$ are always strictly less than 1 *for all the relevant eigenmodes of the semi-infinite periodic stack, with the only exception when EM field value of the eigenmode at the surface of the slab is f_0. In other words, at an inflection point there always will be a positive fraction of the incident energy transmitted through the infinite slab. In fact, by proper design of the slab one can achieve almost 100% transmission of the incident energy. In contrast, at any band edges the transmission is always*

exactly zero and the reflection is always 100%, as we will see from the analysis in the following sections.

More elaborate analysis yields asymptotic expressions for the matrix of reflection coefficients ρ, as determined by (232) and (496), and other related quantities for nonzero by small $\nu = \omega - \omega_0$. Indeed, let us use in the relations (229)–(232) the vectors Φ_1 and Φ_2 defined by

$$\Phi_1(\nu) = \mathfrak{e}_0(\nu), \ \ \Phi_2(\nu) = \mathfrak{h}^\sharp(\nu) = \frac{\mathfrak{e}_{\mathrm{sign}(\acute{\nu})}(\nu) - \mathfrak{e}_0(\nu)}{\mathrm{i}\acute{\nu}(\varsigma_{\mathrm{sign}(\acute{\nu})} - 1)}. \tag{509}$$

Notice that (356) and (359) yield the following representation

$$\begin{aligned}
\mathfrak{e}_0(\nu) &= \big(1 + \mathrm{i}\tau_2\acute{\nu} + O(\acute{\nu}^2)\big)\mathfrak{f}_0 + \big(\mathrm{i}\acute{\nu} + \mathrm{i}\tau_1\acute{\nu}^2\big)\mathfrak{f}_1 - \acute{\nu}^2\mathfrak{f}_2 + O(\acute{\nu}^3),\\
\mathfrak{h}^\sharp(\nu) &= [\tau_2 + O(\acute{\nu})]\mathfrak{f}_0 + \left[1 + \frac{\varsigma_{-\mathrm{sign}(\acute{\nu})} - \mathrm{i}}{\mathrm{i}(\varsigma_{\mathrm{sign}(\acute{\nu})} - 1)}\acute{\nu}\right]\mathfrak{f}_1 + \frac{1 - \varsigma_{-\mathrm{sign}(\acute{\nu})}}{\mathrm{i}(\varsigma_{\mathrm{sign}(\acute{\nu})} - 1)}\acute{\nu}\mathfrak{f}_2 + O(\acute{\nu}^2),\\
\tau_2 &= \frac{[T_1]_{32}}{3\zeta_0\mathfrak{t}_1}, \quad \mathrm{i}\mathfrak{t}_1 = \alpha_0^3 = \frac{6}{\omega'''(k_0)}.
\end{aligned} \tag{510}$$

In particular, (509) and (510) yield for $\nu = 0$

$$\Phi_1(0) = \mathfrak{f}_0, \quad \Phi_1(0) = \tau_2\mathfrak{f}_0 + \mathfrak{f}_1, \tag{511}$$

implying that

$$\{\Phi_1(0), \Phi_2(0)\} \quad \text{are linearly independent.} \tag{512}$$

The relation (512) implies that the condition (492) is satisfied.

Now, let find the value $\Phi(\alpha^+;\nu)$ of the eigenmode corresponding to the incident wave α^+. Using (228), (231), (495) we consequently obtain

$$\check{\Phi}(\alpha^+;\nu) = \begin{bmatrix}\varphi_1(\nu)\\ \varphi_2(\nu)\end{bmatrix} = \begin{bmatrix}\varphi_1(0)\\ \varphi_2(0)\end{bmatrix} + O(\acute{\nu}), \quad \begin{bmatrix}\varphi_1(0)\\ \varphi_2(0)\end{bmatrix} = [Q^+(0)]^{-1}\alpha^+. \tag{513}$$

$$\begin{aligned}
\Phi(\alpha^+;\nu) &= \varphi_1(\nu)\Phi_1(\nu) + \varphi_2(\nu)\Phi_2(\nu) = \varphi_1(\nu)\mathfrak{e}_0(\nu) + \varphi_2(\nu)\frac{\mathfrak{e}_{\mathrm{sign}(\acute{\nu})}(\nu) - \mathfrak{e}_0(\nu)}{\mathrm{i}\acute{\nu}(\varsigma_{\mathrm{sign}(\acute{\nu})} - 1)}\\
&= \frac{\varphi_2(0)}{\mathrm{i}\acute{\nu}(\varsigma_{\mathrm{sign}(\acute{\nu})} - 1)}\big[\mathfrak{e}_{\mathrm{sign}(\acute{\nu})}(\nu) - \mathfrak{e}_0(\nu)\big] + O(1).
\end{aligned} \tag{514}$$

Observe that the decomposition (514) of the vector $\Phi(\alpha^+;\nu)$ into a linear combination of eigenvectors $\mathfrak{e}_0(\nu)$ and $\mathfrak{e}_{\mathrm{sign}(\acute{\nu})}(\nu)$ of the transfer matrix $\mathcal{T}(\nu)$ signifies that the amplitude of the eigenmode inside the slab is

$$\frac{\varphi_2(0)}{\mathrm{i}\acute{\nu}(\varsigma_{\mathrm{sign}(\acute{\nu})} - 1)} + O(1). \tag{515}$$

Combining (500), (502) with (510), (513) we get the following formula for the flux

$$[\Phi(\alpha^+;\nu), \ \ \Phi(\alpha^+;\nu)] = \left|\frac{\varphi_2(0)}{\varsigma_+ - 1}\right|^2[\mathfrak{f}_1, \mathfrak{f}_1] + O(\acute{\nu}) = \frac{\{[Q^+(0)]^{-1}\alpha^+\}_2^2}{3}[\mathfrak{f}_1, \mathfrak{f}_1] + O(\acute{\nu}). \tag{516}$$

The formula (516) together with (237) yield

$$t^2(\alpha^+;\nu) = 1 - r^2(\alpha^+;\nu) = \frac{\{[Q^+(0)]^{-1}\alpha^+\}_2^2}{3|\alpha^+|^2}[\mathfrak{f}_1, \mathfrak{f}_1] + O(\acute{\nu}). \tag{517}$$

More accurate computation based on (499), (496) and (508) implies the following asymptotic formulae for the transmission and reflection coefficients

$$t^2(\alpha^+;\nu) = 1 - r^2(\alpha^+;\nu) = 1 - \frac{|\rho_0\alpha^+|^2}{|\alpha^+|^2} - \frac{2\,\mathrm{Re}\{(\rho_1\alpha^+,\,\rho_0\alpha^+)\}}{|\alpha^+|^2}\acute{\nu} + O(\acute{\nu}^2),$$

$$r^2(\alpha^+;\nu) = \frac{|\rho_0\alpha^+|^2}{|\alpha^+|^2} + \frac{2\,\mathrm{Re}\{(\rho_1\alpha^+,\,\rho_0\alpha^+)\}}{|\alpha^+|^2}\acute{\nu} + O(\acute{\nu}^2), \quad \frac{|\rho_0\alpha^+|^2}{|\alpha^+|^2} < 1,$$

$$\rho_0 = Q_0^-[Q_0^+]^{-1}, \quad \rho_1 = [Q_0^-]^{-1}\big\{Q_0^-Q_1^- - Q_0^+Q_1^+\big\}[Q_0^+]^{-1}. \tag{518}$$

Observe that the formulae (518) involve the matrix ρ_1 requiring more terms in the expressions for the eigenvectors $\mathfrak{e}_0(\nu)$ and $\mathfrak{e}_\pm(\nu)$ (namely we need to compute the matrix Λ_2 as defined in the appendix 2). When the exact value of the matrix ρ_1 is found we can find the exact value of the coefficient $\frac{2\,\mathrm{Re}\{(\rho_1\alpha^+,\rho_0\alpha^+)\}}{|\alpha^+|^2}$ in (518). At this point we are interested in the concrete value of $\frac{2\,\mathrm{Re}\{(\rho_1\alpha^+,\rho_0\alpha^+)\}}{|\alpha^+|^2}$ and for that reason we have not carried out the computation of the matrix Λ_2.

11.2. *Relevant modes near a degeneracy point of order 4*

In this section we study the basic properties of the relevant eigenmodes and, in particular, the space $\mathcal{S}_{\mathrm{T}}(0;\omega)$ as functions of the frequency ω in a vicinity of a degenerate point ω_0 of order $n = 4$, i.e. for $\omega = \omega_0 + \nu$ when ν is small. Without loss of generality we assume $\nu \geq 0$.

Notice that the eigenvector $\mathfrak{e}_0(\nu)$ corresponds to the eigenvalue $\theta_1(\nu)$ for which

$$|\theta_0(\nu)| = 1, \tag{519}$$

and, hence, the corresponding eigenmode is a propagating one.

Using the equalities (388) and (477)–(479) we get the following asymptotic formulae as $\nu \to 0$ for the fluxes

$$[\mathfrak{e}_0(\nu),\,\mathfrak{e}_0(\nu)] = 2\acute{\nu}^3\,\mathrm{Im}[\mathfrak{f}_1,\,\mathfrak{f}_2] + O(\acute{\nu}^4),$$

$$\tau_1 = \frac{[T_1]_{31}}{8\zeta_0\mathfrak{t}_1}, \quad \tau_2 = \frac{[T_1]_{42}}{8\zeta_0\mathfrak{t}_1}, \quad \acute{\nu} = \alpha_0\nu^{1/4}, \quad \alpha_0^4 = \frac{4!}{\omega^{(4)}(k_0)}. \tag{520}$$

Notice now in view of (384) the eigenvector $\mathfrak{e}_1(\nu)$ corresponds to the eigenvalue $\theta_1(\nu)$ for which evidently

$$|\theta_1(\nu)| = |e^{\mathrm{i}k_0 + \mathrm{i}\acute{\nu}\varsigma_1}|(1 + O(\acute{\nu}^2)) = e^{-\acute{\nu}}, \quad \acute{\nu} \geq 0, \tag{521}$$

and, hence, the corresponding eigenmode is an evanescent one.

In view of (519) and (521), we can use the relations (131) and (132) yielding

$$[\mathfrak{e}_1(\nu),\,\mathfrak{e}_1(\nu)] = [\mathfrak{e}_1(\nu),\,\mathfrak{e}_0(\nu)] = 0. \tag{522}$$

Hence, as follows from (519) and (520) the vectors $\mathfrak{e}_0(\nu)$ and $\mathfrak{e}_1(\nu)$ correspond respectively to a propagating and evanescent modes. So based on (193) we get

$$\mathcal{S}_{\mathrm{T}}(0;\omega_0+\nu) = \mathrm{Span}\{\mathfrak{e}_0(\nu),\,\mathfrak{e}_1(\nu)\}. \tag{523}$$

Then using (393) one verifies that the following limit exists

$$\mathcal{S}_{\mathrm{T}}(0;\omega_0) = \lim_{\nu\to 0}\mathcal{S}_{\mathrm{T}}(0;\omega_0+\nu) = \mathrm{Span}\{\mathfrak{f}_0,\,\mathfrak{f}_1\}. \tag{524}$$

Notice the representation (524) for the space $\mathcal{S}_{\mathrm{T}}(0;\omega_0)$ together with (480) yield

$$[\mathfrak{f},\,\mathfrak{f}] = 0 \quad \text{for any } \mathfrak{f} \in \mathcal{S}_{\mathrm{T}}(0;\omega_0). \tag{525}$$

The relation (525) combined with (223) and (224) implies the following very important property of the reflection coefficient $r(\alpha^+;0)$ at the inflection point ω_0, i.e. $\nu = 0$,

$$\text{for every } \alpha^+ \in \mathbb{C}^2 \text{the reflection coefficient } r(\alpha^+) = 1 \quad \text{and } \rho^\dagger \rho = I_2. \tag{526}$$

The relation (526) clearly indicates that the reflection coefficient $r(\alpha^+;0)$ is always exactly 1 for all the relevant eigenmodes of semi-infinite periodic stack In other words, at any degenerate point of order $n = 4$, 100% of the incident energy is reflected and, hence, no energy is transmitted. In contrast, at any inflection point a positive fraction of the incident energy is always transmitted.

More elaborate analysis provides asymptotic expressions for the matrix of reflection coefficients ρ, as determined by (232) and (496), and other related quantities for nonzero, but small, $\nu = \omega - \omega_0$. Indeed, let us use in the relations (229)–(232) the vectors Φ_1 and Φ_2 defined by

$$\Phi_1(\nu) = \mathfrak{e}_0(\nu), \quad \Phi_2(\nu) = \mathfrak{h}_1(\nu) = \frac{\mathfrak{e}_0(\nu) - \mathfrak{e}_1(\nu)}{\acute{\nu}(\mathrm{i}+1)}. \tag{527}$$

Notice that (356)–(359) yields the following representation

$$\begin{aligned} \mathfrak{e}_0(\nu) &= \big(1 + \mathrm{i}\tau_2\acute{\nu} + O(\acute{\nu}^2)\big)\mathfrak{f}_0 + \big(\mathrm{i}\acute{\nu} + \mathrm{i}\tau_1\acute{\nu}^2\big)\mathfrak{f}_1 - \acute{\nu}^2\mathfrak{f}_2 + O(\acute{\nu}^3), \\ \mathfrak{h}_1(\nu) &= (\tau_1 + 3\tau_2)\mathfrak{f}_0 + \mathfrak{f}_1 + O(\acute{\nu}). \end{aligned} \tag{528}$$

In particular, (527) and (528) yield for $\nu = 0$

$$\Phi_1(0) = \mathfrak{f}_0, \quad \Phi_1(0) = (\tau_1 + 3\tau_2)\mathfrak{f}_0 + \mathfrak{f}_1,$$

implying that

$$\{\Phi_1(0), \Phi_2(0)\} \quad \text{are linearly independent.} \tag{529}$$

The relation (529) shows that condition (492) is satisfied.

Now let find the value $\Phi(\alpha^+;\nu)$ of the eigenmode corresponding to the incident wave α^+. Using (228), (231) and (495) we consequently obtain

$$\check{\Phi}(\alpha^+;\nu) = \begin{bmatrix} \varphi_1(\nu) \\ \varphi_2(\nu) \end{bmatrix} = \begin{bmatrix} \varphi_1(0) \\ \varphi_2(0) \end{bmatrix} + O(\acute{\nu}), \quad \begin{bmatrix} \varphi_1(0) \\ \varphi_2(0) \end{bmatrix} = \big[Q^+(0)\big]^{-1}\alpha^+. \tag{530}$$

$$\begin{aligned} \Phi(\alpha^+;\nu) &= \varphi_1(\nu)\Phi_1(\nu) + \varphi_2(\nu)\Phi_2(\nu) = \varphi_1(\nu)\mathfrak{e}_0(\nu) + \varphi_2(\nu)\frac{\mathfrak{e}_0(\nu) - \mathfrak{e}_1(\nu)}{\acute{\nu}(\mathrm{i}+1)} \\ &= \frac{\varphi_2(0)}{\acute{\nu}(\mathrm{i}+1)}[\mathfrak{e}_0(\nu) - \mathfrak{e}_1(\nu)] + O(1). \end{aligned} \tag{531}$$

Observe that the decomposition (531) of the vector $\Phi(\alpha^+;\nu)$ into a linear combination of eigenvectors $\mathfrak{e}_0(\nu)$ and $\mathfrak{e}_1(\nu)$ of the transfer matrix $\mathcal{T}(\nu)$ signifies that the amplitude of the eigenmode inside the slab is

$$\frac{\varphi_2(0)}{\acute{\nu}(\mathrm{i}+1)} + O(1). \tag{532}$$

Combining (520) and (522) with (530) and (520) we get the following formula for the flux

$$\begin{aligned} [\Phi(\alpha^+;\nu), \Phi(\alpha^+;\nu)] &= \left|\frac{\varphi_2(0)}{\mathrm{i}+1}\right|^2 2\acute{\nu}\,\mathrm{Im}[\mathfrak{f}_1, \mathfrak{f}_2] + O(\acute{\nu}^2) \\ &= \{[Q^+(0)]^{-1}\alpha^+\}_2^2\,\mathrm{Im}[\mathfrak{f}_1, \mathfrak{f}_2]\acute{\nu} + O(\acute{\nu}^2) \end{aligned} \tag{533}$$

The formula (533) together with (237) yields

$$t^2(\alpha^+;\nu) = 1 - r^2(\alpha^+;\nu) = \frac{\{[Q^+(0)]^{-1}\alpha^+\}_2^2\,\mathrm{Im}[\mathfrak{f}_1,\mathfrak{f}_2]\acute{\nu}}{|\alpha^+|^2}\acute{\nu} + O(\acute{\nu}^2). \tag{534}$$

An alternative computation based on (499), (496) and (526) (which turns into $|\rho_0\alpha^+|^2 = |\alpha^+|^2$ for all α^+) implies the following asymptotic formulae for the transmission and reflection coefficients

$$\begin{aligned} t^2(\alpha^+;\nu) &= 1 - r^2(\alpha^+;\nu) = -\frac{2\,\mathrm{Re}\{(\rho_1\alpha^+,\rho_0\alpha^+)\}}{|\alpha^+|^2}\acute{\nu} + O(\acute{\nu}^2),\\ r^2(\alpha^+;\nu) &= 1 + \frac{2\,\mathrm{Re}\{(\rho_1\alpha^+,\rho_0\alpha^+)\}}{|\alpha^+|^2}\acute{\nu} + O(\acute{\nu}^2),\\ \rho_0 &= Q_0^-[Q_0^+]^{-1}, \quad \rho_1 = [Q_0^-]^{-1}\{Q_0^-Q_1^- - Q_0^+Q_1^+\}[Q_0^+]^{-1}. \end{aligned} \tag{535}$$

11.3. *Relevant modes near a degenerate point of order 2*

In this section we study the basic properties of the relevant eigenmodes and, in particular, the space $\mathcal{S}_{\mathrm{T}}(0;\omega)$ as functions of the frequency ω in a vicinity of a degenerate point ω_0 of order $n = 2$, i.e. for $\omega = \omega_0 + \nu$ when ν is small. Without loss of generality we assume $\nu \geq 0$.

Notice that the eigenvector $\mathfrak{e}_0(\nu)$ corresponds to the eigenvalue $\theta_1(\nu)$ for which

$$\theta_0(\nu) = e^{\mathrm{i}k_0 + \mathrm{i}\acute{\nu}}(1 + O(\acute{\nu}^2)) : |\theta_0(\nu)| = 1, \tag{536}$$

with the corresponding eigenmode propagating in the positive direction.

Using the equalities (415), (483) and (486)–(488) we get the following asymptotic formulae as $\nu \to 0$ for the fluxes

$$[\mathfrak{e}_0(\nu),\mathfrak{e}_0(\nu)] = -2\,\mathrm{Im}[\mathfrak{f}_0,\mathfrak{f}_1]\acute{\nu} + O(\acute{\nu}^2), \quad \acute{\nu} = \alpha_0\sqrt{\nu}, \quad \alpha_0 = \sqrt{\frac{2}{\omega''(k_0)}}. \tag{537}$$

In particular, for $\nu = 0$ the equality (537) implies

$$[\mathfrak{e}_0(0),\mathfrak{e}_0(0)] = 0. \tag{538}$$

Notice that in view of (384) the eigenvector $\mathfrak{e}_1(\nu)$ corresponds to the eigenvalue $\theta_1(\nu)$ for which

$$\theta_0(\nu) = e^{\mathrm{i}k_0 - \mathrm{i}\acute{\nu}}(1 + O(\acute{\nu}^2)) : |\theta_1(\nu)| = 1, \quad \acute{\nu} \geq 0, \tag{539}$$

with the corresponding eigenmode propagating in the negative direction.

In view of (536) and (539), we can use the relations (131) and (133) yielding

$$[\mathfrak{e}_1(\nu),\mathfrak{e}_0(\nu)] = 0. \tag{540}$$

So, unlike in situations for $n = 3, 4$ in the case $n = 2$ only the vector $\mathfrak{e}_0(\nu)$ belongs to the space $\mathcal{S}_{\mathrm{T}}(0;\omega_0+\nu)$, where another one, namely $\mathfrak{e}_1(\nu)$, does not belong to $\mathcal{S}_{\mathrm{T}}(0;\omega_0+\nu)$ since it corresponds to an eigenmode propagating in the negative direction. Hence, the second vector in $\mathcal{S}_{\mathrm{T}}(0;\omega_0+\nu)$ must be one of $\mathfrak{e}_2(\nu)$ and $\mathfrak{e}_3(\nu)$. Without loss of generality we assume that is $\mathfrak{e}_2(\nu)$, and, hence

$$\mathcal{S}_{\mathrm{T}}(0;\omega_0+\nu) = \mathrm{Span}\{\mathfrak{e}_0(\nu),\mathfrak{e}_2(\nu)\}. \tag{541}$$

Now there can be two possibilities: $|\theta_2(\nu)| < 1$ or $|\theta_2(\nu)| = 1$. The most interesting case is

$$|\theta_2(\nu)| < 1, \ \ \nu \geq 0, \tag{542}$$

when the corresponding mode is an evanescent one. Since we are interested to know if there can be any transmission of energy by a mode related to a regular band edge under assumption (542), the only possibility of the transmission will the mode related to the band edge.

In the case of $|\theta_2(\nu)| = 1$ the corresponding mode will be a common one propagating in the positive direction with non-zero velocity. In this case the calculation is similar to the case (542) with the only difference that we have to pick the single eigenmode related to the band edge and find the corresponding flux and the reflection coefficient. For that mode the result is the same as in the case (542).

So, we assume now that the condition (542) is satisfied. Notice that under the condition (542) in view of (131) and (132) we have

$$[\mathfrak{e}_0(\nu), \mathfrak{e}_2(\nu)] = 0, \quad [\mathfrak{e}_2(\nu), \mathfrak{e}_2(\nu)] = 0, \quad \nu \geq 0 \tag{543}$$

Then it follows from (541) that

$$\mathcal{S}_{\mathrm{T}}(0; \omega_0) = \mathrm{Span}\{\mathfrak{e}_0(0), \mathfrak{e}_2(0)\}. \tag{544}$$

Notice the representation (544) for the space $\mathcal{S}_{\mathrm{T}}(0; \omega_0)$ together with (538) and (543) yields

$$[\mathfrak{f}, \mathfrak{f}] = 0 \quad \text{for any } \mathfrak{f} \in \mathcal{S}_{\mathrm{T}}(0; \omega_0). \tag{545}$$

The relation (545) combined with (223) and (224) implies the following very important property of the reflection coefficient $r(\alpha^+; 0)$ at the inflection point ω_0, i.e. $\nu = 0$,

$$\text{for every } \alpha^+ \in \mathbb{C}^2 \text{ the reflection coefficient} \quad r(\alpha^+) = 1 \quad \text{and} \quad \rho^\dagger \rho = I_2. \tag{546}$$

The relation (526) clearly indicates that the reflection coefficient $r(\alpha^+; 0)$ *is always exactly* 1 *for all the relevant eigenmodes of semi-infinite periodic stack related to the band edge.*

More elaborate analysis yields asymptotic expressions for the matrix of reflection coefficients ρ, as determined by (232) and (496), and other related quantities for nonzero, but small, $\nu = \omega - \omega_0$. Indeed, let us use in the relations (229)–(232) the vectors Φ_1 and Φ_2 defined by

$$\Phi_1(\nu) = \mathfrak{e}_0(\nu), \quad \Phi_2(\nu) = \mathfrak{e}_2(\nu). \tag{547}$$

Notice that generically $\mathfrak{e}_0(0)$ and $\mathfrak{e}_2(0)$ are always linearly independent and, hence,

$$\{\Phi_1(0), \Phi_2(0)\} \text{ are linearly independent.} \tag{548}$$

The relation (548) shows that condition (492) is satisfied.

Now let us find the value $\Phi(\alpha^+; \nu)$ of the eigenmode corresponding to the incident wave α^+. Using (228), (231), (495) we consequently obtain

$$\check{\Phi}(\alpha^+; \nu) = \begin{bmatrix} \varphi_1(\nu) \\ \varphi_2(\nu) \end{bmatrix} = \begin{bmatrix} \varphi_1(0) \\ \varphi_2(0) \end{bmatrix} + O(\acute{\nu}), \quad \begin{bmatrix} \varphi_1(0) \\ \varphi_2(0) \end{bmatrix} = [Q^+(0)]^{-1}\alpha^+. \tag{549}$$

$$\Phi(\alpha^+; \nu) = \varphi_1(\nu)\Phi_1(\nu) + \varphi_2(\nu)\Phi_2(\nu) = \varphi_1(0)\mathfrak{e}_0(0) + \varphi_2(0)\mathfrak{e}_2(0) + O(\acute{\nu}) \tag{550}$$

Observe that the decomposition (550) of the vector $\Phi(\alpha^+; \nu)$ into a linear combination of eigenvectors $\mathfrak{e}_0(\nu)$ and $\mathfrak{e}_1(\nu)$ of the transfer matrix $\mathcal{T}(\nu)$ signifies that the amplitude of the eigenmode inside the slab is

$$\varphi_1(0) + O(\acute{\nu}). \tag{551}$$

Combining (537), (543) with (549), (550) we get the following formula for the flux

$$\begin{aligned} [\Phi(\alpha^+; \nu), \Phi(\alpha^+; \nu)] &= -2|\varphi_1(0)|^2 \operatorname{Im}[\mathfrak{f}_0, \mathfrak{f}_1]\acute{\nu} + O(\acute{\nu}^2) \\ &= -2\{[Q^+(0)]^{-1}\alpha^+\}_1^2 \operatorname{Im}[\mathfrak{f}_0, \mathfrak{f}_1]\acute{\nu} + O(\acute{\nu}^2). \end{aligned} \tag{552}$$

The formula (552) together with (237) yields

$$t^2(\alpha^+;\nu)=1-r^2(\alpha^+;\nu)=-\frac{2\{[Q^+(0)]^{-1}\alpha^+\}_1^2\,\mathrm{Im}[\mathfrak{f}_0,\mathfrak{f}_1]}{|\alpha^+|^2}\acute{\nu}+O(\acute{\nu}^2). \tag{553}$$

An alternative computation based on (499), (496) and (546) (which turns into $|\rho_0\alpha^+|^2=|\alpha^+|^2$ for all α^+) implies the following asymptotic formulae for the transmission and reflection coefficients

$$\begin{aligned}
t^2(\alpha^+;\nu)&=1-r^2(\alpha^+;\nu)=-\frac{2\,\mathrm{Re}\{(\rho_1\alpha^+,\rho_0\alpha^+)\}}{|\alpha^+|^2}\acute{\nu}+O(\acute{\nu}^2),\\
r^2(\alpha^+;\nu)&=1+\frac{2\,\mathrm{Re}\{(\rho_1\alpha^+,\rho_0\alpha^+)\}}{|\alpha^+|^2}\acute{\nu}+O(\acute{\nu}^2),\\
\rho_0&=Q_0^-[Q_0^+]^{-1},\quad \rho_1=[Q_0^-]^{-1}\{Q_0^-Q_1^--Q_0^+Q_1^+\}[Q_0^+]^{-1}.
\end{aligned} \tag{554}$$

11.4. *Asymptotic analysis summary*

The final results on the reflection coefficients, transmission and flux are formulated in Section "relevant modes at degenerate points" .

We reiterate that for any relevant eigenmode of a semi-infinite slab the following fundamental relation holds for its energy flux $[\Phi,\Phi]$ and the reflection and transmission coefficients

$$t^2(\alpha^+)=1-r^2(\alpha^+)=\frac{[\Phi(\alpha^+),\Phi(\alpha^+)]}{|\alpha^+|^2}$$

where the two-dimensional vector α^+ describes the incident wave in a properly chosen basis and $\Phi(\alpha^+)$ is the corresponding EM field at the surface of the slab.

One the most important quantitative results of the analysis of the reflection coefficient in a vicinity of band edges and inflection points is summarized by the following formulae for the reflection coefficient r as $\nu=\omega-\omega_0\to 0$

$$\text{inflection point } n=3: r^2=r_0^2+c_{\mathrm{sign}\,\nu}|\nu|^{1/3},\quad 0\le r_0<1;$$

$$\text{regular band edge } n=2: r^2=1-c_0|\nu|^{1/2},\quad \begin{cases}\nu\ge 0 \text{ for a lower edge}\\ \nu\le 0 \text{ for an upper edge}\end{cases};$$

$$\text{degenerate band edge } n=4: r^2=1-c_0|\nu|^{1/4},\quad \begin{cases}\nu\ge 0 \text{ for a lower edge}\\ \nu\le 0 \text{ for an upper edge}\end{cases}.$$

where $c_{\mathrm{sign}\,\nu}$ denotes one of the constants $c_\pm$ corresponding to the sign of ν.

The above formulae for the reflection coefficient indicate clearly that on approach to a band edge the reflection coefficient approaches 1. In contrast, in a vicinity of an inflection point the reflection coefficient approaches a less than 1 number r_0 and can be made arbitrarily small for properly designed structures.

The table below shows the asymptotic behavior of the slow mode group velocity, the saturation amplitude, and the semi-infinite slab transmittance as the frequency approaches the respective stationary point.

Rank of degeneracy	Group velocity	Saturation amplitude	Transmittance
2 (regular band edge)	$\lvert\nu\rvert^{1/2}$	1	$\lvert\nu\rvert^{1/2}$
3 (stationary inflection pint)	$\lvert\nu\rvert^{2/3}$	$\lvert\nu\rvert^{-1/3}$	1
4 (degenerate band edge)	$\lvert\nu\rvert^{3/4}$	$\lvert\nu\rvert^{-1/4}$	$\lvert\nu\rvert^{1/4}$

Using this table we summarize the basic properties of the eigenmodes at frequencies close to the band edges and inflection points as follows.

1. For a regular band edge there are no energy relevant Floquet modes, and as $\nu \to 0$ the group velocity and the maximal flux vanish as $|\nu|^{1/2}$, whereas the saturation amplitude remains finite. The light does slow down in the vicinity of a regular band edge, but only a vanishing fraction enters the photonic slab, while the rest is reflected back to space.
2. For a stationary inflection point there is a relevant Floquet mode at ω_0, and as $\nu = \omega - \omega_0 \to 0$ the group velocity vanishes at the rate $|\nu|^{2/3}$ with the maximal flux remaining finite, and the saturation amplitude diverging as $|\nu|^{-1/3}$. The slab transmittance at $\omega = \omega_0$ remains finite and can even be close to unity.
3. For a 4-fold degenerate band edge, there is a relevant non-Bloch Floquet mode. As $\nu \to 0$, the respective slow mode group velocity vanishes as $|\nu|^{3/4}$, while the saturation amplitude diverges as $|\nu|^{-1/4}$. The transmitted energy flux, along with the slab transmittance, vanishes as $|\nu|^{1/4}$.

12. Summary

Although the existence of slow electromagnetic modes in photonic crystals is quite obvious, the next question is whether and how such modes can be excited by incident light. In other words, we need to know whether or not a significant fraction of the incident light energy can be converted into a slow mode with virtually zero group velocity in a semi-infinite photonic crystal. We have shown that it can be done, but only if the slow mode is associated with a stationary inflection point of the dispersion relation $\omega(k)$. In this special case, the incident light with the proper frequency, polarization, and direction of incidence is completely converted into the slow frozen mode with huge amplitude and vanishingly small group velocity. Such a phenomenon constitute the frozen mode regime. By contrast, if a slow electromagnetic mode relates to a photonic band edge, the incident wave will be reflected back to space. Not every photonic crystal can have the dispersion relation with a stationary inflection point and, thereby, support the frozen mode regime. For instance, one-dimensional periodic arrays (periodic layered structures) must include specially oriented anisotropic layers, in order to support the proper dispersion relation and the frozen mode regime. Photonic crystals with three-dimensional periodicity are not required to have anisotropic constitutive components.

Generally, the possibility of conversion of an incident wave into a slow mode appears to be directly related to the character of the respective Bloch dispersion relation $\omega(k)$ of the periodic structure. This fundamental relation exists regardless of the specific physical realization of the periodic structure supporting such a dispersion relation. For instance, although neither periodically modulated waveguides, nor periodic arrays of coupled resonators are formally photonic crystals, still, as soon as the respective Bloch electromagnetic dispersion relation develops a stationary inflection point, one can expect the frozen mode regime at the respective frequency.

Not every periodic array can have the dispersion relation with a stationary inflection point. Symmetry-based considerations similar to those applied above to the case of periodic layered arrays, can provide a meaningful guidance on how to find the proper structure.

Acknowledgment and Disclaimer

Effort of A. Figotin and I. Vitebskiy is sponsored by the Air Force Office of Scientific Research, Air Force Materials Command, USAF, under grant number FA9550-04-1-0359.

References

[1] Brillouin, L., 1960, Wave Propagation and Group Velocity (Academic, New York).
[2] Landau, L. D., Lifshitz, E. M. and Pitaevskii, L. P., 1984, Electrodynamics of continuous media (Pergamon, N.Y.)
[3] Yariv, A. and Yeh., Pochi, 1984, Optical Waves in Crystals ("A Wiley-Interscience publication").
[4] Sommerfeld, A., 1907, *Phys. Z.*, **8**, 841.
[5] Kuzmich, A., Dogariu, A., Wang, L. J., Milonni, P. W. and Chiao, R. Y., 2001, *Phys. Rev. Lett.*, **86**, 3925.
[6] Boyd, R. W. and Gauthier, D. J., 2002, in Progress in Optics, E. Wolf, Ed (Elsevier, Amsterdam) **43**.
[7] Milonni, P. W., 2002, *J. Phys.*, B 35, R31.
[8] Veselago, V. G., 1968, The electrodynamics of substances with simultaneously negative values of ε and μ Soviet Physics USPEKHI. **10**, 509–514.
[9] Hau, L., Harris, S., Dutton, Z. and Behroozi, C., 1999, Light speed reduction to 17 metres per second in an ultracold atomic gas. *Nature*, **397**, 594–598.
[10] Kash, M., Sautenkov, V., Zibrov, Al., Hollberg, L., Welch, G., Lukin, M., Rostovtsev, Yu., Fry, E. and Scully, M., 1999, Ultraslow group velocity and enhanced nonlinear optical effects in a coherently driven hot atomic gas. *Phys. Rev. Lett.*, **82**, 5229–5232.
[11] Budker, D., Kimball, D. F., Rochester, S. M. and Yashchuk, V. V., 1999, Nonlinear Magneto-optics and Reduced Group Velocity of Light in Atomic Vapor with Slow Ground State Relaxation. *Phys. Rev. Lett.*, **83**, 1767.
[12] Lukin, M. and Imamoglu, A., 2001, Controlling photons using electromagnetically induced transparency. *Nature*, **413**, 273–276.
[13] Phillips, D. F., Fleischhauer, A., Mair, A. Walsworth, R. L. and Lukin, M. D., 2001. Storage of light in atomic vapor. *Phys. Rev. Lett.*, **86**, 783–786.
[14] Turukhin, A. V., Sudarshanam, V. S., Shahriar, M. S., Musser, J. A., Ham, B. S. and Hemmer, P. R., 2002, Observation of ultraslow and stored light pulses in a solid. *Phys. Rev. Lett.*, **88**, 023602.0
[15] Bigelow, Matthew S., Lepeshkin, Nick N. and Boyd, Robert W., 2003, Observation of Ultraslow light propagation in a ruby crystal at room temperature. *Phys. Rev. Lett.* **90**, 113903.
[16] Bigelow, Matthew S., Lepeshkin, Nick N. and Boyd, Robert W., 2003, Superluminal and slow light propagation in a room-temperature solid. *Science*, **301**, 200.
[17] Yanik, M. and Fan., S., 2004, Stopping light all optically. *Phys. Rev. Lett.*, **92**, 083901.
[18] Heebner, J. and Boyd., R., 2002, Slow and stopped light. 'Slow' and 'fast' light in resonator-coupled waveguides. *Journal of modern optics*, **49**, 2629.
[19] Heebner, J. and Boyd, R., 2002, Slow light, induced dispersion, enhanced nonlinearity, and optical solitons in a resonator-array waveguide. *Phys. Rev., E***65**, 036619.
[20] Melloni, A., Morichetti, F. and Maritelli, M., 2003, Linear and nonlinear pulse propagation in coupled resonator slow-wave optical structures. *Optical and Quantum Electronics*, **35**, 365.
[21] Poon, J., Scheuer, J., Xu, Y. and Yariv, A., 2004, Designing coupled-resonator optical waveguide delay lines. *J. Opt. Soc. Am., B*, **21**.
[22] Scheuer, J., Paloczi, G., Poon, J., and Yariv, A., 2005, Toward the slowing and storage of light. *OPN*, **16**, 36.
[23] Khurgin, J. B., 2005, Optical buffers based on slow light in electromagnetically induced transparent media and coupled resonator structures: comparative analysis. *J. Opt. Soc. Am., B* **22**, 1062.
[24] Khurgin, J. B., 2005, Expanding the bandwidth of slow-light photonic devices based on coupled resonators. *Optic Letters*, **30**, 513.
[25] Notomi, M., Yamada, K., Shinya, A., Takahashi, J., Takahashi, C. and Yokohama, I., 2001, Extremely large group-velocity dispersion of line-defect waveguides in photonic crystal slabs. *Phys. Rev. Lett.* **87**, 253902.
[26] Scalora, M., Flynn, R. J., Reinhardt, S. B., Fork, R. L., Bloemer, M. J., Tocci, M. D., Bowden, C. M., Ledbetter, H. S., Bendickson, J. M., Dowling, J. P., and Leavitt, R. P., 1996, Ultrashort pulse propagation at the photonic band edge: Large tunable group delay with minimal distortion and loss. *Phys. Rev. E*, **54**, R1078.
[27] Bloemer, M., Myneni, K., Centini, M., Scalora, M. and D'Aguanno, G., 2002, Transit time of optical pulses propagating through a finite length medium. *Phys. Rev., E* **65**, 056615.
[28] Soljacic, M., Johnson, S., Fan, S., Ibanescu, M., Ippen, E. and Joannopoulos, J. D., 2002, Photonic-crystal slow-light enhancement of nonlinear phase sensitivity. *J. Opt. Soc. Am. B.*, **19**, 2052.
[29] Figotin, A. and Vitebskiy, I., 2003, Electromagnetic unidirectionality in magnetic photonic crystals. *Phys. Rev., B* **67**, 165210.
[30] Figotin, A. and Vitebskiy, I., 2003, Oblique frozen modes in layered media. *Phys. Rev., E* **68**, 036609.
[31] Ballato, J., Ballato, A., Figotin, A. and Vitebskiy, I., 2005, Frozen light in periodic stacks of anisotropic layers. *Phys. Rev., E* **71**.
[32] Molchanov, S. and Vainberg, B., 2004, Slowdown of the wave packages in finite slabs of periodic media. *Waves Random Media*, **14**, 411.

[33] Figotin, A. and Vitebskiy, I., 2005. Gigantic transmission band-edge resonance in periodic stacks of anisotropic layers. *Phys. Rev., E* **72**, 036619.
[34] Figotin, A. and Vitebskiy, I., 2006, Electromagnetic unidirectionality and frozen modes in magnetic photonic crystals. *JMMM*, **300**, 117.
[35] Harris, S. E., 1997, Electromagnetically induced transparency. *Physics Today*, **50**, 36.
[36] Joannopoulos, J., Meade, R. and Winn, J., 1995, Photonic Crystals (Princeton University Press).
[37] Yeh, Pochi, 1988, "Optical Waves in Layered Media," (Wiley, New York).
[38] Weng Cho Chew, 1990,"Waves and Fields in Inhomogeneous Media," (Van Nostrand Reinhold, New York).
[39] Notomi, M., 2000, Theory of light propagation in strongly modulated photonic crystals: Refractionlike behavior in the vicinity of the photonic band gap. *Phys. Rev., B* **62**, 10696.
[40] Figotin, A. and Vitebsky, I., 2001, *Nonreciprocal magnetic photonic crystals*. *Phys. Rev., E* **63**, 066609.
[41] Berreman, D. W., 1972, *J. Opt. Soc. Am., A* **62**, 502–10
[42] Abdulhalim, I., 2000, Analytic propagation matrix method for anisotropic magneto-optic layered media. *J. Opt. A: Pure Appl. Opt.* **2**, 557.
[43] Abdulhalim, I., 1999, Analytic propagation matrix method for linear optics of arbitrary biaxial layered media, *J. Opt. A: Pure Appl. Opt*. **1**, 646.
[44] Bellman, R., 1997, Introduction to matrix analysis (SIAM. Philadelphia.)
[45] Coddington, E. and Carlson, R., 1997, Linear ordinary differential equations (SIAM, Philadelphia).
[46] Bogaevski, V. N. and Povzner, A., 1991, Algebraic methods in nonlinear perturbation theory, Springer-Verlag, New York.
[47] Figotin, A. and Godin, Yu., 2001, Spetral properties of thin-film photonic crystals. *SIAM J. APPL. MATH.*, **61**, 1959–1979.
[48] Kato, T., 1995, Perturbation theory of linear operators. Springer.
[49] Lancaster, P. and Tismenetsky, M., 1985, The theory of matrices, Academic Press.
[50] Wilkinson, J., 1996, The algebraic eigenvalue problem, Oxford University Press.

Appendix 1: basic properties of the transfer matrix

According to (91), the 4×4 matrix $\mathcal{T}(\nu)$, $\nu = \omega - \omega_0$ satisfies the following identity

$$\mathcal{T}^{-1}(\nu) = J\mathcal{T}^*(\nu)J. \tag{555}$$

The identity implies, in particular that

$$|\det \mathcal{T}(\nu)| = 1 \tag{556}$$

$$\text{if } \zeta \text{ is an eigenvalues of } \mathcal{T}(\nu) \text{ then } 1/\zeta^* \text{ is also an eigenvalue.} \tag{557}$$

In other words, the statement (557) yields that if $\zeta = \rho e^{\mathrm{i}\phi}$ is the polar form of an eigenvalue ζ and $\rho \neq 1$ then

$$\zeta = \rho e^{\mathrm{i}\phi} \quad \text{and} \quad \zeta = \rho^{-1} e^{\mathrm{i}\phi} \text{ are both eigenvalues of } \mathcal{T}(\nu) \tag{558}$$

and that if ζ is an eigenvalue of $\mathcal{T}(\nu)$ then $1/\zeta^*$ is an eigenvalue too.

The above properties of eigenvalues of $\mathcal{T}(\nu)$ imply the following statements.

1. Suppose that $\zeta(\nu)$ is an eigenvalue of $\mathcal{T}(\nu)$ depending on ν continuously. Suppose also that $\zeta(0)$ has multiplicity 1 and $|\zeta(0)| = 1$. Then there exists a sufficiently small $\delta > 0$ such that

$$|\zeta(\nu)| = 1 \quad \text{for any } |\nu| \leq \delta. \tag{559}$$

To show (559) we need the following elementary implication:

$$\text{if } |\zeta_0| = 1 \quad \text{and } |\zeta - \zeta_0| \leq \epsilon \leq \frac{1}{2} \quad \text{then} \quad \left|\frac{1}{\zeta^*} - \zeta_0\right| \leq 6\epsilon. \tag{560}$$

Assume now that the assumption of (560) holds. Notice that

$$\frac{1}{\zeta^*} \equiv \frac{\zeta}{|\zeta|^2} \tag{561}$$

and

$$||\zeta|-1| = ||\zeta|-|\zeta_0|| \le |\zeta-\zeta_0| \le \epsilon \le \frac{1}{2}. \tag{562}$$

with then implies that

$$1-\epsilon \le |\zeta| \le 1+\epsilon. \tag{563}$$

Now using (561) we get

$$\left|\frac{1}{\zeta^*}-\zeta_0\right| = \left|\frac{\zeta}{|\zeta|^2}-\zeta_0\right| = \left|\left(\frac{1}{|\zeta|^2}-1\right)\zeta+\zeta-\zeta_0\right|$$
$$\le \left|\left(\frac{1}{|\zeta|^2}-1\right)\zeta\right| + |\zeta-\zeta_0| = \frac{1-|\zeta|^2}{|\zeta|} + |\zeta-\zeta_0| \tag{564}$$

The inequalities (562), (564) together with $\epsilon \le \frac{1}{2}$ yield

$$\left|\frac{1}{\zeta^*}-\zeta_0\right| \le \frac{1-(1-\epsilon)^2}{1-\epsilon} + \epsilon = \epsilon\frac{3-2\epsilon}{1-\epsilon} \le 6\epsilon, \tag{565}$$

which is the desired inequality (560).
Using the fact the $\zeta(0)$ has multiplicity one and applying the standard perturbation theory arguments we can always find $0 < \epsilon_0 < 1$ and $\delta_0 > 0$ such that

$$\text{for} |\nu| \le \delta_0 \text{ the eigenvalue } \zeta(\nu) \text{ is the only one in the circle } |\zeta-\zeta(0)| \le \epsilon_0. \tag{566}$$

Now using the continuity of $\zeta(\nu)$ we can always find a positive $\delta < \delta_0$ such that

$$\text{for } |\nu| \le \delta < \delta_0 \text{ we have } |\zeta(\nu)-\zeta(0)| \le \frac{\epsilon_0}{6} \le \frac{1}{6}. \tag{567}$$

Observe that (565) and (567) imply that

$$\left|\frac{1}{\zeta^*(\nu)}-\zeta(0)\right| \le \epsilon_0 \quad \text{for } |\nu| \le \delta < \delta_0. \tag{568}$$

Assume for the sake of the argument that for some $|\nu| \le \delta$ we have $|\zeta(\nu)| \ne 1$. Then based on (568) and general properties of $\mathcal{T}(\nu)$ we have to conclude that $\frac{1}{\zeta^*(\nu)} \ne \zeta(\nu)$ is another eigenvalue of $\mathcal{T}(\nu)$ residing in the circle $|\zeta-\zeta(0)| \le \epsilon_0$. But this clearly contradicts to (566) implying the desired relation (559).

2. Suppose that for $0 < |\nu| < \delta$ the matrix $\mathcal{T}(\nu)$ has four different eigenvalues $\zeta_j(\nu)$, $j = 1, \dots 4$ each continuously depending on ν and having the following properties:

$$\text{There exists a } \zeta_0 \text{ such that } \lim_{\nu\to 0}\zeta_j(\nu) = \zeta_0, \quad j = 1,2,3, \text{ and } \zeta_4(0) \ne \zeta_0. \tag{569}$$

In other words, for small $|\nu|$ the eigenvalue $\zeta_4(\nu)$ has multiplicity one and is well separated from the other 3 different eigenvalues $\zeta_j(\nu)$, $j = 1,2,3$ which converge as $\nu \to 0$ to a ζ_0. Then we claim that

$$|\zeta_0| = 1 \quad \text{and } |\zeta_4(0)| = 1, \tag{570}$$

and there exists a $\delta > 0$ such that

$$|\zeta_j(\nu)| = 1 \quad \text{for at least one } j = 1,2,3 \text{ and } |\nu| < \delta. \tag{571}$$

$$|\zeta_4(\nu)| = 1 \quad \text{for } |\nu| < \delta. \tag{572}$$

Observe, first, that the first equality in (569) follows from the conditions of (569) and general properties of $\mathcal{T}(\nu)$, since if $|\zeta_0| \neq 1$, we would have three more eigenvalues $\frac{1}{\zeta_j^*(\nu)}$, $j = 1, 2, 3$ with the total number of eigenvalues 6. That is, of course, impossible for 4×4 matrix implying that the first equality in (569) holds. As to the second, it follows from proving that $|\zeta_0| = 1$ and the identity (556), since then we must have $|\zeta_0|^3 |\zeta_4(0)| = 1$.

To show (571) we use the limit conditions in (569) and the fact that $\frac{1}{\zeta_j^*(\nu)}$ is also an eigenvalue. Indeed, if, for the sake of the argument, we assume that (569) does not hold we have to conclude that in a infinitesimally small vicinity of ζ_0 there will be at least four different eigenvalues which is impossible in view of the second condition in (569). This completes the proof of (571). As to the proof of (572) it follows from the statement (559).

Appendix 2: perturbation theory for a diagonal matrix

Particular constructions of the perturbation theory we discuss here follow from [46] and [47]. Suppose that

$$W(\nu) = W_0 + \nu W_1 + \nu^2 W_2 + \cdots \tag{573}$$

and T_0 is a diagonal matrix with distinct elements, i.e.

$$W_0 = \begin{bmatrix} w_1 & 0 & \dots & 0 \\ 0 & w_2 & \ddots & \vdots \\ \vdots & \ddots & \ddots & 0 \\ 0 & \dots & 0 & w_n \end{bmatrix}, \quad \text{where } w_m \neq w_j \text{ if } m \neq j. \tag{574}$$

To diagonalize $T(\nu)$ we use the approach outlined in [46] and used in [47]. Namely, there exists the following representation for the diagonal form X of $T(\nu)$

$$\zeta = e^{-S(\nu)} W e^{S(\nu)} = W_0 + \nu\zeta_1 + \nu^2\zeta_2 + \cdots, \quad S(\nu) = \nu S_1 + \nu^2 S_2 + \cdots, \tag{575}$$

where the matrices $S_1, S_2, \dots$ do not depend on ν and $X_1, X_2, \dots$ are diagonal. To find S_j and X_j we use the Hausdorf's representation

$$X = e^{-S} W e^{S} = W + [W, S] + \frac{1}{2!}[[W, S], S] + \cdots, \quad \text{where} \tag{576}$$

where the brackets denote the commutator of two matrices

$$[A, B] = AB - BA.$$

Substituting (575) into (576) and equating the terms of like powers in ν, we obtain the following expressions for the matrices X_j

$$X_1 = [T_0, S_1] + T_1, \quad X_2 = [T_0, S_2] + T_2 + [T_1, S_1] + \frac{1}{2}[[T_0, S_1], S_1], \dots. \tag{577}$$

To find X_j we introduce for a matrix Y its representation as the sum of its diagonal $\bar{Y}$ part and the remaining part $\mathring{Y}$ with zero diagonal elements (so called integrable matrix [46])

$$Y = \bar{Y} + \mathring{Y}, \quad \bar{Y} = \operatorname{diag}(Y), \quad \mathring{Y} = Y - \operatorname{diag}(Y). \tag{578}$$

Then

$$X_1 = [W_0, S_1] + \bar{W}_1 + \mathring{W}_1, \tag{579}$$

and to get rid of the integrable part $\mathring{W}_1$ of W_1 we take S_1 to be the solution of the equation

$$[W_0, S_1] = -\mathring{W}_1. \tag{580}$$

The solution to this equation is

$$[S_1]_{jm} = \frac{1}{w_m - w_j}[\mathring{W}_1]_{jm}, \quad j \neq m; \quad [S_1]_{jj} = 0. \tag{581}$$

Consequently,

$$X_1 = \mathrm{diag}(W_1) = \bar{W}_1. \tag{582}$$

To find X_2 we recast the equation (577) as

$$X_2 = [W_0, S_2] + \bar{Y}_2 + \mathring{Y}_2, \quad Y_2 = W_2 + [W_1, S_1] + \frac{1}{2}[[W_0, S_1], S_1]. \tag{583}$$

Applying to this equation the same approach as for (579) we get

$$X_2 = \mathrm{diag}(Y_2) = \bar{Y}_2, \quad Y_2 = W_2 + [W_1, S_1] + \frac{1}{2}[[W_0, S_1], S_1].$$

$$[S_2]_{jm} = \frac{1}{w_m - w_j}[\mathring{Y}_2]_{jm}, \quad j \neq m; \quad [S_2]_{jj} = 0. \tag{584}$$

Using (580)–(583) we can recast (584) as

$$X_2 = \mathrm{diag}(W_2 + \frac{1}{2}[\mathring{W}_1, S_1]),$$

$$[S_2]_{jm} = \frac{1}{w_m - w_j}[\mathring{Z}_2]_{jm}, \quad j \neq m; \quad [S_2]_{jj} = 0; \quad Z_2 = W_2 + [W_1 - \frac{1}{2}\mathring{W}_1, S_1]. \tag{585}$$